NTNU – Trondheim
Norwegian University of
Science and Technology

A Case Study of How MPD Techniques Can Be Used to Adapt to Uncertain Pore and Fracture Pressure Gradients

Anders Wenaas

Petroleum Geoscience and Engineering (2 year)
Submission date: June 2014
Supervisor: John-Morten Godhavn, IPT

Norwegian University of Science and Technology
Department of Petroleum Engineering and Applied Geophysics

Abstract

This thesis aims to identify the potential and limitations of using Managed Pressure Drilling (MPD) in deepwater fields where narrow and unpredictable mud weight windows are encountered. A significant effort has been done to understand the methods used to estimate and verify the underground pressure and stress environment.

Some of the worlds largest conventional oil fields are located in the deep waters beyond the continental shelves. As the industry engage in these highly productive and promising deepwater fields, major obstacles are encountered during drilling which leads to high amounts of costly Non-Productive Time (NPT). With unique challenges such as lost circulation, narrow drilling windows and vast amounts of salt, there is a need for innovative techniques to develop these fields in a safe and effective manner.

MPD is presented as a favourable solution to overcome challenges associated with uncertain and narrow mud windows. Being able to control the annular pressure profile throughout the wellbore and react to pressure fluctuations within seconds allows drilling to proceed safely and uninterrupted, while keeping the operational problems to a bare minimum. In addition to increased operational flexibility, MPD has shown positive effects on lost circulation, which is a major well cost driver in conventional drilling.

A case study is conducted for a deepwater exploration well in the Gulf of Mexico. Based on estimations of the pore and fracture pressure gradients, drilling programs are designed for respectively conventional drilling, and the two MPD variants: Constant Bottom-Hole Pressure (CBHP) and Controlled Mud Level (CML). Where the latter is a Dual Gradient Drilling (DGD) approach. The deepwater well is then drilled with the planned drilling programs and real pore and fracture pressure gradients. This case study shows the unique flexibility MPD entails when deviations from the plan are encountered.

Sammendrag

Denne oppgaven tar sikte på å avklare potensialet og begrensningene boreteknikken "Managed Pressure Drilling" (MPD) innehar i dypvannsfelt, hvor uforutsigbare og smale borevinduer ofte er tilstede. En betydelig innsats er lagt ned i å forstå de metodene som brukes for å estimere samt verifisere det underjordiske trykk- og spenningsmiljøet.

Noen av verdens største konvensjonelle oljefelt befinner seg på dypt vann utenfor kontinentalsoklene. Ettersom bransjen engasjerer seg i disse svært produktive og lovende dypvannsfeltene, er store hindringer møtt under boring som medfører mye kostbar ikke-produktiv tid. Med unike utfordringer som tapt sirkulasjon, smale borevinduer og store lag med salt, er det behov for innovative teknikker for å utvikle disse feltene på en sikker og effektiv måte.

MPD er presentert som en gunstig løsning for å overvinne utfordringene knyttet til usikre og smale borevinduer. Mulighetene for presis kontroll av trykket i annulus samt hurtig reaksjon på trykkforandringer åpner muligheten for at boringen kan fortsette trygt og uforstyrret, samtidig som de operasjonelle problemene holdes på et minimum. I tillegg til økt operasjonell fleksibilitet, har MPD vist positive effekter på tapt sirkulasjon, noe som er en stor kostnadsdriver i konvensjonell boring.

En casestudie er gjennomført for en dypvannsbrønn i Mexicogolfen. Basert på beregninger av pore- og bruddtrykk er boreprogram designet for henholdsvis konvensjonell boring, og de to MPD variantene: "Constant Bottom-Hole Pressure" (CBHP) og Controlled Mud Level (CML), der den sistnevnte er en "Dual Gradient Drilling" (DGD) metode. Dypvannsbrønnen er deretter boret med de planlagte boreprogrammene med reelle pore- og fraktureringstrykk. Denne studien viser den unike fleksibiliteten MPD innehar når avvik fra boreplanen oppstår.

Acknowledgements

This Master Thesis was written in the spring of 2014 at the Department of Petroleum Engineering and Applied Geophysics at the Norwegian University of Science and Technology (NTNU).

First, I would like to thank my supervisor John-Morten Godhavn for his insightful advice and feedback throughout the thesis.

Secondly, I would like to thank Kristian Eliassen for the much appreciated comments on structuring and language improvements.

Last but not least, I would like to thank my mother, Tove Baugerød, in addition to my stepfather, Dagfinn Heie, for their continuous support and encouragement.

Contents

List of Figures

List of Tables

Chapter 1

Introduction

A widely used expression states that the days of so-called "easy oil" are over, making it more complicated and expensive to meet the worlds ever-increasing demand for oil and gas. This reality was first acknowledged by the chairman and chief executive officer of Chevron, David O'Reilly, whom in 2005 stated that "*the era of easy oil is over* [1]." Not only are many of the existing fields experiencing a decline in production, he noted, but the new discoveries are mainly occurring in places where they are difficult to extract. In the attempt to meet the worlds increasing energy demand, the petroleum industry has been "forced" into more remote and challenging environments such as offshore at great water depths. As illustrated in Figure 1.1, early in the 2000s, oil production from deepwater (300 - 1 500 meters) and ulta-deepwater (> 1 500 meters) reservoirs in the Gulf of Mecico surpassed the production from shallow water (< 300 meters) reservoirs [1, 2].

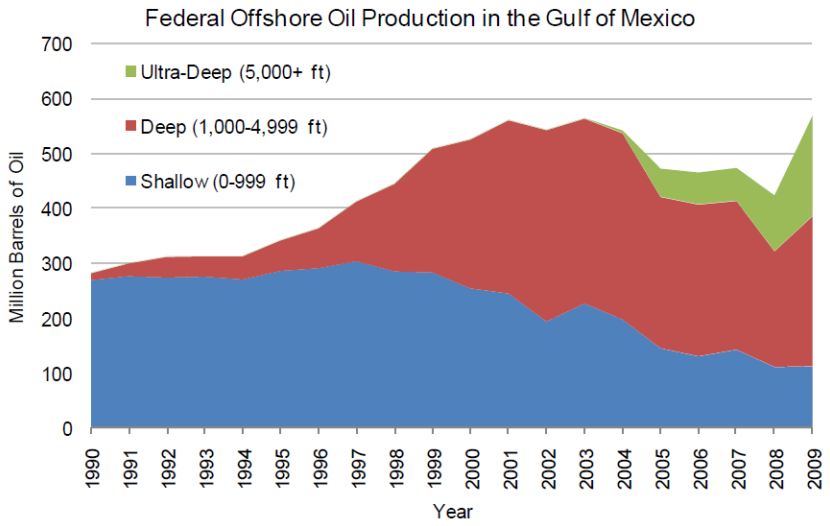

Figure 1.1: Offshore oil production in the Gulf of Mexico per year (*1 barrel = 159 litres*) [2].

In the early 1990s, the oil industry discovered that huge amounts of oil and gas are resting in the deep waters beyond the continental shelves. It is believed that as much as 7 % of the worlds oil and gas resources are located in the deep offshore. That is approximately 340 billion barrels (54,1 billion m^3) of oil equivalents which is sufficient to cover the global consumption for roughly six to seven years [3, 4]. As of 2014, the service company *Schlumberger* states that: "*Deep waters are among the most important and challenging exploration and production frontiers today, the success of which offers a unique opportunity for adding significantly to the worlds proven oil reserves* [5]."

As the exploration and production (E&P) companies engage in these promising deepwater and ultra-deepwater fields, they are encountering challenges that increase costs, NPT and risk. Narrow mud weight windows, unstable boreholes caused by changes in pore and fracture pressures, and reservoirs located beneath vast amounts of salt are among the experienced issues. The mud weight window defines the maximum and minimum well pressure that is acceptable during drilling, most commonly bound by the pore and fracture pressure. A peculiar challenge encountered in deep waters is that this margin tends to decrease with increasing water depth, commonly spoken of as *narrow mud weight windows*. If the well pressure either exceeds or drops below the defined pressure margin, problems related to kicks, lost circulation and unstable boreholes are experienced. Such incidents may in a worst case scenario lead to blowout, that is, an uncontrollable flow of hydrocarbons to the environment [6, 7].

The aforementioned challenges encountered in deep water drilling does often result in very expensive wells. It is not uncommon for a deepwater well in the Gulf of Mexico (GOM) to target a formation at 30 000 feet (9 145 meters) vertical depth. As illustrated in Figure 1.2, this is far deeper than some of the wells drilled on the Norwegian continental shelf. In order to drill these wells in a safe en effective manner, innovative technology is required. An exploration well in the deep waters of the Gulf of Mexico can typically cost from 100 to 200 million US dollars, and an exploration well may cost twice as much. The aforementioned problems related to NPT contributes significantly to these costs in addition to safety concerns. The industry is therefore seeking new techniques that are able to mitigate these problems so that deep wells in deep waters can be drilled in a safe and effective manner [8].

From a conventional point of view, drilling is conducted with an open-to-atmosphere drilling fluid circulation system and with a single fluid gradient. However, the relatively modern drilling technique Managed Pressure Drilling challenges this point of view. MPD utilizes a closed-to-atmosphere drilling fluid circulation system and enables the bottom-hole pressure

(BHP) to be kept constant during the entire drilling operation. In 2004, the International Association of Drilling Contractors (IADC) defined MPD as: "'*An adaptive drilling process used to precisely control the annular pressure profile throughout the wellbore* [9].' As stated by IADC, MPD is an adaptive drilling process, meaning that MPD is able to handle and control sudden underground pressure deviations in a safe and effective manner. MPD is able to detect influx/losses at very small values and, through quick regulation of the BHP, brings the situation effectively under control. This feature combined with a CBHP, enables each section to be drilled longer prior to running casing/liner. The overall advantage of MPD is increased drillability in narrow and uncertain pressure environments, increased safety and reduced NPT. This gives reason to believe that several of the experienced issues in deepwater drilling will be mitigated through the use of this technique rather than conventional drilling [10].

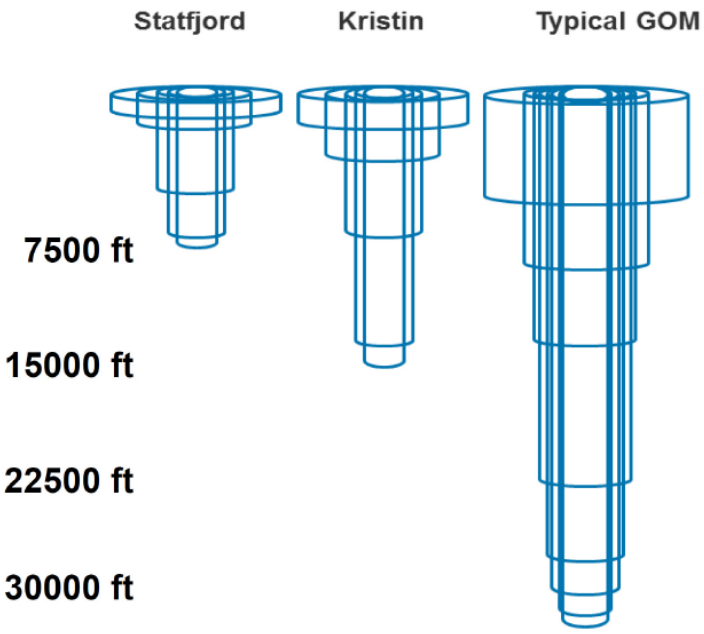

Figure 1.2: Comparison between typical casing programs for respectively a well drilled at Statfjord, Kristin and a typical deep well drilled in the deep waters of the GOM [8].

1.1 Scope of thesis

Prior to drilling, a mud weight window is constructed based on estimations of the underground pressure and stress environments. There are, however, uncertainties related to these estimates, and unpleasant "surprises" may therefore be encountered during drilling. The purpose of this thesis is to investigate and elaborate on how MPD can be used to adapt to these uncertainties, particularly in deep waters.

My supervisor, John-Morten Godhavn, has provided estimated and real pore and fracture pressure gradients for a deepwater exploration well in the Gulf of Mexico. First, based on the estimated values, drilling programs are designed for respectively conventional drilling and the two MPD variants: *Constant Bottom-Hole Pressure* and *Controlled Mud Level*. Where the latter is a DGD approach. The well is then drilled, on paper, using the planned drilling programs and real pore and fracture pressure gradients. When deviations are encountered it will require the drilling program to be updated. A special focus are given towards the additional flexibility offered by MPD when such deviations are encountered.

1.2 Outline of thesis

The outline of the thesis is as follow:

Chapter 2 Describes the importance of pressure control during drilling and explains how the mud weight window is estimated prior to drilling and later updated by using real information during drilling.

Chapter 3 Discusses deepwater drilling and elaborates on the challenges and concerns related to this.

Chapter 4 Describes the fundamentals of the various drilling techniques, but with a special focus towards MPD and the advantages offered by the various MPD variants

Chapter 5 Contains a case study performed on a deepwater exploration well in the Gulf of Mexico.

Chapter 6 Presents the final discussion of the thesis.

Chapter 7 Contains the concluding remarks of the thesis.

Appendix A Describes commonly used equipment in MPD.

Appendix B Presents an overview of the various DGD approaches and systems.

Appendix C Contains the details of the planned and actual drilling programs presented in the case study.

Chapter 2

Pressure control during drilling

A fundamental requirement for a safe and responsible drilling operation is proper control of the wellbore pressure. The wellbore pressure must be sufficiently high to avoid a collapsed borehole situation and/or unwanted influx of formation fluids, referred to as a *kick*. Meanwhile, the pressure in the wellbore must not exceed the maximum pressure the formation is able to withstand. If this occur, fractures will be formed along the borehole wall and drilling fluid will be lost to the formation, referred to as *lost circulation*. The pressure conditions at which these incidents occur are commonly presented in a plot known as the *mud weight window*, further discussed Section 2.1 [11, 12].

Until the early 1900s, drilling after hydrocarbons were conducted without any form of pressure control whatsoever. The hydrocarbons encountered during drilling would flow uncontrolled to the surface and lead to a blowout. An unwanted influx of formation fluid is, as mentioned above, referred to as a kick. However, if the ability to control this influx is lost and hydrocarbons are flowing with an uncontrollable rate towards the surface, the situation has developed to a much more serious situation, namely a blowout. Such a situation may potentially inflict large economic consequences, and in a worst case scenario involve loss of human lives. The aforementioned drilling strategy in the early 20th century caused several blowouts to occur, such as the Spindletop blowout on January 10, 1901. On that day, it was reported in the morning news that a solid stream of Petroleum were rising out of the earth, 200 feet (61 meter) into the air. The Spindletop well was flowing uncontrolled for nine days before it was finally brought under control, leaking up to 100 000 barrels (15 900 m^3) per day. A picture taken of the Spindletop blowout is presented in Figure 2.1 [12, 13].

Figure 2.1: The Spindletop blowout in 1901 [12].

The blowout incidents in the early 20th century functioned as an eye-opener for the industry regarding the importance of pressure control and safety during drilling, completion and production operations. Weighted drilling fluids, and hence overbalanced drilling, was invented to mitigate the occurrence of kicks/blowouts during drilling [12]. "*It has been said that Spindletop was where oil became an industry. Its impact had to be felt* [13]."

2.1 Mud weight window

The mud weight window, occasionally referred to as the *drilling operating window* or the *drilling window*, defines the maximum and minimum well pressure that is acceptable during drilling. On the low side, the well pressure is bound by the formation-pore pressure, P_f, or the collapse pressure of the formation, $P_{Collapse}$. Whichever of them has the highest value determines the lower well pressure margin. Whereas on the high side, the well pressure is bound by the formation-fracture pressure, P_{frac}. The well pressure, P_w, during drilling is then governed by the following pressure boundaries [10, 11]:

$$P_f \text{ or } P_{Collapse} < P_w < P_{frac} \tag{2.1}$$

Prior to drilling, a mud weight window is constructed based on estimations of the underground stress and pressure environment. These estimations are then further used to plan an optimal well design. The primary purpose of the planned well is to reach a certain location of interest, either in the search for new hydrocarbon prospects or to ensure optimum drainage of an already discovered hydrocarbon zone. This entails that well design primarily is governed by the well trajectory required to reach the location of interest. The suggested well trajectory is then evaluated against the estimated mud weight window to assess the drillability of the well. This enables an optimal drilling plan to be constructed prior to drilling, aiming towards an economical and safe drilling operation [11].

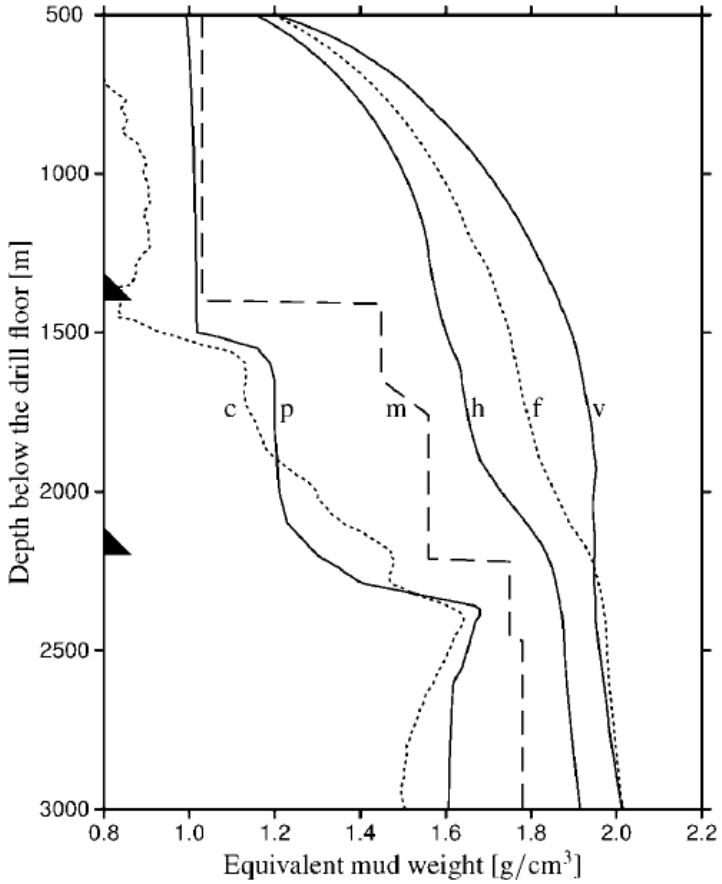

Figure 2.2: Example of an estimated mud weight window for a planned well on the Norwegian Continental Shelf. Courtesy of Statoil [11].

An estimated mud weight window is illustrated in Figure 2.2. The two black triangles seen on the depth axis represents the casing shoe depths, and from respectively left to right the lines are: estimated collapse pressure gradient (c), estimated pore pressure gradient (p), planned mud weights gradient (m), estimated minimum horizontal stress gradient (h), estimated fracture pressure gradient (f) and the estimated overburden stress gradient (v).

A brief introduction about the underground stress regime is presented in Section 2.2. On the figure, it is seen that from roughly 1 900 to 2 300 meter depth, the collapse pressure gradient exceeds the pore pressure gradient. This implies that the lower pressure margin is governed by the collapse pressure in this interval. It is seen that casing strings are set when it becomes challenging/impossible to continue the drilling operation with the current mud weight. The placed casing seals off and protects the upper part of the well, enabling the mud weight to be increased and drilling to continue. This illustrates the two most important features for a stable borehole: The ability to adjust the wellbore pressure and the casing program [11].

During the drilling phase, there is a relatively high possibility of encountering unexpected pore and fracture pressure, potentially resulting in influx/losses. If the pressure margin allows it, a kick is handled by increasing the wellbore pressure and losses are handled by decreasing the wellbore pressure. However, if the wellbore pressure is touching the limits set by the mud weight window, this may trigger the need to cease drilling and run casing/liner earlier than planned. This may cause challenges in reaching target depth, especially if several sections has to be cased and secured earlier than planned. In order to handle the unexpected pressure gradients in a safe manner, various verification methods and drilling techniques has been developed, aiming to reduce the uncertainties and handle the encountered deviations in a safe manner.

2.1.1 Pressure gradients

When pressures are related to mud density, it is customary to convert the pressure value at a specific depth to a density value. This is often referred to as an equivalent mud weight (EMW) or a pressure gradient, making the mud weight window more comprehensible:

$$EMW = \frac{Pressure}{g \cdot TVD} \tag{2.2}$$

where, in SI-units, EMW is noted kg/m^3, pressure in Pa (pascal), g is the gravity constant (9,81 m/s^2) and TVD is the total vertical depth in meters.

2.1.2 Well killing

The content in this section is taken from a previous paper written at NTNU in the unit "TPG 4140 Naturgass" [14]. When a kick is experienced, it is important to take action to prevent further loss of control of the well. For drillers it is important to be able to predict gas behavior, as small volumes of gas can potentially be dangerous because of the huge expansion.

Provided that the maximum allowable annular surface pressure (MAASP) is larger than the shut-in casing pressure (SICP), then killing the well is the standard procedure. The MAASP value determines the maximum pressure that can be applied from the surface before exceeding the fracture pressure at the casing shoe. When a kick is experienced, the well is shut in (the blow out preventer (BOP) is closed) and the annular surface pressure is read. In order to kill a well, a new overbalance in the borehole must be restored. Pumping drilling mud with higher density restores this overbalance. There exists a number of different killing methods, but the two main killing-methods used in the industry are:

- *Driller's method*: The formation fluid is displaced before injecting the kill mud. This is the most common method of restoring an overbalance after a kick has been detected.
- *Engineer's method*, alternatively called the *wait and weight method*: Kill mud is pumped into the well immediately and the formation fluids are circulated out of the wellbore.

2.2 Underground stresses

Stress acting on a material is defined as force over area ($\sigma = \frac{F}{A}$) and is commonly divided into a perpendicular and parallel stress vector. Respectively normal stress, σ_n, and shear stress, τ. This is illustrated in Figure 2.3 [15].

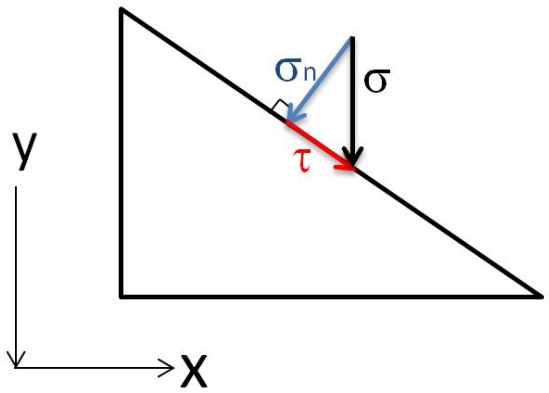

Figure 2.3: Shear- and normal stress acting on a 1-dimensional plane [15].

For special orientations of the coordinate system, the stress state can be expressed in a particularly simple form. This occurs when the coordinate system is oriented θ degrees so that the shear stress vector vanishes. The total stress is then equal to the normal stress,

which for this unique situation is referred to as principal stress, σ_i. This is illustrated for a one-dimensional system in Figure 2.4 [15].

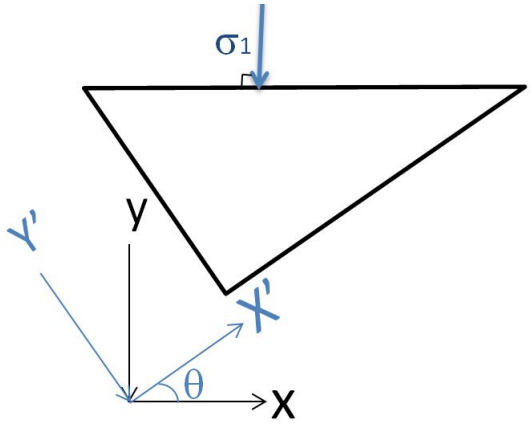

Figure 2.4: Illustration of principal stress [15].

The same principle applies in a three-dimensional system, such as the underground. The difference being that the stress state is expressed by three principal stresses as opposed to one. In the underground, these three principal stresses are called vertical stress, σ_v, maximum horizontal stress, σ_H, and minimum horizontal stress, σ_h. Where the normal case is that $\sigma_v > \sigma_H > \sigma_h$. The principal stresses acting on a vertical wellbore is illustrated in Figure 2.5 [15].

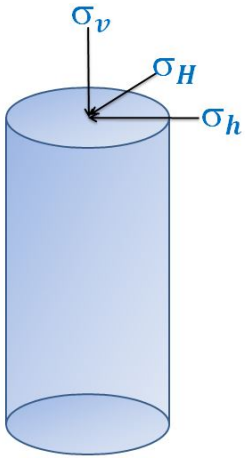

Figure 2.5: Underground stresses acting on a vertical wellbore.

2.2.1 Vertical stress

The vertical stress is fairly straightforward to estimate, whereas the two horizontal stresses are slightly more complex. At a certain vertical depth, the vertical stress component is estimated as follows [15]:

$$\sigma_v = P_{ovb} = \int_0^{TVD} \rho \cdot g \cdot TVD \, dTVD \tag{2.3}$$

where P_{ovb} is the overburden pressure and ρ is the overburden rock density. It is seen by Equation 2.3 that the vertical stress at a particular point in the underground is solely given by the densities of the overburden rocks [15].

2.2.2 Horizontal stress

The two horizontal stresses are also to a great extent determined by the overburden pressure. However, as rocks has the ability to resist shear stresses, the three principal stresses are commonly not of equal magnitude. Mainly caused by tectonic movement which induces tectonic stresses in the underground. For simplicity, the maximum horizontal stress is often assumed equal to the minimum horizontal stress, that is, $\sigma_H = \sigma_h$. This is often the case because no straightforward method exists for accurate determination of σ_H. Estimation and verification of the minimum horizontal stress is further discussed in Sections 2.4.2 and 2.4.3 [15].

2.3 Pore pressure

The pore pressure contained within a saturated formation is directly related to its burial depth. Increased burial depth implies increased overburden pressure, which in turn, leads to compaction of the sediments within the formation. If fluids are expelled from the saturated formation with the same rate as the rate of compaction, a normal pore pressure gradient will develop. That implies that the pore pressure is solely determined by the hydrostatic head of fluid, most commonly saline water. However, if the rate of compaction is higher than the rate of fluid expulsion, a higher-than-normal pore pressure is established, referred to as *abnormal pore pressure*. Abnormal pore pressure may also be induced by tectonic movement, pore fluid generation or expansion by a thermal or chemical process. A typical pore pressure versus depth plot is illustrated in Figure 2.6. The depth scale on this plot is in meters [11].

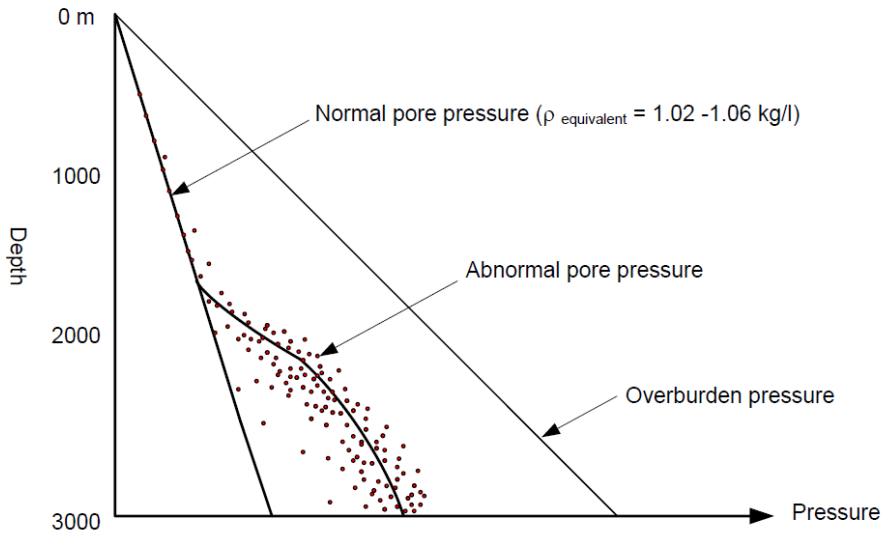

Figure 2.6: Typical formation-pore pressure development in a sedimentary basin [16]

If an abnormally pressured zone is encountered unprepared during drilling, the outcome may potentially be catastrophic. Problems related to collapsed boreholes, kicks, lost circulation and stuck pipe may be experienced. In an attempt to battle the formation fluid influx, the first response of the driller may be to increase the mud weight, as was discussed in Section 2.1.2. This may potentially stop the influx, but at the same time induce a risk of exceeding the fracture pressure further up in the wellbore. If the driller is unable to bring this situation under control, it may develop to a blowout. From a safety and economical point of view, accurate prediction and verification of the pore pressure is therefore a key parameter, enabling a safe drilling operation and optimal well design [11, 16].

2.3.1 Pore pressure prediction

A predrill estimate of the underground pore pressure environment can be obtained from seismic surveys. A seismic survey is performed by generating acoustic waves at the surface and then transmitting them with a high speed through the earth's upper crust. As the waves are passing through the underground, a large amount of echoes are created. At the surface, several acoustic receivers are mounted to record the wave velocity of the reflected echoes, which primarily are used to map the structure of the underground. This information can also be used to make a predrill estimate of the subsurface pore pressure environment [11].

Eaton's method from 1975 is the most frequently used method for making estimation of the pore pressure based on acoustic wave velocity. The method derived by Eaton is an

improvement of Hottman and Johnson's method of equivalent depth, proposed in 1965. Both of these methods rely upon Terzaghi's effective stress principle from 1925. Terzaghi defined the effective stress in a given direction, σ_i', to be equal to the total stress in the same direction, σ_i, minus the support from pore fluid pressure, P_f [17]:

$$\sigma_i' = \sigma_i - P_f \tag{2.4}$$

Eaton's method is based on Terzaghi's principle in the vertical direction:

$$\sigma_v' = \sigma_v - P_f \tag{2.5}$$

As was defined by Equation 2.3, the vertical stress at a certain vertical depth is equal to the overburden pressure. The pore fluid pressure at a given vertical depth can then be expressed as:

$$P_f = P_{ovb} - \sigma_v' \tag{2.6}$$

In 1975, Eaton defined the pore pressure to be a function of the overburden pressure, the hydrostatic normal pore pressure and the ratio between the observed versus normal acoustic wave velocity. The following relationship is known as Eaton's equation [17]:

$$P_f = P_{ovb} - ((P_{ovb} - P_{normal})(\frac{\Delta t_{normal}}{\Delta t})^3) \tag{2.7}$$

where P_{normal} is the normal pore pressure at the point of interest, Δt_{normal} is the normal acoustic wave velocity in m/s and Δt is the actual acoustic wave velocity. The subscript *normal* refers to the trend line the sonic log would follow in normally pressured environments. This normal trend is established by comparing log data from various wells in areas where the mud weight indicates a normal pore pressure gradient [17]. This is however not a straightforward process and, as Eaton said it: "*The methods used to establish normal trends vary as much as the number of people who do it* [17]."

When seismic measurements are used to predict the underground pressure environment, one have to bear in mind that there are uncertainties related to the obtained values. This uncertainty increases rapidly with increasing distance from a known control point such as a well log. Basically, this means that if drilling is to be conducted in an unknown area, such as often is the case during exploration drilling, the obtained values may be quite uncertain. However, if the well is to be drilled in a well-known area, such as for a field in production, the uncertainties are less substantial, as information from known control points are available. It is important to determine and take these uncertainties into account prior to a drilling operation. This will provide a better understanding of the potential

challenges that may be encountered during drilling, and enables a more informed drilling plan to be constructed. A case study, conducted in the Green Canyon in the Gulf of Mexico, regarding the uncertainties in the estimated mud weight widow is illustrated in Figure 2.7. This figure represents the P10-P50-P90 ranges for both pore and fracture pressure gradients which are obtained through Eaton's method. P10, P50 and P90 means that the chance of encountering a lower pore pressure than these values are respectively: 10 %, 50 % and 90 %. Hence, the chance of encountering a pore pressure between the P10 and P90 values are 80 % [18].[1] Estimation of the fracture pressure is discussed in Section 2.4.2.

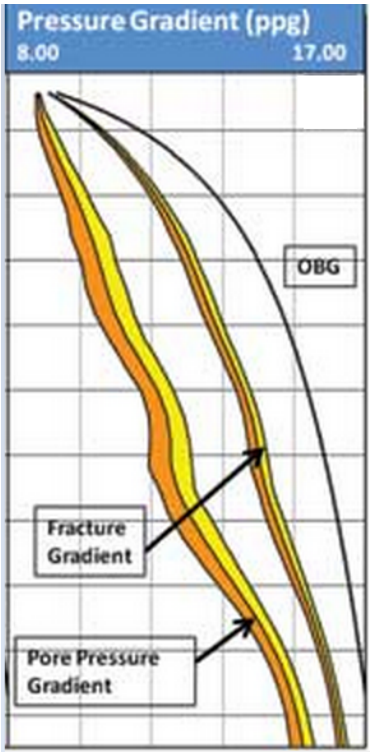

Figure 2.7: P10-P50-P90 values for pore and fracture pressure gradients [18].

2.3.2 Pore pressure verification

Various methods has been developed to provide measurements and real-time information about the pore pressure during drilling. If the measured pore pressure strongly deviates from the predicted pore pressure, it entails that a non-optimal mud weight is being used. This may potentially cause losses/influx to occur which may trigger the need to adjust the mud weight and/or running the casing/liner earlier than planned. The following techniques/properties are commonly used to verify the pore pressure during drilling [16]:

[1] John-Morten Godhavn, personal communication (e-mail), 15.04.2014.

- Measurements while drilling (MWD)
- Rate of penetration (ROP)
- Mud properties

Measurements while drilling

In the later years, MWD has more or less replaced wireline logging, especially in expensive offshore wells. A challenge with wireline logging is that logging cannot be commenced before drilling of a section has been completed. As a result, the information obtained from the logs are available long after the formations were actually drilled through. With the MWD technology however, information is obtained almost instantaneous through pressure pulses in the returning drilling fluid. The MWD tool, positioned approximately 15 meters above the bit, is used to gather information such as pore pressure, well trajectory, mud temperature and well pressure (referred to as pressure-while-drilling (PWD)). Real-time pore pressure data provided by a MWD tool is based on the same principle as pore pressure prediction from seismic data, that is, Eaton's method. Eaton did, in addition to Equation 2.7, also derive relationships between pore pressure and respectively resistivity and the dc-exponent [16, 17]:

$$P_f = P_{ovb} - ((P_{ovb} - P_{normal})(\frac{R}{R_{normal}})^{1,2}) \tag{2.8}$$

$$P_f = P_{ovb} - ((P_{ovb} - P_{normal})(\frac{d_c}{d_{c,normal}})^{1,2}) \tag{2.9}$$

where R is the actual measured resistivity and d_c is the dc-exponent (a drilling parameter discussed below). Hence, pore pressure information can be obtained through either a sonic log, a resistivity log or through the dc-exponent. This provides more accurate information than the predictions obtained through seismic as the travel length of the waves are much shorter. The subscript *normal* refers to the trend lines the different input logs would follow in normally pressured environments [17].

Rate of penetration/d'exponent

The rate of penetration during drilling is governed by the following parameters [16]:

- Rock properties
- Bottom hole cleaning
- Bit weight
- Rotary speed
- Fluid properties
- Bit type
- Bit wear
- Differential pressure between the wellbore and the formation

The ROP is strongly related to the difference between pore and wellbore pressure. This implies that if the other parameters are kept more or less constant, a change in pore pressure will have an immediate effect on the ROP. The higher the differential pressure is between the well and the formation ($P_w - P_f$), the lower the ROP is, meaning that an increase in pore pressure causes the ROP to increase (provided that the mud weight is kept constant). This relationship is illustrated in Figure 2.8 [16].

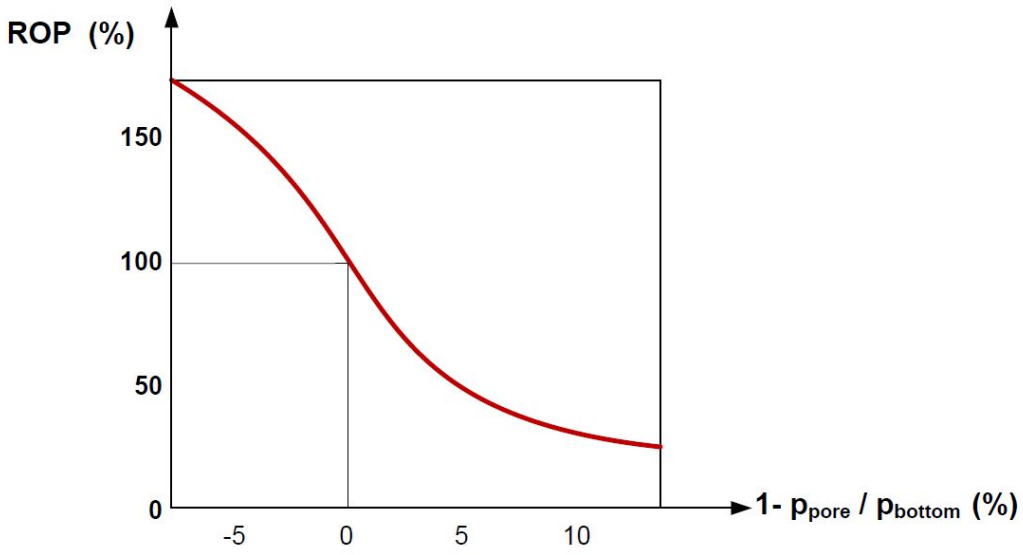

Figure 2.8: ROP VS. ΔP at wellbore bottom [16].

The d'exponent is a way of normalizing the ROP to extract information about the drillability and hardness of the formation. The following relationship was developed by Jordan and Shirley in 1966 [17]:

$$d = \frac{log\frac{ROP}{60 \cdot RPM}}{log\frac{12 \cdot WOB}{10^6 \cdot d_{bit}}} \tag{2.10}$$

where d represents the deviation in ROP induced by the differential pressure between the wellbore and the formation, RPM is the rotary speed (revolutions per minute), WOB is weight on bit and d_{bit} is the bit diameter. As for many other parameters, drilling rate will decrease with depth due to higher compaction, meaning that the normal trend line for the d'exponent follows the normal compaction trend line. During drilling, real-time pore pressure is estimated by comparing the measured d'exponent versus the normal d'exponent. It was suggested by Rehm and McClendon in 1971 to use the d_c-exponent rather than the d'exponent. They corrected the d'exponent to also include variations in drilling fluid density [16, 17]:

$$d_c = d \cdot \frac{Normal\ pressure\ gradient}{\rho_m} \tag{2.11}$$

where ρ_m is the drilling fluid density. A plot illustrating how the d_c-exponent is used to provide real-time pore pressure information is presented in Figure 2.9. It is seen that a deviation from the normal trend occurs at the point marked *Departure from trend line*, causing the pore pressure gradient to increase from roughly 1,1/1,2 kg/l to 1,4/1,5 kg/l. 1 kg/l is equal to 1 000 kg/m^3.

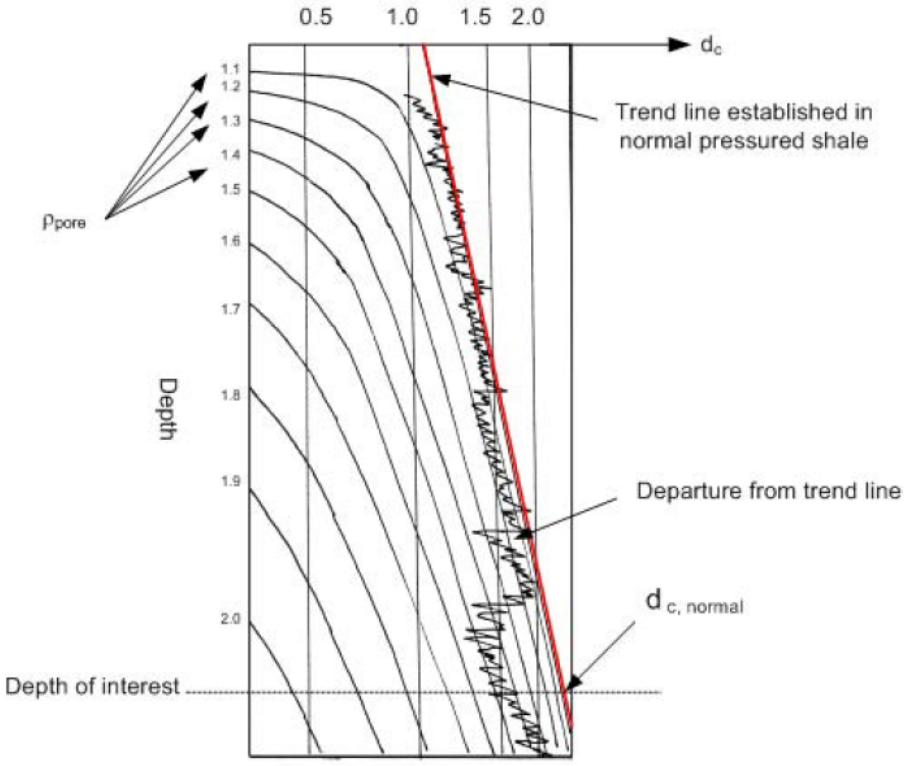

Figure 2.9: Relationship between the d_c-exponent and pore pressure [16].

Mud properties

An early warning of increased pore pressure can be detected by measuring the gas content and temperature of the returning mud. A permeable, abnormally pressured, gas-bearing formation can be detected if the overlying sealing rocks contains gas and this is measured in the returning drilling fluid. The gas has been present in the underground for millions of years, making it reasonable to assume that a small portion of it has migrated up into the overlying low-permeable rocks. When the overlying rocks are drilled through, gas will follow the returning drilling fluid and, if measured, function as an early warning of the abnormally pressured gas-bearing formation located beneath [16].

Regarding the measured mud temperature, it has been found that low compaction (which is the case for abnormally pressured zones as the trapped fluids hinders further compaction of the sediment) implies low thermal conductivity. Meaning that an abnormally pressured zone will function as an isolator, causing the temperature in the overlying layers to be lower than anticipated as illustrated in Figure 2.10. This implies that if the measured mud temperature is lower than expected, an abnormally pressured zone may be encountered [16].

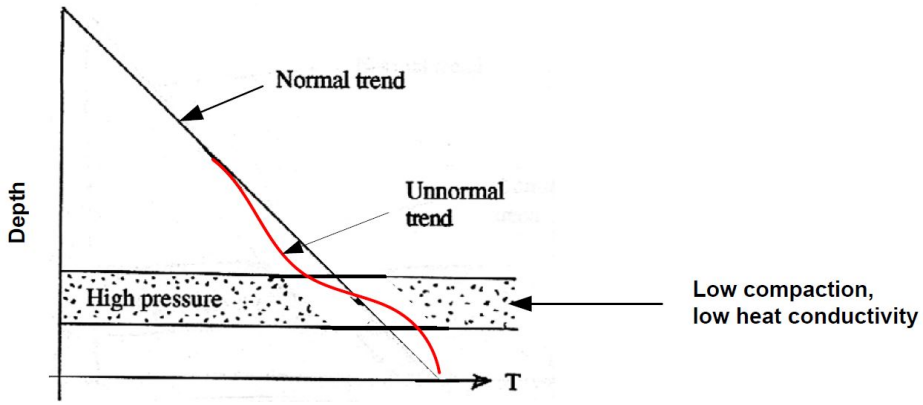

Figure 2.10: Relationship between pore pressure and temperature [16].

2.4 Borehole failure

Borehole failure is a result of rock deformation and rock failure around the borehole, caused by the alterations inflicted on the underground during drilling. The consequence of borehole failure is normally a deformed borehole of some kind. However, it is important to note that such deformations not necessarily are dramatic from a drilling point of view. The term borehole failure is therefore not synonymous with a lost well [11].

When an underground formation is penetrated during drilling, it involves that rocks are crushed, removed and replaced by drilling fluid. Hence, after drilling, the borehole wall is only supported by the pressure exerted from the drilling fluid. This pressure is, however, rarely equal to the in-situ formation pore pressure. According to Terzaghi's principle does this entail that the effective stress regime acting on the borehole has been altered. When a rock is exposed to a certain amount of force/stress, it will experience deformation and eventually failure of some kind. Rock failure induced during drilling is either a result of shear or tensile failure. Shear failure occur at low well pressures, resulting in breakouts in the borehole wall, and tensile failure occur at high well pressures, resulting in fractures. An illustration of the direction for these two failure principles in a vertical borehole are presented in Figure 2.11. Since tensile failure occurs at high well pressure and shear failure at low pressure, these two failure modes are normally not observed at the same depth. This may, however, be the case if the wellbore has been subjected to large variations in pressure [10, 11, 15].

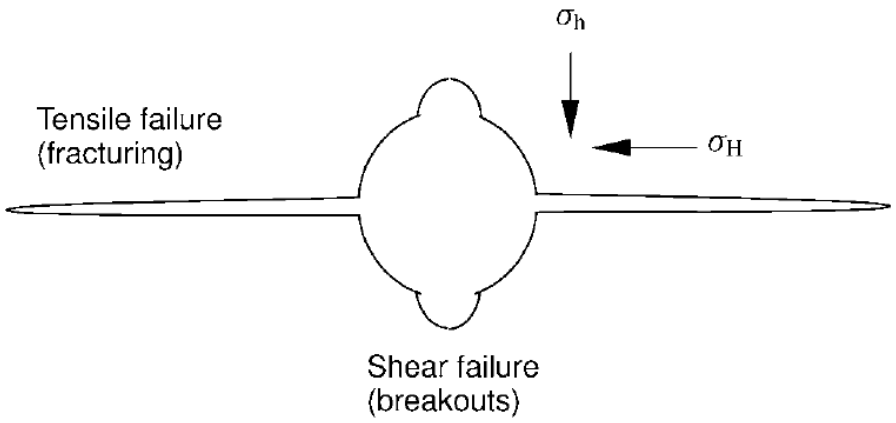

Figure 2.11: Illustration of shear and tensile failure around a vertical borehole [11].

2.4.1 Collapse pressure

A collapsed borehole occurs if the formation near the borehole fails mechanically due to shear failure (occasionally caused by tensile failure), generally leading to a reduced borehole diameter. The collapse pressure is then equal to the pressure at which shear failure will occur. A rock will suffer shear failure if the shear stress along a plane is sufficiently high, resulting in the development of a fault zone. Several methods exist for estimation of shear failure, such as the Tresca criterion, the Mohr-Coulomb criterion, the Griffith criterion and the Hoek-Brown criterion. The most general and frequently used criterion is the Mohr-Coulomb criterion, which for shear failure is expressed as [11, 15]:

$$\sigma_1' = C_0 + \sigma_3' tan^2\beta \tag{2.12}$$

where σ_1' and σ_3' are respectively the maximum and minimum effective stress. If the right hand side of the equation is equal to or larger than the maximum effective stress, then shear failure will occur, potentially leading to a collapsed borehole. When referring to the normal underground stress environment, the Mohr-Coulomb criterion becomes:

$$\sigma_v' = C_0 + \sigma_h' \cdot tan^2\beta \tag{2.13}$$

where C_0 is the *uniaxial compressive strength*, which is the maximum stress a material is able to withstand without loosing its strength, and β is the failure angle caused by shear failure. Laboratory measurements of sand and sandstone has shown that the failure angle typically lies in the range of $55^0 - 70^0$. A plot referred to as *Mohr's circle* is often used to graphically illustrate the Mohr-Coulomb criterion, illustrated in Figure 2.12. The increasing linear line seen on the figure is the failure line. If a rock holds combinations of τ and σ' located at or above this line, then shear failure will occur for these values. The parameter S_0 seen on the figure is the *inherent shear strength* (also known as *cohesion*) of the material whereas the parameters φ (*angle of internal friction*) defines the angle of the failure line. The following relationship applies between φ and β [11, 15].

$$\varphi + \frac{\pi}{2} = 2\beta \tag{2.14}$$

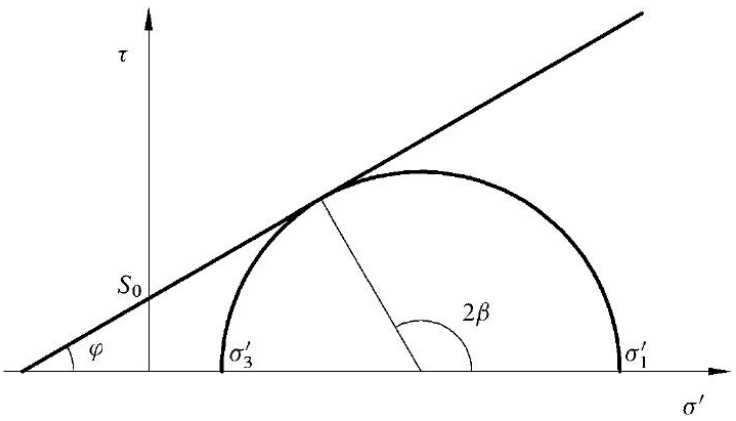

Figure 2.12: The Mohr-Coulomb criterion illustrated in $\tau - \sigma'$ space, the increasing linear line is known as the failure line [11].

Fjær et.al. 2008 argues that the risk of mechanical hole collapse increases if:

- The formation strength is low
- The failure angle is low, often encountered in shale where β is 50^o - 55^o.
- The pore pressure is high, often the case in the cap rock above the reservoir.

2.4.2 Fracture pressure

A rock will suffer tensile failure if the wellbore pressure exceeds the sum of the minimum horizontal stress and the tensile strength of the rock, T_0. In drilling language, the pressure at which tensile failure occur is commonly referred to as the fracture pressure, which is equal to [11, 16]:

$$P_{frac} = \sigma_h + T_0 \tag{2.15}$$

A rocks tensile strength defines the maximum tension it can withstand before it parts. "*Most sedimentary rocks have a rather low tensile strength, typically only a few MPa or less. In fact, it is a standard approximation for several applications that the tensile strength is zero* [11]." This is typically the case if the formation contains natural fractures. A good practice during drilling is therefore to keep the wellbore pressure below the minimum horizontal stress to avoid fracturing the formation.[2] The fracture pressure can then be considered as approximately equal to the minimum horizontal stress [11, 15]:

$$P_{frac} \approx \sigma_h \tag{2.16}$$

In 1982, *Breckels and van Eekelen* published various empirical relationships between minimum horizontal stress and vertical depth, derived for the U.S Gulf Coast, Venezuela and Brunei. The relationships are based on empirical data, gathered from hydraulic fracture operations. In addition to depth, the derived relationships also takes abnormal pore pressure into account. Breckels and van Eekelen concluded that the relationship derived for the U.S Gulf Coast also suits other normally pressured and tectonically relaxed areas such as the North Sea [11, 19]:

$$\sigma_h = 0.0053D^{1.145} + 0,46(P_f - P_{normal}) \qquad (Depth < 3500\ m) \tag{2.17}$$

$$\sigma_h = 0.0264D - 31,7 + 0,46(P_f - P_{normal}) \qquad (Depth > 3500\ m) \tag{2.18}$$

[2] John-Morten Godhavn, personal communication (e-mail), 14.01.2014.

where D is the vertical depth in meters, P_f is the formation-pore pressure (can be predicted with Eaton's equation) in MPa (megapascal), P_{normal} is the normal formation-pore pressure (corresponding to a gradient of 10.5 MPa/km) and σ_h is the minimum horizontal stress in MPa. The relationships presented above were developed at zero or shallow water depths. According to *Fjær et.al. 2008*, it is experienced that these relationships provide fairly good estimates for depths down to about 3 500 meters and in water depths of up to 300 meters. If the water depth is above 300 meter, predictions of σ_h with these relationships should be avoided [11].

It is quite difficult to determine the fracture pressure accurately prior to drilling, especially if little or no information is available from previous wells in the area. The relationships presented by *Breckels and van Eekelen* may provide reasonable estimates, but should always be correlated and/or calibrated against known test data and fracture tests (discussed below) performed during drilling [11].

2.4.3 Fracture tests

The only fully reliable method for accurate determination of the minimum horizontal stress is achieved by pressurizing the formation until it fractures, and then record the pressure at which the fracture closes. Several downhole test methods utilize the idea of applying pressure on the formation, such as the Leak-Off Test (LOT), the Extended Leak-Off Test (XLOT) and the Formation Integrity Test (FIT). Of which, the XLOT is the only one that enables the minimum horizontal stress to be determined accurately [11].

The purpose of a LOT is to determine the maximum well pressure that can be applied in the next section, without fracturing the formation and experience loss of drilling fluid. After a casing has been run and cemented in place, the casing shoe is drilled out and a few meters of the new formation is penetrated. Pressure is then applied from the surface, performed by pumping fluid with a constant rate, until fluids begin to enter the formation below the casing shoe. As pumping is performed with a constant rate, loss of fluid is detected when the pressure response begins to deviate from the expected linear line. This point is seen as the *Leak-Off Pressure* (LOP) in Figure 2.13. A LOT is normally ceased shortly after this deviation is encountered and the LOP is used as the upper design value for the mud density in the next section [11].

However, the LOP is not necessarily directly related to the minimum horizontal stress. If the purpose is to determine this stress, then pumping must be continued beyond the LOP and until a stable fracture propagation pressure (FPP) is achieved. This has led to the so-called *Extended Leak-Off Test*. When a stable FPP is obtained, pumping is ceased and the

minimum horizontal stress is determined by monitoring the shut-in phase and the flowback phase of the fluid, locating the Fracture Closure Pressure (FCP) $\sim \sigma_h$. An illustration of an XLOT test is presented in Figure 2.13 [11].

When several wells has been drilled in a field, it is quite common to perform Formation Integrity Tests rather than Leak-Off Tests. A FIT is conducted by increasing the wellbore pressure up to a predefined level which is considered sufficiently high for drilling of the next section. This implies that this test normally ends in the linear part prior to reaching the LOP. A FIT can therefore not be used for stress determination, but it provides very useful information with respect to the upper well pressure that can be applied in the next section [11].

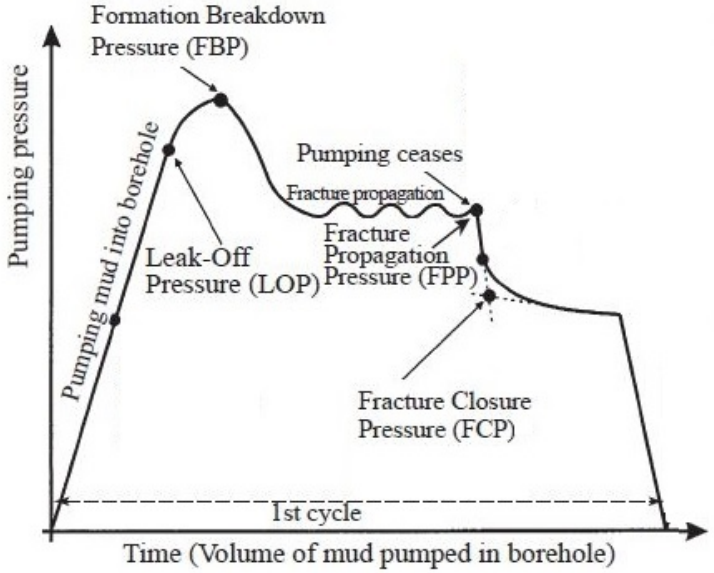

Figure 2.13: Illustration of an Extended Leak-Off Test. *Modified after reference* [11].

Chapter 3

Deepwater drilling

When drilling is conducted in deep waters rather than in shallow waters, a markedly change in conditions is experienced. Not only does the water depth increase, but the sea bottom and geology becomes more complex as well. On the continental shelf in shallow water depths, there is generally a continuous deposition of sand and shale. As the water depth increases beyond the continental shelves, the depositional environment changes and can be largely dominated by turbidites. Turbidites are sediments that are deposited episodically during underwater avalanches. This can create thick layers of very well sorted sand, yielding attractive reservoir properties such as high porosity and high permeability. These properties make turbidites some of the best oil and gas reservoirs with high production rates [20].

In the early 1990s, the petroleum industry discovered that huge amounts of hydrocarbons are located beyond the continental shelves. In pursuit of these resources, drilling contractors and engineers faced technological challenges unlike any previously experienced. "*They took on an operating environment nearly as foreign to them as deep space had been to aeronautical engineers in the 1950s* [4]." Due to the complexities of drilling in deep waters, developing a major deepwater oil field can cost a tremendous amount of money, greatly exceeding the cost of a shallow water development. To justify such developments from an economical point of view, highly productive reservoirs and high-productivity wells are required. This makes deepwater turbidite reservoirs an ideal target. A productive shallow water well typically produce at rates of a few thousand barrels (1 barrel of oil is equivalent to 159 litres) of oil per day. Deepwater wells however, are able to produce at rates exceeding 10 000 barrels of oil per day. The high productivity experienced in deepwater reservoirs is not only a product of favourable geology, it is also a reflection of the abnormally high pressures often encountered deep below the surface. As illustrated in Figure 3.1, the majority of the worlds proven and unproven deepwater reserves are located in North America (northern part of Gulf of Mexico), South America (Brazil) and Africa (west Africa) [4, 20].

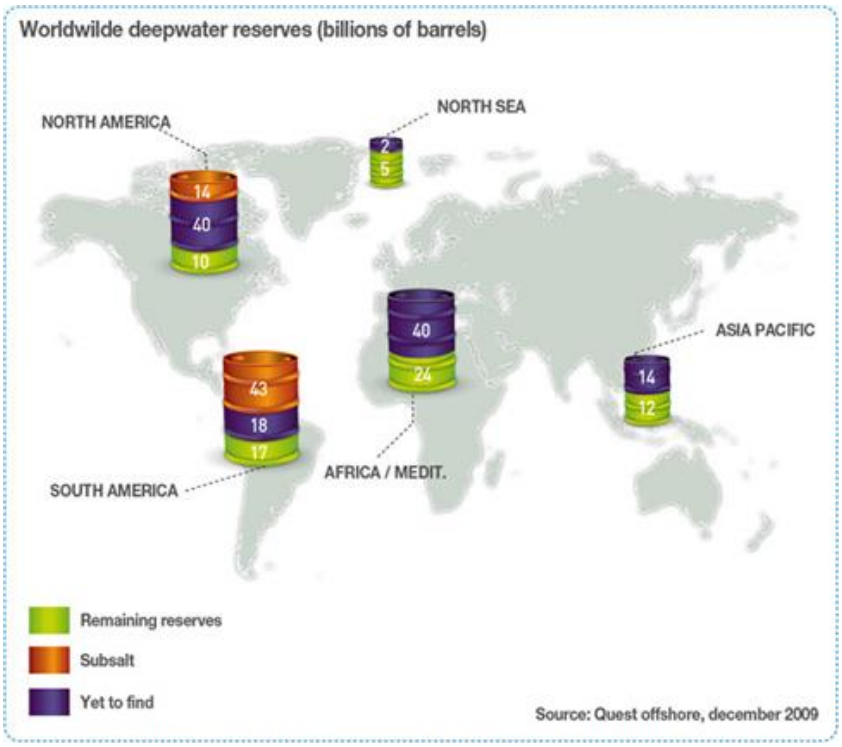

Figure 3.1: Worlds deepwater proven and unproven reserves as of 2009 [3].

3.1 Deepwater challenges

Drilling in deep waters are commonly considered more challenging than drilling in shallow waters due to [4]:

- Narrow mud weight windows
- High variations in temperature.
- Reservoirs occasionally located beneath vast amounts of salt.

As illustrated in Figure 3.1, a substantial amount of the deepwater reservers in respectively the Gulf of Mexico and Brazil are located beneath vast amounts of salt, referred to as *subsalt*. Before the intensified interest in drilling through salt arose, best practice among drilling engineers were considered to avoid such zones. Salt tends to move in the underground, forming an unstable rubble zone at the salts base and sides. One of the most critical concerns occur when the salt zone is exited and the rubble zone entered. This because it is highly difficult to predict the pore pressure, fracture pressure and the extent of natural fractures below the base of the salt. An overview of the average NPT experienced in shallow water and deepwater wells are presented in Table 3.1. The information presented are based on wells drilled in the Gulf of Mexico between 2004 and 2010. It is seen that

the deepwater wells targeting subsalt formations were the most time-consuming to drill, considerably associated with the high amounts of NPT induced by: kicks, lost circulation, stuck pipe and borehole instability [4, 7].

Table 3.1: Average percentage for NPT caused by kicks, lost circulation, stuck pipe and borehole instability for shallow and deepwater wells [7].

Cause of NPT	263 non-subsalt wells WD < 600ft (180m)	99 non-subsalt wells WD > 3000ft (910m)	65 subsalt wells WD > 3000ft (910m)
	% of total drill time	% of total drill time	% of total drill time
Kick	1,2 %	0,8 %	1,9 %
Lost circulation	2,3 %	2,0 %	2,4 %
Stuck pipe	2,2 %	0,7 %	2,9 %
Borehole instability	0,7 %	0,9 %	2,9 %
Other	5,6 %	12,6 %	19,9 %
Total NPT	**12,0** %	**17,0** %	**30,0** %
Average days to drill	35 days	54 days	97 days

3.1.1 Narrow mud weight window

When drilling is conducted below deep water depths, the high column of water above the seabed causes both the collapse and fracture pressure gradients to be reduced. As pointed out in Section 2.1.1, it is customary to convert pressure values at a specific depth to density values. When a wellbore is drilled offshore, this specific depth is given by the sum of the water depth, D_w, and the depth measured from the seabed, $D_{formation}$, which yields the following expression:

$$EMW = \frac{Pressure}{g \cdot (D_{formation} + D_w)} \tag{3.1}$$

The pressure at which a formation will suffer failure, either collapse or fracturing, is given by the sum of the corresponding failure pressure in absence of water, P_i, and the hydrostatic head of water, P_{water}. In terms of EMW this yields [11]:

$$EMW_i = \frac{P_i + P_{water}}{g \cdot (D_{formation} + D_w)} \tag{3.2}$$

where the subscript i refers to the condition at which either collapse or fracturing occur. As previously discussed, the pore pressure gradient is determined by the overlying hydrostatic head of fluid (provided normal pressure conditions), and is therefore not affected by increasing water depth. At the seabed ($D_{formation}$=0), this implies that the mud weight window is non-existent as the fracture, collapse and pore pressure gradients are given by

the water density. At shallow depths below the seabed, the effect of water depth still dominates. This causes the collapse and fracture pressure gradients to be lower than they would have been if drilling took place onshore, or in shallow water for that matter. The effect water depth has on the mud weight window is illustrated in Figure 3.2. Reaching target depth under such conditions, with the technology available in the early days of deepwater drilling, often required a high amount of casing stings to be run. This often resulted in a very small production string diameter, and hence, the produced volumes were generally too small to be justified from an economical point of view. As of today, new drilling techniques and approaches has been developed, aiming to overcome the problems experienced when drilling in narrow deepwater mud weight windows. This is further discussed in Chapter 4 [4, 11].

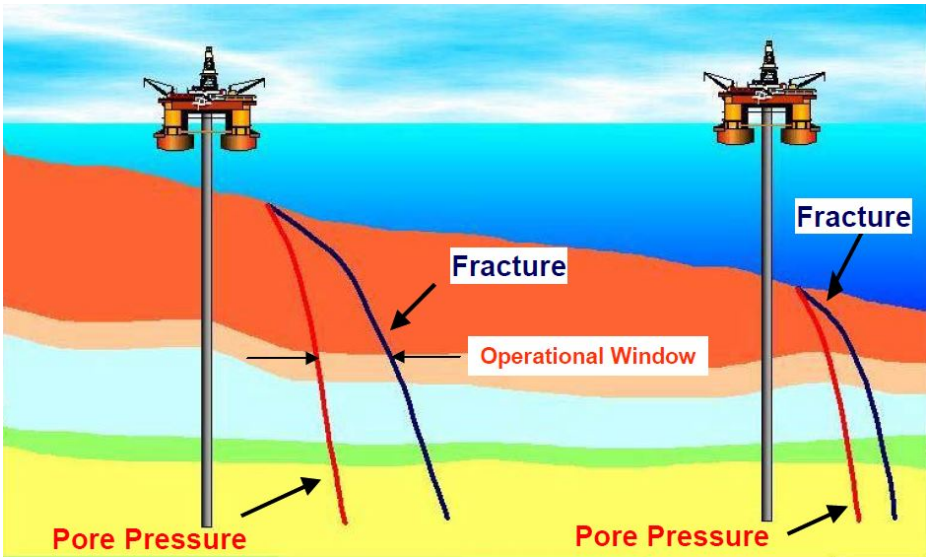

Figure 3.2: Mud weight window in shallow water compared to deep water [21].

3.1.2 Temperature variations

Drilling and completion fluids used in deepwater drilling are exposed to a roller coaster of temperature variations. In pursuit of fluids able to handle such conditions, the oil industry chemistry has been pushed to its limit. The fluids experiences everything from surface temperature at the rig, near-freezing conditions at the seabed, and reservoir temperature at target depth. In time, new drilling and completion fluids has been developed which are able to operate under such conditions [4].

Similarly, produced reservoir fluids are also exposed to these extreme temperature variations. Reservoir fluid flows up to the wellhead, which is bathed in freezing waters, and is

further transported through several kilometres of ocean-bottom flowlines. This may create flow-assurance problems, especially if the production suddenly stops and the fluids are cooled down to freezing conditions. When gas and water are mixed at a relatively high pressure and low temperature, gas hydrates may form, illustrated in Figure 3.3. Gas hydrates are solid ice-like structures containing gas molecules. This may potentially cause subsea equipment and/or pipes to become clogged and cause flow-assurance problems. Such problems can be avoided through heated flowlines. In the event of planned stop in production, antifreeze liquid can be injected into the pipeline [4, 14].

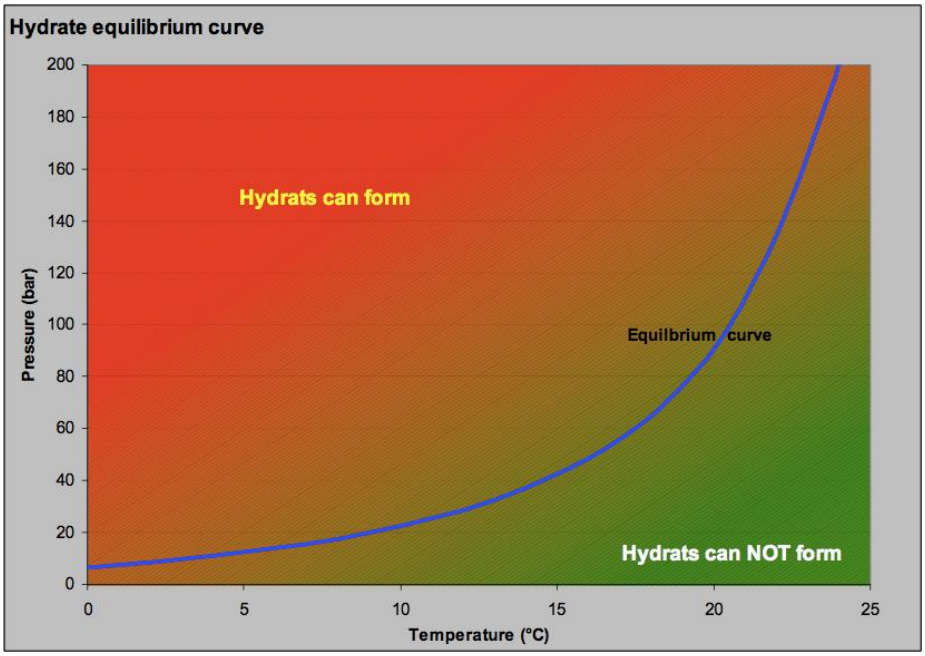

Figure 3.3: Gas hydrate phase diagram [14].

3.1.3 Drilling through vast layers of salt

The task of drilling into these deepwater reservoirs became even more daunting when it was discovered that they are often buried beneath vast layers of salt. As illustrated in Figure 3.4, deepwater salt formations are present in areas targeting deepwater reservoirs such as the Gulf of Mexico, Brazil and West Africa [4].

From a conventional point of view, drilling through salt is considered a risky business, mainly due to its unique characteristics. As opposed to other solid materials, salt remains a relatively low density even after burial. This entails that salt sheets tend to be less dense than formations located above and below. If the overlying sediments provide little resistance against salt migration, then salt rises. This movement generates an unstable

Figure 3.4: Potential exploration targets buried beneath vast amounts of salt (marked white) [4].

rubble zone below and at the sides of the salt, which is difficult to model. When salt is drilled through, one of the most critical concerns occur when the salt is exited and the rubble zone entered. It is highly difficult to predict the pore pressure, fracture pressure and the extent of natural fractures below the salt, making pressure control a critical issue when exiting the salt. When seismic waves encounter salt, they travel with a higher velocity than in surrounding non-salt formations. Surface seismic surveys have therefore historically provided only poor images below or near a salt structure. This leaves considerable margin for error in estimating the properties of the salt itself and the formations located beneath. Therefore, extreme care must be taken when exiting the salt layer. The mud pit volume must be continuously checked to monitor for gains or losses. A gain indicates a kick whereas losses indicate lost circulation. After the base of the salt has been breached, drilling is continued with a low ROP and a continuous focus towards losses/kicks and borehole instability. The consequences of lost control at this point may potentially be catastrophic, including loss of wellbore [4].

Penetrating salt during drilling presents a unique challenge. Under a continuous constant stress, salt deforms significantly as a function of time. This effect is known as *creep*, and allows salt to flow into the wellbore and replace the salt that previously has been removed by the drill bit. Salt creep may occur quickly enough to cause the drill pipe to become stuck, and the situation may be so severe that the operator is forced to either sidetrack or abandon the well. For salt formations, the in-situ stresses are assumed equal in all directions and only governed by the overburden pressure. The rate at which a wellbore closes due to salt creep, increases with increasing temperature and difference between the wellbore pressure and formation stress. Chloride and sulphate salts containing water are most prone to

creep, whereas halite moves relatively slow and anhydrite and other carbonate evaporates are considered immobile [4].

In the Gulf of Mexico, where the salt composition is up to 96 % halite, creep is a less substantial problem than in other parts of the world. There has, however, been incidents of casing collapse in a number of wells drilled in the Gulf of Mexico. As illustrated in Figure 3.5, movement of salt can lead to severe casing displacement. Best practice to avoid such situations include under-reaming (make a wellbore larger than its original drilled size), proper drilling fluid composition and cementing particles that improve stress distribution [4].

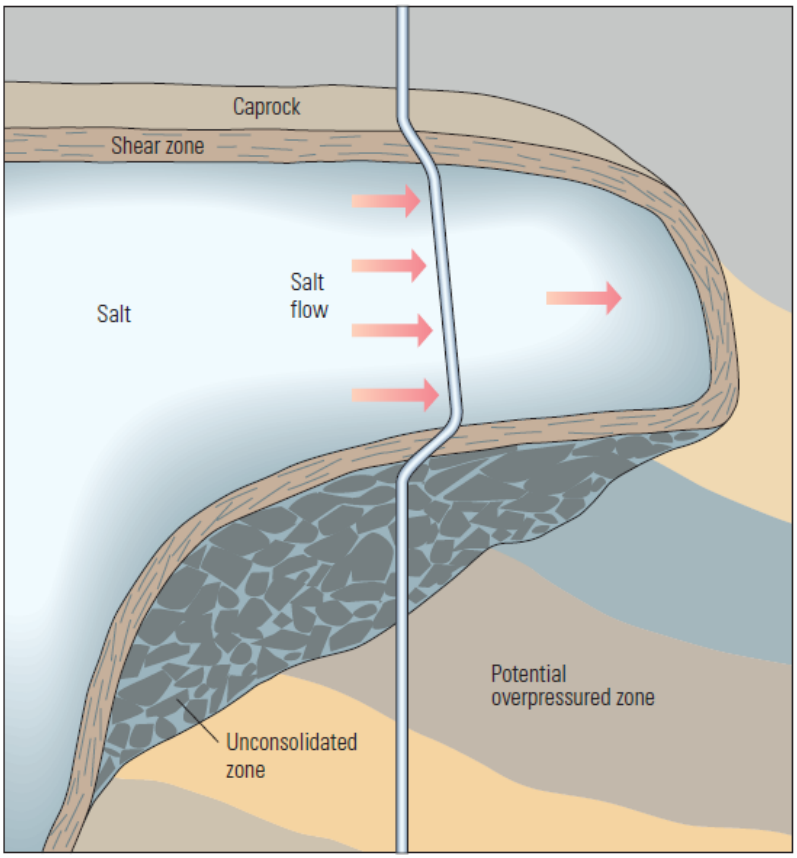

Figure 3.5: Casing displacement induced by salt movement [4].

The unique characteristics of salt does, however, offer certain advantages. A wide mud weight window is often experienced when drilling through salt, which allows long sections to be drilled between casing points. In addition, the low permeability of salt provides a reliable hydrocarbon trapping mechanism. Hence, problems experienced in permeable formations, such as kicks, are virtually non-existent within the salt itself. There may, however, be permeable formations within the salt structure of higher or lower pore pressure than the

surrounding salt. As a consequence, lost circulation or kick incidents may be experience if such formations are encountered [4].

3.2 Deepwater concerns

If a blowout should occur when working deep below the surface, a myriad of problems are experienced. Containment is a difficult task, as was experienced during the *Deepwater Horizon accident* (further discussed below). Up to this accident, little attention was devoted towards containment in the case of a blowout, mainly because it was considered so unlikely to occur. The biggest risk is probably what made deepwater drilling so attractive in the first place. The high pressures and associated high flow rates becomes the enemy in the case of a blowout, as this will result in huge uncontrollable amounts of oil and gas released to the environment [2].

Equipment placed in the deep offshore are exposed to higher pressures and lower temperatures than equipment placed in shallow waters or onshore. These effects in combination with powerful underwater currents put extra stress on critical subsea equipment such as the BOP. An article published in *Drilling Contractors* in 2007 describes the extreme operating conditions a deepwater subsea BOP must deal with. "*Today, a subsea BOP can be required to operate in water depths of greater than 10,000 ft* (3 048 meters)*, at pressures of up to 15,000 psi* (1 035 $\cdot 10^5$ Pa) *and even 25,000 psi* (1 724 $\cdot 10^5$ Pa)*, with internal wellbore fluid temperatures up to 400^0 F* (204^0 C) *and external immersed temperatures coming close to freezing (34^0 F)* (1^0 C) [22]." It is further said that for a single well, the subsea BOP can be placed at the seabed for roughly 45 to 90 days. However, if drilling and completion on multiple wells are required, the BOP may be placed at the seabed for more than a year. In the case of an uncontrollable flow of hydrocarbons, the BOP is relied upon to function as a last line of defence. It is the main barrier protecting human lives, equipment and the environment from an uncontrollable flow of hydrocarbons. This entails that the BOP must function flawless when it is relied upon to seal the wellbore [2, 22].

3.2.1 Deepwater Horizon accident

On the evening of April 20, 2010, a catastrophic well control incident occurred in the deep waters of the Central Gulf of Mexico, known as the *Deepwater Horizon accident*. At the time, Transocean's semi-submersible drilling rig *Deepwater Horizon* was, on behalf of BP and its partners, drilling the *Macondo* exploration well. The well had penetrated a hydrocarbon-bearing zone, and it was decided to temporarily abandon it before completing it as a production well later. As the well was prepared for temporarily abandonment, well

control was lost and the BOP did not manage to seal the wellbore properly. This led to an uncontrollable flow of hydrocarbons up through the wellbore and onto the drilling rig. The hydrocarbons ignited and caused explosions and fire on board the rig. Eleven people lost their lives and seventeen were injured. On the April 22, after burning for roughly 36 hours, the rig sank to the seabed at approximately 5 000 feet (1 524 meters) below the surface. Hydrocarbons were discharged uncontrolled to the environment until July 15, 2010, causing an oil spill of national significance, estimated in the range of five million barrels (0,8 million m^3) [23, 24].

Figure 3.6: Deepwater Horizon accident [25].

Before April 20, it was a common belief that drilling might be safer in deep waters than in shallow waters. As deepwater rigs are working farther off the coast, it was considered that a potential leak would use longer time to reach the shore, and hence give more time to take proper action. In the aftermath of the accident, however, speculations towards the safety culture in the industry began. The National Commission (2011) on the accident found [2, 24]:

"*The immediate causes of the Maconde well blowout can be traced to a series of identifiable mistakes made by BP, Halliburton, and Transocean that reveal systematic failures in risk management that they place in doubt the safety culture of the entire industry* [24]."

On May 27, 2010, the President of the United States, Barack Obama, announced a wide-ranging moratorium (postpone) on deepwater drilling in the Gulf of Mexico. After this

announcement, Secretary of the Interior, Ken Salazar issued an order on May 30, 2010 to postpone all new deepwater wells (in this context, deepwater is considered deeper than 150 meters) for six months. Production on existing deepwater wells was not affected by this order. The purpose of this moratorium was to postpone deepwater drilling until the risk of these operations were better understood and appropriate steps to remedy them could be identified and undertaken. On October 12, 2010 the moratorium was ended, allowing new wells to be drilled if they followed the new safety rules. The drilling rigs must for instance certify they have a working BOP and standards for well cementing. In addition, containment resources must be available in the event of a blowout [26, 27].

The legacy after the Deepwater Horizon accident stays a strong reminder of the consequences and potential risks of deepwater drilling. An article published in the Forbes, on April 29, 2014, has the following predictions about the future for deepwater drilling: "*Nevertheless, in the absence of further major debacles in the near future, deepwater drilling will continue apace, driven in large part by continuing increases in global demand for energy that may only intensify in coming years if emerging markets continue to grow robustly* [28]."

Chapter 4

Managed pressure drilling

4.1 Drilling techniques

The introduction of weighted drilling fluid, and thus overbalanced drilling in 1901, was the first step towards today's sophisticated and advanced drilling techniques. Over the last century, the search for oil and gas has gradually moved into ever-more demanding environments. This has led to the development of new and safe drilling techniques that are able to cope with these situations. As of today, the various drilling techniques are commonly differentiated between [12, 29]:

- Conventional drilling
- Underbalanced drilling (UBD)
- Managed Pressure drilling (MPD)

While conventional drilling is performed with an "open-to-the-atmosphere" drilling fluid circulation system, both UBD and MPD are performed with a closed and usually pressurized circulation system. As illustrated in Figure 4.1, one of the main differences between these drilling techniques lies in the drilling operating pressures of the various techniques. During an underbalanced operation, the annular pressure is maintained below formation-pore pressure. Conversely, in conventional drilling the annular pressure is maintained far above the pore pressure. Whilst in MPD, the annular pressure is maintained at, or just above the formation pore pressure [30].

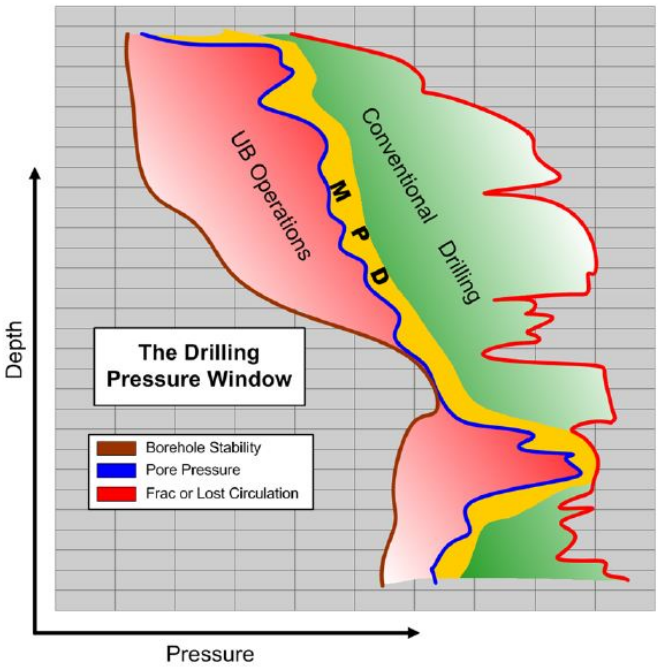

Figure 4.1: Operational window for the different drilling techniques [29].

4.1.1 Conventional Drilling

Conventional drilling is performed with a bottom-hole wellbore pressure, BHP, higher than the formation-pore pressure. This scenario is referred to as overbalanced drilling:

$$BHP > P_f \tag{4.1}$$

During a drilling operation, the mud pumps are, for various reasons, turned off and on frequently, for instance during tripping and connection operations. When circulation of drilling fluid and cuttings are ceased, static wellbore conditions apply, whereas when circulation occur, dynamic wellbore conditions apply. The static BHP during conventional drilling is solely determined by the hydrostatic head of drilling fluid in the wellbore (Figure 4.2), expressed as:

$$BHP_{stat} = P_{hydrostatic} = \rho_m \cdot g \cdot TVD \tag{4.2}$$

where BHP_{stat} is the static bottom hole pressure, ρ_m is the drilling fluid density, g is the gravity constant (9,81m/s^2) and TVD is the total vertical depth. During dynamic conditions, the term "equivalent circulating density" (ECD) is commonly used to describe the actual density exerted on the formation. The dynamic bottom hole pressure, BHP_{dyn}, is then expressed as:

$$BHP_{dyn} = ECD \cdot g \cdot TVD \tag{4.3}$$

According to the drilling lexicon provided by the IADC is ECD defined as: "*The sum of pressure exerted by hydrostatic head of fluid, drilled solids, and friction pressure losses in the annulus divided by depth of interest* [31]." Thus, ECD can be expressed as:

$$ECD = \rho_m + \frac{P_{AF} + P_C}{g \cdot TVD} \tag{4.4}$$

where P_{AF} is the annular friction pressure, and P_C is the pressure exerted by cuttings. As illustrated by Figures 4.2 and 4.3, the wellbore pressure increases as circulation of drilling fluid and transport of cuttings occur, thus $BHP_{dyn} > BHP_{stat}$. It is important to consider both the static and the dynamic wellbore pressures during the planning- and drilling phase of a well. The static wellbore pressure must be sufficient to keep the wellbore pressure above the formation-pore pressure, whereas the dynamic wellbore pressure must stay below the formation-fracture pressure. This may pose problems in narrow mud weight windows, and thus cause losses/influx to occur which eventually may trigger the need for setting casing/liner earlier than planned.

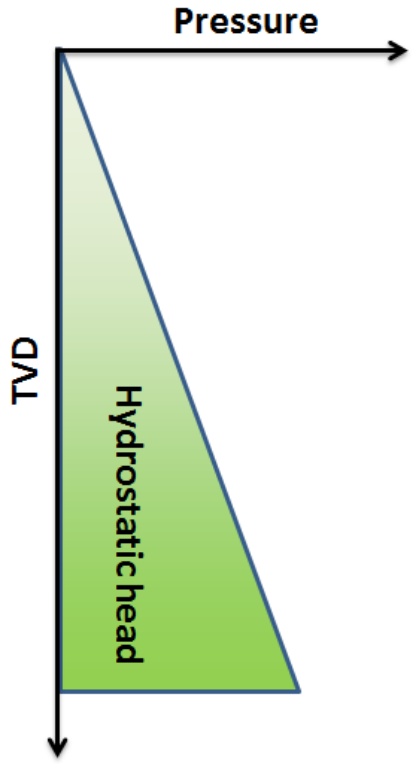

Figure 4.2: Static wellbore pressure during conventional drilling

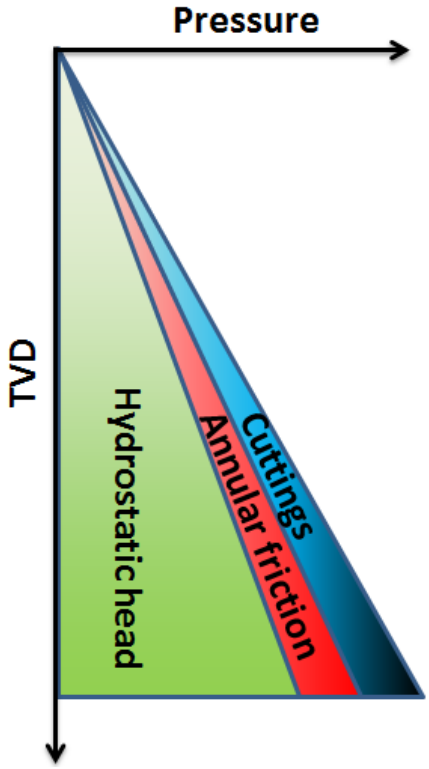

Figure 4.3: Dynamic wellbore pressure during conventional drilling

4.1.2 Underbalanced Drilling

Underbalanced drilling is, as opposed to conventional drilling, successfully achieved when the effective circulating borehole pressure is less than the formation-pore pressure, thus [32]:

$$BHP < P_f \tag{4.5}$$

This implies that an influx of formation fluid is intentionally invited into the wellbore. In order to accurately control and regulate the wellbore underbalance, and thus the amount of formation fluid influx, external back pressure is applied from the surface (further explained in Appendix A.2). The static bottom hole pressure during UBD is then expressed as [32]:

$$BHP_{stat} = \rho_m \cdot g \cdot TVD + P_{BP,stat} \tag{4.6}$$

where $P_{BP,stat}$ is the amount of back pressure applied during static conditions. When the mud pumps are turned on and circulation initiated, the bottom-hole pressure is expressed as [32]:

$$BHP_{dyn} = ECD \cdot g \cdot TVD + P_{BP,dyn} \tag{4.7}$$

where $P_{BP,dyn}$ is the amount of back pressure applied during dynamic conditions. As illustrated by Figure 4.4 and 4.5, the amount of back pressure applied during static and dynamic conditions may be regulated so that a more stable bottom-hole pressure is obtained.

If a porous fluid containing formation is drilled through underbalanced, fluids will enter the wellbore. This makes it more complicated to estimate the bottom-hole pressure during both static and dynamic conditions. Especially if the formation fluid is gas, which will displace and replace drilling fluid. This will cause the wellbore pressure to decrease as gas normally has a lower density than drilling fluid. The relatively low density of gas combined with fluid circulation, causes the gas to migrate towards the surface. As gas rises and the hydrostatic fluid pressure decreases, the gas will expand and cause even more drilling fluid to be displaced. From a conventional point of view, the situation described above is considered as a kick, that is an uncontrolled influx of formation fluid. However, during underbalanced drilling it is the intention to invite drilling fluid into the wellbore. Through the invention of back pressure, such a situation can effectively be controlled in a safe manner. If suddenly the flow of formation fluids exceeds a wanted value, the back pressure can be increased slightly, thus avoiding an uncontrollable situation [32].

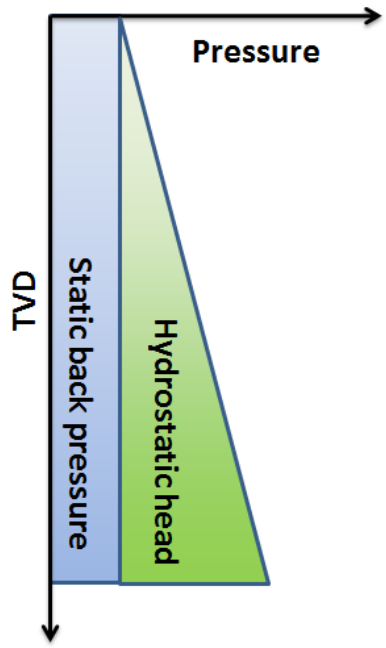

Figure 4.4: Static wellbore pressure during underbalanced drilling. *Free after reference* [32].

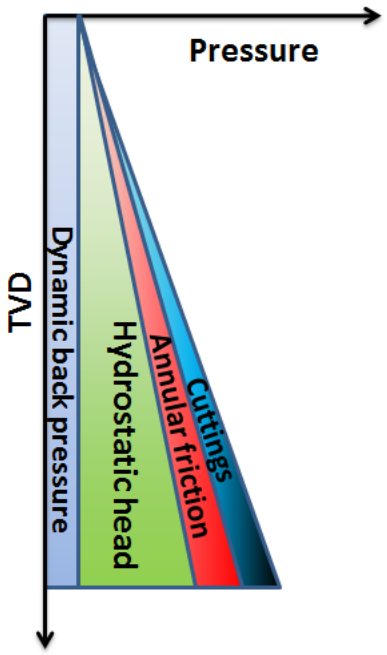

Figure 4.5: Dynamic wellbore pressure during underbalanced drilling. *Free after reference* [32].

Underbalanced drilling is normally more costly and time-consuming than conventional drilling. Despite this, underbalanced drilling has evolved to become a relatively common procedure. Mainly because an underbalanced well induces very little damage to the formation, which is especially appreciated when drilling the reservoir section. Oil/gas production is thus enhanced and the need for expensive well stimulation is eliminated. In addition, masked or subtle hydrocarbon pay zones may be discovered during underbalanced drilling (reveals itself by generating a kick) [32, 33]. There are however some disadvantages associated with UBD, such as [34, 35]:

- Increased overall production risk.
- Wellbore instability.
- Well control issues.
- Increased drill string vibration and higher torque and drag.
- Problems with the MWD mud pulse signals.
- Problems related to flaring, storing or injection of the formation fluids transported to surface during drilling.

4.1.3 Managed Pressure Drilling

In 2004, the IADC defined MPD as: "*An adaptive drilling process used to precisely control the annular pressure profile throughout the wellbore* [9]." The stated objectives are to: "*Ascertain the downhole pressure environment limits and to manage the annular hydraulic pressure profile accordingly* [9]." The IADC effectively differentiates MPD from UBD by stating the following: "*It is the intention of MPD to avoid continuous influx of formation fluids to the surface. Any influx incidental to the operation will be safely contained using an appropriate process* [9]." In order to achieve this stated intention, MPD is performed with a BHP at, or slightly above the pore pressure, thus:

$$BHP \geq P_f \tag{4.8}$$

The IADC further defines MPD as [9]:

- "*MPD process employs a collection of tools and techniques which may mitigate the risks and costs associated with drilling wells that have narrow downhole environmental limits, by proactively managing the annular hydraulic pressure profile.*
- *MPD may include control of back pressure, fluid density, fluid rheology, annular fluid level, circulating friction, and hole geometry, or combinations thereof.*
- *MPD may allow faster corrective action to deal with observed pressure variations. The ability to dynamically control annular pressures facilitates drilling of what might otherwise be economically unattainable prospects.*"

The various equipment and software commonly used in an automated MPD operation is presented in Appendix A. As stated by IADC, the BHP may be, but not necessarily, adjusted and regulated through back pressure. Whether or not this is the case largely depends on the variant of MPD being used. The various MPD variants are presented and discussed in Section 4.3. The static and dynamic bottom hole pressure during MPD are thus commonly equal to Equation 4.6 and 4.7.

MPD may either be used as a contingency plan or as a primary plan during a drilling operation. These two various approaches are respectively referred to as the "Reactive approach" and the "Proactive approach" [36].

Reactive approach

"*Well is designed conventionally, but equipment is rigged up to quickly react to unexpected pressure changes in the well* [37]." This means that the reactive approach uses MPD meth-

ods and/or equipment as a contingency, in case problems should arise during conventional drilling. This approach does not fully utilize all the advantages provided by MPD, discussed in *Section 4.2* [36].

Proactive approach

"*Equipment is rigged up to actively alter the annular pressure profile, potentially extending or eliminating casing points* [37]." This means that the entire drilling operation is planned and conducted as MPD. This approach enables the wide range of tools and techniques MPD provides to be utilized, thus all the advantages provided by MPD can be exploited [36].

4.2 Advantages of MPD

MPD were primarily invented to overcome the following drilling related problems, commonly encountered in narrow mud weight windows [38]:

- Lost circulation
- Wellbore kicks
- Differential sticking
- Excessive amount of casing strings necessary to reach target depth

The overall advantages of MPD, achieved through mitigation of the aforementioned problems, are increased drillability in narrow mud weight windows, increased safety during drilling and reduced costs caused by NPT [38].

4.2.1 Lost circulation and wellbore kicks

Problems related to lost circulation and wellbore kicks can to a great extent be mitigated through MPD. If it is sensed that drilling fluid is being lost to the formation, the back pressure can quickly be reduced to bring the wellbore pressure below the formation-fracture pressure. The amount of drilling fluid actually lost and the damage exerted on the formation is then very low due to the rapid response (further described in Appendix A.6). The same principle applies if a kick is detected. The back pressure is increased to bring the wellbore pressure above the formation-pore pressure, thus quickly bringing the situation under control [38].

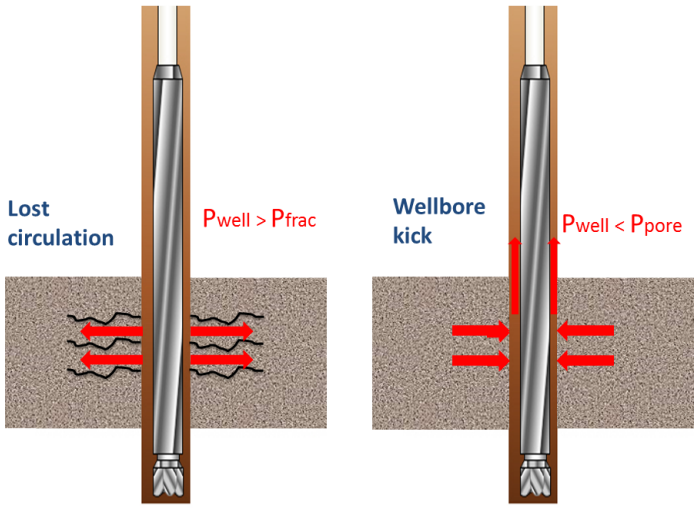

Figure 4.6: Lost circulation to the left and a wellbore kick to the right, *free after reference* [39].

4.2.2 Differential sticking

During overbalanced drilling in porous/permeable formations, a filter cake is formed along the borehole wall. This filter cake consists of cuttings and precipitated particles from the drilling fluid. The pressure gradient in the filter cake varies from wellbore pressure to pore pressure at the borehole wall. If a sufficient amount of the drill string is embedded in the filter cake, movement/rotation of it becomes impossible. This situation is referred to as a differentially stuck pipe, illustrated in Figure 4.7. Differential sticking is the most frequent stuck pipe cause, and thus a great contributor of NPT. As the wellbore overbalance is kept very low during MPD, the occurrence of differential sticking is greatly reduced with this drilling technique [30].

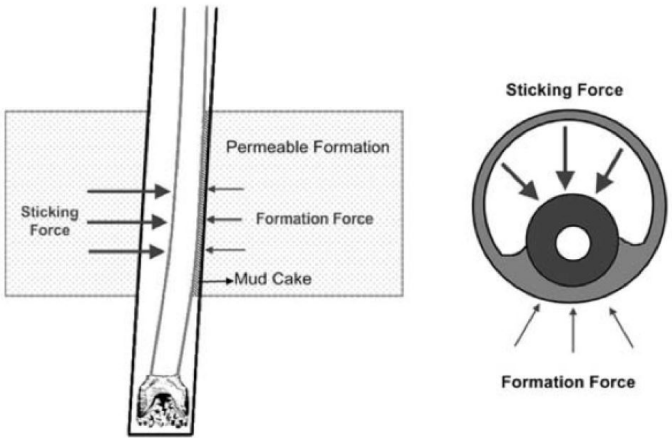

Figure 4.7: Illustration of differential sticking [38].

4.2.3 Reducing casing strings

A problem encountered in narrow mud weight windows are the excessive amounts of casing strings sometimes required to reach target depth. The two MPD variants "Constant Bottom-Hole Pressure" and "Dual Gradient Drilling" offers manipulation and real-time adjustment of the bottom hole pressure. This enables the sections to be drilled deeper and longer within the mud weight window. Ultimately, this extends and reduces the amount of casing strings required to reach the desired depth. These two drilling techniques are further explained in respectively Sections 4.3.1 and 4.3.3 [30, 38].

4.3 MPD variations

Several variations of MPD has been developed in recent time, with the aim towards precise control of the annular pressure profile. The following four variants are commonly considered as the main variations [40]:

- Constant Bottom-Hole Pressure (CBHP).
- Pressurized Mud-Cap Drilling (PMCD).
- Dual Gradient Drilling (DGD).
- Returns-Flow-Control (RFC).
  - Alternatively called the health, safety and environmental (HSE) variant.

4.3.1 Constant Bottom-Hole Pressure

Generally, the MPD variant known as CBHP, refers to a process that enables the annular pressure during drilling to remain more or less constant at a predefined depth. As discussed in Section 4.1.1, the wellbore pressure during conventional drilling is frequently fluctuating between dynamic and static conditions. When drilling is conducted in a narrow mud weight window, this inconsistency in wellbore pressure may lead to problems. Sudden pressure fluctuations may be sufficient to "move" the wellbore pressure out of the mud weight window, thus potentially causing lost circulation or a kick to occur. A situation where mud circulation "pushes" the wellbore pressure out of the mud weight window is illustrated in Figure 4.8 [10].

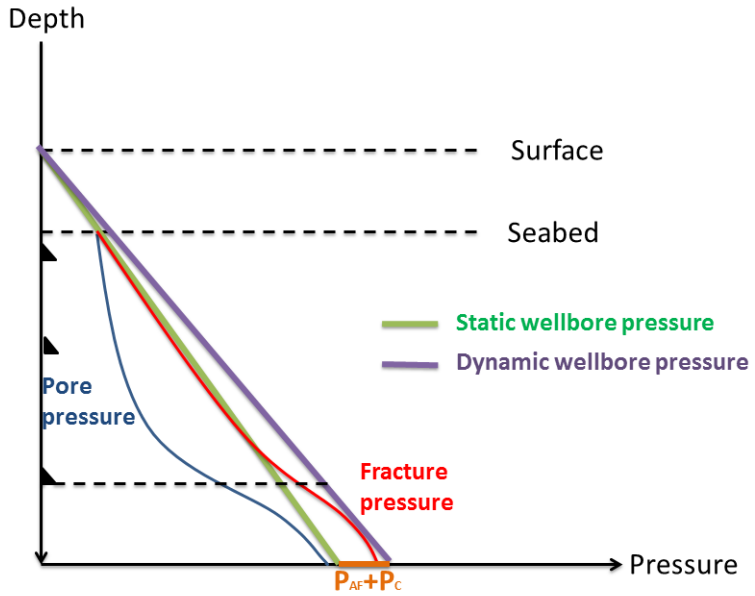

Figure 4.8: Downhole pressure gradients during conventional drilling. *Free after reference* [10].

The CBHP variant has been developed to mitigate the aforementioned problems with fluctuating wellbore pressure. A low density mud combined with annular back pressure enables high flexibility and quick response to sudden underground pressure changes. During static conditions, the BHP is expressed as:

$$BHP_{stat} = \rho_m \cdot g \cdot TVD + P_{BP,stat} \tag{4.9}$$

whereas the dynamic BHP is:

$$BHP_{dyn} = ECD \cdot g \cdot TVD + P_{BP,dyn} \tag{4.10}$$

The intention of this method is as mentioned to enable constant annular pressure at a specific depth. This entails that at this depth, the static and dynamic wellbore pressures must be of equal magnitude:

$$BHP_{stat} = BHP_{dyn} \tag{4.11}$$

$$\Rightarrow \quad \rho_m \cdot g \cdot TVD + P_{BP,stat} = ECD \cdot g \cdot TVD + P_{BP,dyn} \tag{4.12}$$

The point of constant annular pressure are usually set at bit depth. However, under

certain conditions, it may be better to keep the annular pressure at the casing shoe depth constant. This may typically be the case if the mud weight window at this depth is very narrow whereas further down, it expands. As prevously discussed, this can be seen when subsalt formations are encountered [41]. By replacing the ECD term in Equation 4.12 with Equation 4.4 and removing the hydrostatic pressure contributions (equal during both static and dynamic conditions), the following expression is found:

$$P_{BP,stat} = P_{AF} + P_C + P_{BP,dyn} \tag{4.13}$$

As shown by Equation 4.13, it is through control of the back pressure that the BHP can be maintained at a constant value. Figure 4.9 illustrates this scenario. The equipment and software used to regulate, measure and adjust the applied back pressure are presented in Appendix A [10].

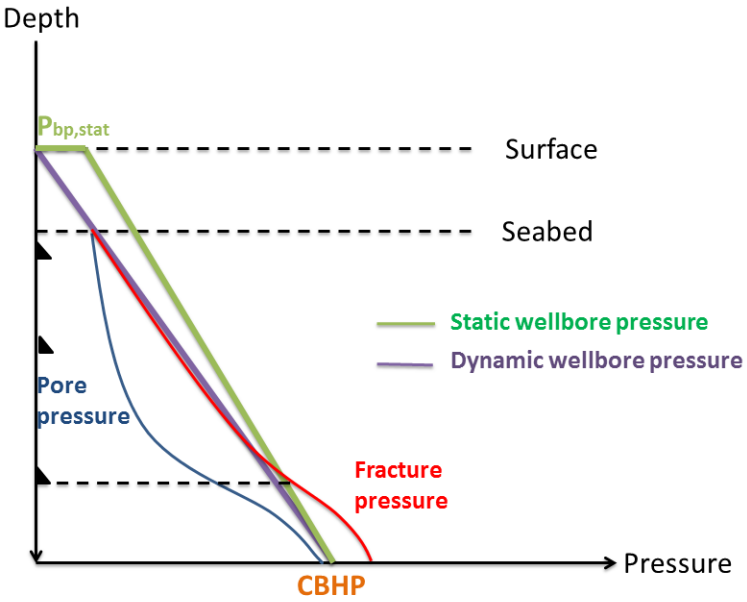

Figure 4.9: Downhole pressure gradients with the CBHP MPD variant. *Free after reference* [10].

The CBHP MPD makes it possible to drill longer sections in narrow mud weight windows, thus reducing the amount of casing strings required to reach target depth. An inherent risk that is mitigated through CBHP is wellbore instability induced by fluctuating wellbore pressure, making the wellbore more stable. A flow meter, if installed, enables quick detection and immediate reaction in case mud losses or influx occur. The flow meter compares the measured flow rate out of the wellbore against a calculated, predicted flow rate. If the two values differ with a certain amount, the choke manifold is signalled to either decrease

or increase the back pressure slightly. The situation is then quickly and automatically brought under control. See Appendix A.6 for further information about the flow meter used in MPD [10, 30]

4.3.2 Pressurized Mud-Cap Drilling (PMCD)

The PMCD method, also variously called "pressured mud cap", "light annular mud cap" or "closed-hole circulation drilling", allows drilling to continue in cases where extreme fluid losses are encountered. This method is illustrated in Figure 4.10. Such drilling challenges are most frequently encountered in highly depleted or naturally fractured carbonate formations. If such a formation is encountered with conventional methods, common problems are related to total loss of circulation, pressure control, increased NPT and a risk of never reaching target depth. The PMCD technique has a slightly different approach towards fluid losses than conventional methods. Instead of trying to avoid them they are encouraged [10, 42]. This method is by the IADC defined as:

"*A variation of Managed Pressurised Drilling (MPD), that involves drilling with no returns to surface and where an annulus fluid column, assisted by surface pressure (made possible with the use of a Rotating Control Device (RCD)), is maintained above a formation that is capable of accepting fluid and cuttings* [43]."

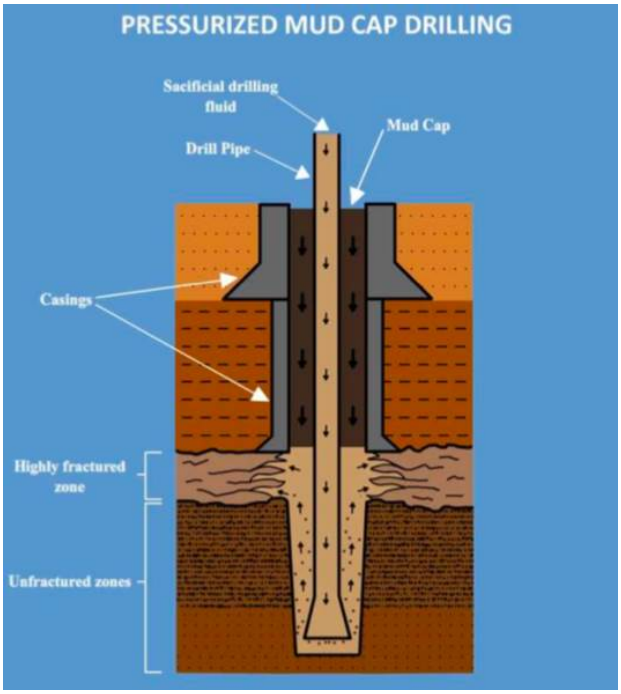

Figure 4.10: Drilling with the PMCD technique. Both cuttings and sacrificial fluid is injected into the fractured zone [30].

In order for this technique to function properly, total loss of circulation must be present. As stated by the IADC, PMCD is performed without any returns to surface. This implies that the fractured or depleted formation must accept the entire accumulated volume of drilling fluids and cuttings. If the losses are only partial or sustainable, then lost circulation material (LCM) should be added prior to utilizing the PMCD method. A well planned to be drilled with this method can either be drilled conventional, or with another MPD variant, prior to total losses are encountered [42, 44].

When total losses are faced, PMCD is enabled by filling the annulus with mud of less density than required to balance out the formation-pore pressure, referred to as *light annular mud* (LAM). The LAM forms a mud cap in the annulus which functions as an annular seal, thus preventing formation fluids from escaping up through the annulus. In order to ensure proper pressure control, back pressure is applied on top of the mud cap. During static conditions, the hydrostatic mud pressure combined with back pressure is equal to the formation-pore pressure at the depth of the fractured zone, expressed as [42, 44]:

$$BHP_{stat} = P_{mud} = \rho_{LAM} \cdot g \cdot h_{top\ frac} + P_{BP,stat} \tag{4.14}$$

where ρ_{LAM} is the light annular mud density and $h_{top\ frac}$ is the vertical depth down to the first fractured zone. Drilling is conducted through a rotating annular seal surface (see Appendix A.1), enabling back pressure to be applied in the annulus. Sacrificial drilling fluid (preferably an economical and non-damaging one, such as water) is pumped down the drill string. Drilling is now conducted through the fractured zone and sacrificial fluids and cuttings are forced into the loss zone [10].

During drilling, the annular surface pressure is read, and used as a continuous indicator of the downhole situation. If the pressure begins to increase, gas has most likely entered the annulus and is migrating upwards. When/if the annular pressure exceeds a predefined limit, LAM is bullheaded down the annulus and the gas pushed back into the loss zone. This implies that the annular pressure is raised above formation-pore pressure at the depth of the fractured zone. When the annular pressure is brought back to its original level, bullheading is ceased. This enables control over the well and avoids undesirable material like hydrogen sulfide, H_2S, from reaching the surface [10].

PMCD provides a safe and cost-efficient solution to drilling problems encountered in highly depleted- or naturally fractured formations. A typical scenario encountered in such formations are the *kick-loss cycle*. Such a cycle involves a very unstable wellbore which may prove impossible to drill to the desired depth. This problem is effectively prevented by the PMCD technique as the annulus fluid column is sealed off, thus annular pressure control is

remained even when total losses occur. "*In this manner, PMCD solves one of the most difficult challenges faced by conventional drilling methods. And in doing so, makes previously undrillable wells drillable* [45]."

4.3.3 Dual Gradient Drilling

The IADC defines DGD as: "*Two or more pressure gradients within selected well sections to manage the well pressure profile* [9]." This means that DGD relies on two, or more, fluid gradients to provide the same BHP normally provided by a single fluid gradient, illustrated in Figure 4.11 [46]. The static BHP during DGD is then expressed as:

$$BHP_{stat} = \rho_1 g h_1 + \rho_2 g h_2 \tag{4.15}$$

where ρ_1 is the upper fluid/gas density (usually sea water or air, dependent on the method being used), h_1 is the vertical height of the upper fluid/gas, ρ_2 the lower fluid density and h_2 the vertical height of the lower fluid. During dynamic conditions, the following equation applies:

$$BHP_{dyn} = \rho_1 g h_1 + \rho_2 g h_2 + P_{AF} + P_C \tag{4.16}$$

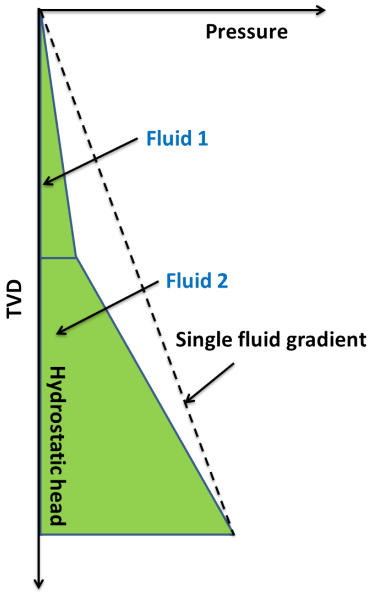

Figure 4.11: Basic static pressure profile with the DGD method.

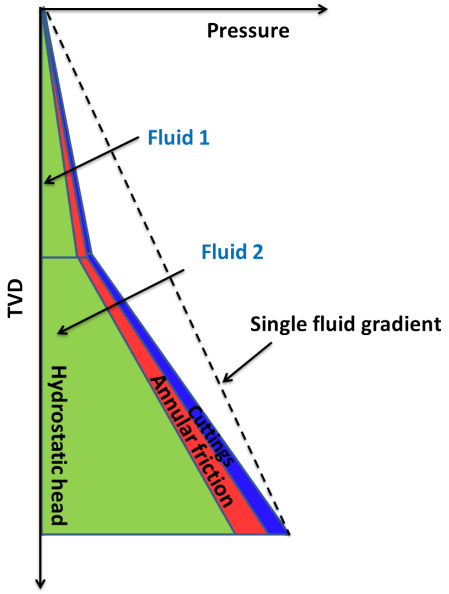

Figure 4.12: Basic dynamic pressure profile with the DGD method.

The idea of using dual gradients during drilling was first considered in the early 1960s. At that time, the goal was to eliminate the need of drilling risers, thus the concept was originally designated *Riserless Drilling*. However, the need for such a technique proved to be quite limited as the water depths contemplated were shallow, thus conventional riser-based drilling covered the needs [46].

In the early 1990's however, several deepwater discoveries were made in the Gulf of Mexico. This led to an increased interest in deepwater prospects, but the amount of rigs suited for such water depths were limited. This motivated both operator and contractor companies to find methods that would extend the capabilities of these shallow water rigs. The answer became *Riserless Drilling* as this would eliminate the need of a heavy riser and reduce the amounts of drilling fluid needed on board the rig, ultimately reducing the rig weight. This would allow smaller rigs to move into deeper waters. A number of joint venture projects and field trials were carried out, aiming towards success in utilizing this technique, but it proved to be quite challenging [46].

The research and development performed on DGD in the 1990s revealed that the technique had other, interesting qualities to offer besides reduced rig weight. This led to a slight change in motivation for developing the technique. "*Ultimately, the driver to developing dual gradient drilling became the need to manage the narrow margin between pore pressure and fracture pressure gradients in deepwater* [46]." As Figure 4.13 illustrates, DGD overcomes a significant deepwater drilling challenge. It enables a reduction in the amount of casing strings required to reach target depth [46].

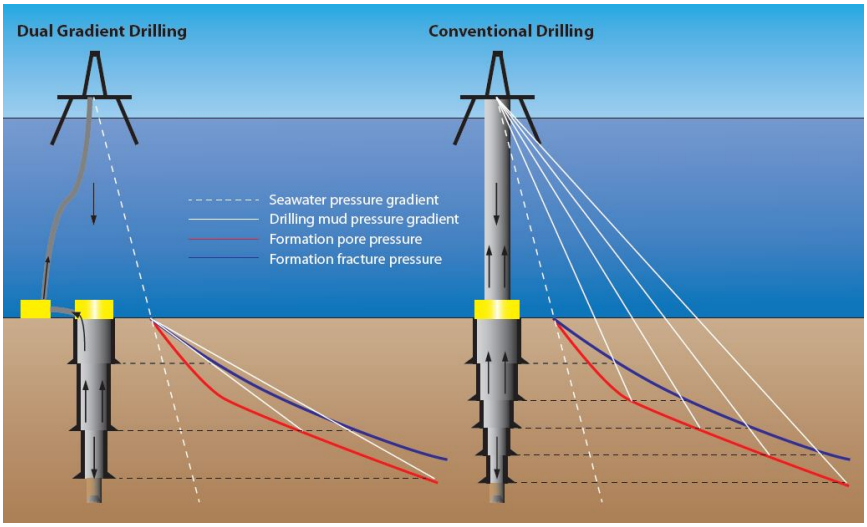

Figure 4.13: Comparison between conventional drilling and DGD in a narrow mud weight window. As seen on the figure, the amount of casing strings required to reach target depth is reduced from five to three through DGD [30].

SubSea MudLift technique

The first successful field trial utilizing the principle of dual gradients was achieved in 2001. It was the product of one of the largest and most significant joint industry projects (JIPs) so-far experienced, named the "SubSea MudLift Drilling JIP". The price tag on the project was nearly fifty million dollars and it took in total five years to finalize it. A subsea pump placed on the seabed, was used to pump the returning drilling fluid and cuttings back to the rig. As for the riser, the original motivation was to eliminate it. However, after various alternatives had been discussed, it was decided to keep it and use a marine drilling riser filled with seawater. As Figure 4.14 illustrates, the drill string is filled with drilling fluid whereas the marine riser is filled with seawater. This difference in pressure outside and inside of the drill string induces a high risk of u-tubing to occur. In an attempt to equalize the pressure difference, fluid will flow in the direction of least resistance. In this case, that will be from the drill string and into the annulus. A *Drillstring Valve* (DSV) (similar to a non return valve) was therefore installed in the *bottom-hole assembly* (BHA) with the purpose to "arrest" this u-tube effect from occurring during static conditions. In addition, a *Rotating Diverter* (similar to a RCD) was developed with the function to form a mechanical seal between the wellbore and the riser. This hinders drilling fluid, cuttings and formation fluids from entering into and mixing with the riser fluid [46].

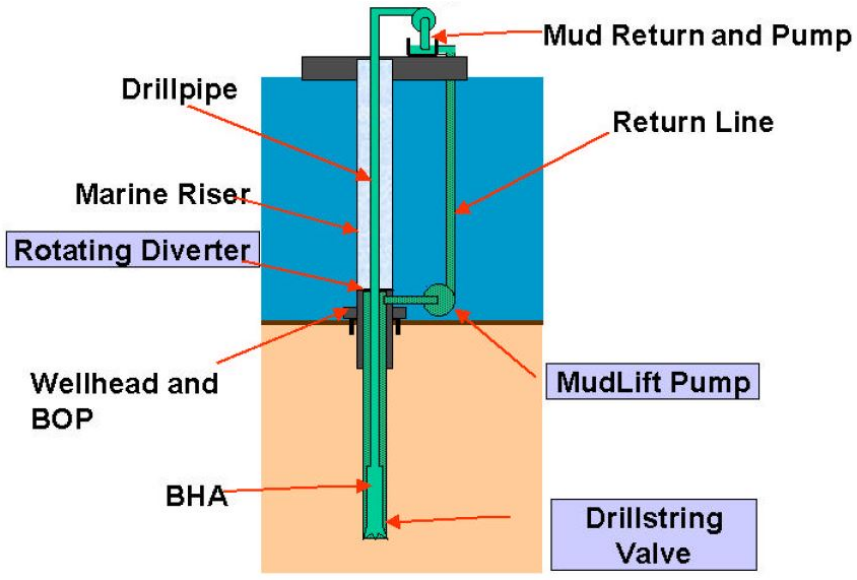

Figure 4.14: The first successful field trial utilizing the dual gradient technique.

In the fall of 2001, the SubSea MudLift technique was successfully tested in the Green Canyon Block 136 in the Gulf of Mexico, operated by Texaco. The water depth at the drill site was 910 feet (275 meters), and the field trial was deemed a big success. In 2002, all

the team members were honoured with the "Special Meritorious Awards for Engineering Innovation." "*Field trial participants put the system through its paces: circulating, drilling, tripping, running casing, cementing, and well control simulations. Aside from some instrumentation issues at the outset, the system performed as designed and even better than expected* [47]." Despite the success the Subsea MudLift technique was regarded as it never reached the goal of becoming commercially developed. This new technique did not only require extensive rig modifications, it also entailed a basic change in existing ideas and methods. At the time the industry was not ready for such a paradigm shift [46, 47].

Half a decade later, in 2006, various operator and contractor companies had gained significantly more experience with deepwater drilling. Chevron and a few other operator companies had drilled wells in waters depths over 10 000 feet (3 050 meters). The total depths of these wells lied in the range of 25 000 - 30 000 feet (7620 - 9140 meters). When drilling these deep wells, a problem encountered was the high difference between static and dynamic wellbore pressures. At total depth, the difference was often in the range of 0,5 - 1 ppg (pounds per gallen, 1 ppg = 119,8kg/m^3), making it challenging to reach target depth. This triggered several drilling engineers to reconsider the DGD concept [47].

"*Today several developmental projects are under deployment on a commercial scale, primarily in the Gulf of Mexico, the North Sea and several areas of the world* [9]." As of today, the only industrial commercially available DGD technique is the *Riserless Mud Return* (RMR) method, offered by AGR Subsea AS since 2003. As shown in Appendix B, the RMR method is a "Pre-BOP" DGD approach, meaning that it can only be applied in the upper wellbore sections. This method is further discussed below. Another interesting DGD approach that is discussed in this thesis is the *Controlled Mud Level* system, also referred to as *Mid-Riser Pumping* system. In Appendix B, this system is found below "Post-BOP" DGD systems.

Riserless Mud Return

The RMR method is a top-hole drilling technique that utilizes a subsea pump to bring drilling fluids and cuttings from the seabed to the drilling rig, see Figure 4.15. In this manner, the RMR system is quite similar to the SubSea MudLift Technique, the difference is that the RMR method is performed without a riser. The RMR method is therefore only applied in the upper sections prior to installing the drilling riser and BOP. As of today, the RMR method has been used in more than 200 wells all over the world. The majority of these wells operated in less than 2 000 feet (610 meter) water depths, but the technique has been tried in water depths close to 5 000 feet (1 525 meter). According to AGR,

this method enables the top holes to be drilled more stable, with a higher quality and low environmental impact as fluids and cuttings are brought back to the rig rather than dumped on the seabed [10, 48].

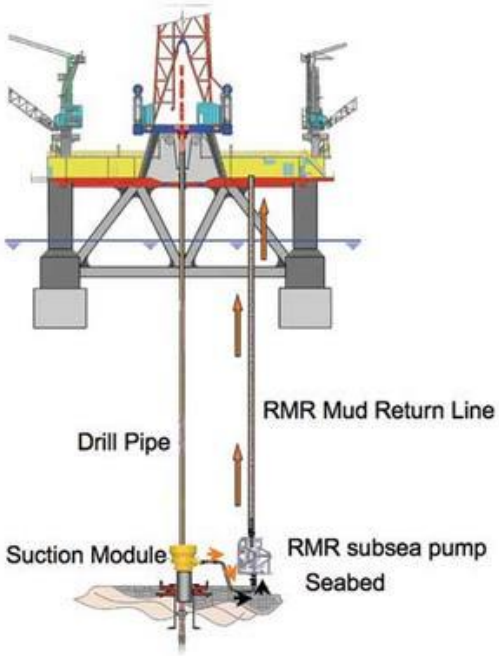

Figure 4.15: Riserless Mud Return [49].

Controlled Mud Level

The Norwegian company "Ocean Riser Systems" (ORS) developed a technique called "Low Riser Return System" (LRRS). From a conventional point of view, wellbore pressure is adjusted and regulated through mud density control. The LRRS technique challenges this mindset. Rather than adjusting the density, the mud level in the marine riser is adjusted. A subsea pump placed in a separate conduit, transports drilling fluid and cuttings from the marine riser and up to the drilling rig, see Figure 4.16. The mud level in the riser is adjusted by changing the flow rate through the subsea pump. Reducing the flow rate causes the mud level to increases whereas increasing the flow rate causes the mud level to drop [50].

The LRRS can be used in two application modes. In the first mode, the riser is filled during static conditions and when mud circulation is initiated, the mud level decreased to compensate for the annular friction and cuttings transport. The second technique involves using a higher-than-conventional mud weight and a partly evacuated riser for both static

and dynamic conditions. Both of these application modes improves the safety margins, enables better pressure control and increased efficiency for most well operations [50].

Figure 4.16: Low Riser Return System [50].

In July 2012, Ocean Riser Systems AS merged with the Enhanced Drilling Solutions (EDS) department of AGR and formed AGR EDS-ORS. The Enhanced Drilling department has developed a DGD technique named "EC-Drill", illustrated in Figure 4.17. This method, which is designed for use on semi-submersible, jack-up and drilling ships, has been used on several deepwater wells to date. The system is based on the same idea as the LRRS, namely to alter the wellbore pressure through changing the mud level in the marine riser [51].

The key feature enabled with the "Controlled Mud Level" approach is the ability to manipulate the mud level in the riser, and in that manner control the BHP. Through mud level adjustments during static and dynamic conditions, a near constant BHP can be established, hence ECD management. In addition, kicks/losses can be detected at an early stage through volume management. All together, this results in increased flexibility with respect to rapid down-hole pressure adjustment [52].

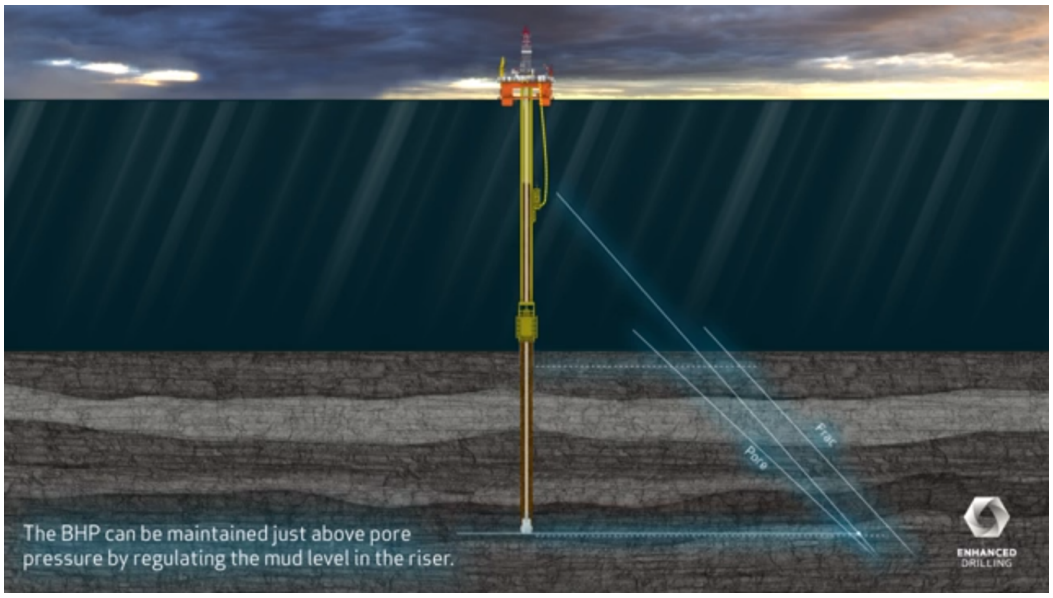

Figure 4.17: The EC-Drill technique

A constant BHP is enabled as follow:

$$BHP_{stat} = BHP_{dyn} \tag{4.17}$$

When Equation 4.15 is replaced with BHP_{stat} and Equation 4.16 with BHP_{dyn}, the following relationship is obtained:

$$(\rho_1 g h_1 + \rho_2 g h_2)_{stat} = (\rho_1 g h_1 + \rho_2 g h_2)_{dyn} + P_{AF} + P_C \tag{4.18}$$

The medium above mud line commonly consists of air at atmospheric pressure, hence this pressure is equal during both static and dynamic conditions and can thus be removed from Equation 4.18:

$$(\rho_2 g h_2)_{stat} = (\rho_2 g h_2)_{dyn} + P_{AF} + P_C \tag{4.19}$$

This can be written as:

$$\rho_2 \cdot g \cdot (h_{2,stat} - h_{2,dyn}) = P_{AF} + P_C \tag{4.20}$$

Which means that during mud circulation and cuttings transport, the riser mud line must be lowered equivalent to:

$$\Delta h = \frac{P_{AF} + P_C}{\rho_2 \cdot g} \tag{4.21}$$

4.3.4 Returns-Flow-Control (RFC)

During conventional drilling, the drilling fluid return system is, as mentioned, open to the atmosphere. Thus, chemicals and gasses contained in the drilling fluid can escape to the atmosphere. If a formation containing high amounts of toxic gasses, like hydrogen sulfide (H_2S), is encountered with an *open-to-atmosphere* fluid returns system, it may entail serious health, safety and environmental (HSE) concerns. Especially with respect to the crew members on the rig [53].

A MPD variant, *Returns-Flow-Control*, has been developed for this particular situation. The variant utilizes the *closed-to-atmosphere* fluid returns system and the RCD to safely contain any toxic gasses within the drilling fluid. Hence, the primary objective of this MPD variant is not increased downhole pressure control, but increased HSE during drilling [30, 53].

Chapter 5

Case Study

In this chapter, a case study of a vertical deepwater exploration well drilled by Statoil in the Gulf of Mexico is presented and discussed. My supervisor, John-Morten Godhavn, has provided both expected and real pore and fracture pressure gradients for this well. First, based on expected pore and fracture pressure gradients, drilling programs for respectively conventional drilling, CBHP MPD and the CML MPD DGD approach are designed. The well is then drilled theoretically, on paper, using the planned programs and real pore and fracture pressure gradients. In this case study, a special focus is given towards MPD and the additional flexibility this drilling technique offers in uncertain pressure environments. The pressure gradients versus depth data provided by John-Morten Godhavn are given in respectively ppg (pound per gallon) and feet. These units are used throughout this Chapter. 1 feet is equivalent to 0,3048 meter and 1 ppg is equivalent to 119,8 kg/m^3.

As previously discussed, both conventional drilling and MPD are performed overbalanced. This entails that the planned wellbore pressure are bound by the following pressure boundaries:

$$P_{f,\,est} < P_{well,planned} < P_{frac,\,est} \tag{5.1}$$

where $P_{f,\,est}$ is the estimated formation-pore pressure, $P_{well,planned}$ is the planned wellbore pressure and $P_{frac,\,est}$ is the estimated fracture pressure. In addition, internal and/or local regulations may require additional margins between the wellbore pressure and the pressure boundaries. In the Gulf of Mexico, the following requirements apply [8]:

- *Minimum mud weight*: Statoil requires that the minimum mud weight shall be 0,17 ppg higher than the maximum expected pore pressure gradient in that section.
- *Maximum mud weight*: The Bureau of Safety and Environmental Enforcement(BSEE) and Statoil requires that the maximum mud weight shall be 0,5 ppg below the lesser

of the casing shoe integrity test or the lowest estimated fracture pressure gradient in that section. The ECD must be kept below the lesser of the casing shoe integrity test or the lowest estimated fracture pressure gradient in that section.

The minimum horizontal stress is usually lower than the fracture pressure gradient. If the wellbore pressure exceeds the fracture pressure, and drilling fluid is lost to the formation, the fracture will not close before the wellbore pressure descends below the fracture closure pressure, which is approximately equal to σ_h, see Section 2.4.3 and Figure 2.13. The mud weight should therefore be kept below the minimum horizontal stress. In case losses should occur during drilling, the mud pumps are turned off to bring the well pressure below the σ_h, and hence close the initiated fractures. A good practice during drilling is therefore to keep the mud weight below the minimum horizontal stress [8].

In terms of density, the pressure boundaries for the planned drilling program profile then becomes:

$$\rho_{f,\,est} + 0,17ppg < \rho_{well,planned} < \rho_{frac,\,est} - 0,5ppg \tag{5.2}$$

When the well is drilled in real pressure environment with an estimated drilling plan, deviations from this plan are expected. This may lead to pressure related incidents like fluid losses and/or formation fluid influx. Knowledge obtained through such situations are used to continuously discuss the need for updating the drilling plan. During the theoretical drilling part, real-time wellbore pressure is obtained through a PWD tool. In addition, real-time pore pressure information has been assumed provided through MWD logs. The lower pressure boundary is then dictated by the largest value of the estimated and measured pore pressure. After a section has been cased and cemented, a Leak-Off Test is performed which offers accurate fracture pressure information at the casing shoe depth. The fracture pressure is then updated and checked prior to drilling a new section. This opens up for modifications of the planned drilling program in case the deviations are of a substantial magnitude. The pressure boundaries for the real drilling program then becomes:

$$(\rho_{f,\,est}\ or\ \rho_{f,\,measured}) + 0,17ppg < \rho_{well,actual} < (\rho_{frac,\,LOT}\ or\ \rho_{frac,\,est}) - 0,5ppg \tag{5.3}$$

where $\rho_{well,actual}$ is the actual well pressure gradient and $\rho_{frac,\,LOT}$ is the fracture pressure gradient measured at the casing shoe depth. It has been decided to keep both the static and dynamic well pressure gradients within this limit, even though it is not a requirement to keep the dynamic well pressure 0,5 ppg below the lesser of the LOT or the lowest estimated fracture pressure gradients. If either the static or dynamic well pressure exceeds

the defined pressure boundaries, measures must be taken to bring the situation back within the acceptance criteria. The static and dynamic pressure gradients presented in the drilling programs are given in terms of equivalent mud weight, defined in Section 2.1.1.

The equations presented and derived for static and dynamic wellbore pressures in Section 4.3 are given in terms of EMW in the two following tables:

Table 5.1: Static well pressure gradients in terms of equivalent mud weight.

Drilling technique	$\mathbf{EMW_{stat}}$
Conventional drilling:	$EMW_{stat} = \rho_m$
"Constant Bottom-Hole Pressure" MPD:	$EMW_{stat} = \rho_m + \frac{P_{BP,\,stat}}{g \cdot TVD}$
"Controlled Mud Level" DGD, MPD:	$EMW_{stat} = \frac{\rho_1 \cdot h_1 + \rho_2 \cdot h_2}{TVD}$

Table 5.2: Dynamic well pressure gradients in terms of equivalent mud weight.

Drilling technique	$\mathbf{EMW_{dyn}}$
Conventional drilling:	$EMW_{dyn} = \rho_m + \frac{P_{AF} + P_C}{g \cdot TVD}$
"Constant Bottom-Hole Pressure" MPD:	$EMW_{dyn} = \rho_m + \frac{P_{AF} + P_C + P_{BP,\,dyn}}{g \cdot TVD}$
"Controlled Mud Level" MPD, DGD:	$EMW_{dyn} = \frac{\rho_1 \cdot h_1 + \rho_2 \cdot h_2}{TVD} + \frac{P_{AF} + P_C}{g \cdot TVD}$

The pressure exerted by friction and cuttings in the annulus during drilling are mainly governed by the fluid flow velocity. In vertical wells ($< 60^0$), an upper and lower boundary condition, with respect to annular fluid flow velocity, are therefore commonly designed. The upper one is normally designed so that turbulence flow does not develop around the drill collars, whereas the lower one is set by the concentration of cuttings in the annulus. The amount of cuttings with respect to drilling fluid must be lower than four volume percent. If it gets higher, problems related to accumulation of cuttings (like stuck pipe) has shown to occur with an increasing trend [54].

Pressure exerted by cuttings

In vertical wells, hole cleaning and transportation of cuttings are a matter of sufficient fluid flow rate and velocity to counteract the vertical slipping velocity of cuttings. The amount of cuttings, Q_C $[m^3/s]$, generated during drilling is found by multiplying the cross-sectional area, A $[m^2]$, of the bit with the ROP $[m/s]$:

$$Q_C = A \cdot ROP \quad \Rightarrow \quad Q_C = \frac{\pi}{4} \cdot d_{bit}^2 \cdot ROP \tag{5.4}$$

During drilling, the initial concentration of cuttings, $C_{C,i}$ [%], are found by dividing the amount of cuttings generated by the total annular flow rate, $Q_{tot,a}$ $[m^3/s]$:

$$C_{C,i} = \frac{Q_C}{Q_{tot,a}} \qquad where \qquad Q_{tot,a} = Q_C + Q_m \tag{5.5}$$

where Q_m $[m^3/s]$ is the drilling fluid flow rate. In vertical wells, the slipping velocity of cuttings, v_{slip} $[m/s]$, causes the concentration of cuttings in the borehole to increase. A ratio known as the *cuttings transport ratio*, R_t, defines the impact the slipping velocity has on the cuttings concentration. This ratio expresses the relationship between cuttings transport velocity, v_t $[m/s]$, and average fluid velocity, $\bar{v}$ $[m/s]$ [54]:

$$R_t = \frac{v_t}{\bar{v}} \qquad where \qquad v_t = \bar{v} - v_{slip} \tag{5.6}$$

The average concentration of cuttings in the well, $\bar{C}_C$ [%], is found by dividing the initial concentration of cuttings with the cuttings transport ratio [54]:

$$\bar{C}_C = \frac{C_{C,i}}{R_t} \tag{5.7}$$

In vertical holes, the cuttings transport ratio has a typical value of 0,75. The well discussed in this case study is, as mentioned, a vertical well. This typical value of 0,75 has therefore been applied for estimating the average cuttings concentration during drilling in the case study [55].

The amount of cuttings generated during drilling alters the average annular density, $\bar{\rho}_a$. As cuttings enters the annulus, a part equivalent to $\bar{C}_C$ will consist of cuttings and 1-$\bar{C}_C$ of drilling fluid. This will cause the average annular density to increase, provided that the density of the cuttings are larger than the drilling fluid density [54]:

$$\bar{\rho}_a = \rho_m \cdot (1 - \bar{C}_C) + \rho_C \cdot \bar{C}_C \tag{5.8}$$

where ρ_C is the cuttings density. At shallow depths, ρ_C may be as low as 2 000 kg/m^3, whereas at large depths (> 5000 meter TVD) in zero-porosity environments, ρ_C is typically in the range of 2 800 kg/m^3. According to *Skalle, P*, 2 300 kg/m^3 is a good estimate of the average cuttings density. The additional pressure exerted by cuttings during drilling is found by subtracting the hydrostatic drilling fluid pressure from the average annular hydrostatic pressure [54]:

$$P_c = (\bar{\rho}_a - \rho_m) \cdot g \cdot TVD \tag{5.9}$$

Annular friction pressure

As the upper boundary condition, with respect to annular flow velocity, is governed by the flow pattern of the fluid. The Reynolds number, Re, must be calculated to determine whether the flow is in a laminar or turbulent state [54]:

$$Re = \frac{\rho_{mud} \cdot \bar{v} \cdot (d_o - d_i)}{\mu_{eff}} \tag{5.10}$$

where $\bar{v}$ is the fluid velocity, d_o the outer annulus diameter, d_i the inner annulus diameter and μ_{eff} the effective fluid viscosity. If the Reynolds number is below 2 300, the flow is commonly considered to be in a laminar state, whereas a Reynolds number above 4 000 implies turbulent flow. A Reynolds number between these two values are considered to be in a transition state. The average fluid velocity in the annulus is expressed as:

$$\bar{v} = \frac{Q_{tot,a}}{A} \tag{5.11}$$

where $Q_{tot,a}$ is the total annular flow rate, see Equation 5.5, and A is the cross-sectional area of the annulus:

$$A = \frac{\pi \cdot (d_o^2 - d_i^2)}{4} \quad \Rightarrow \quad \bar{v} = \frac{4 \cdot Q_{tot}}{\pi \cdot (d_o^2 - d_i^2)} \tag{5.12}$$

Prior to calculating the effective fluid viscosity, it must first be determined which of the following rheological models that best describes the drilling fluid behaviour [54]:

- Newtonian
- Bingham
- Power law
- Herschel Buckley

For the purpose of annular friction estimation and effective fluid viscosity, it is suggested to simplify by choosing one of the aforementioned models and base the estimation of effective fluid viscosity on the SI-approach. This will, according to *Skalle, P*, increase the accuracy of the calculations [54].

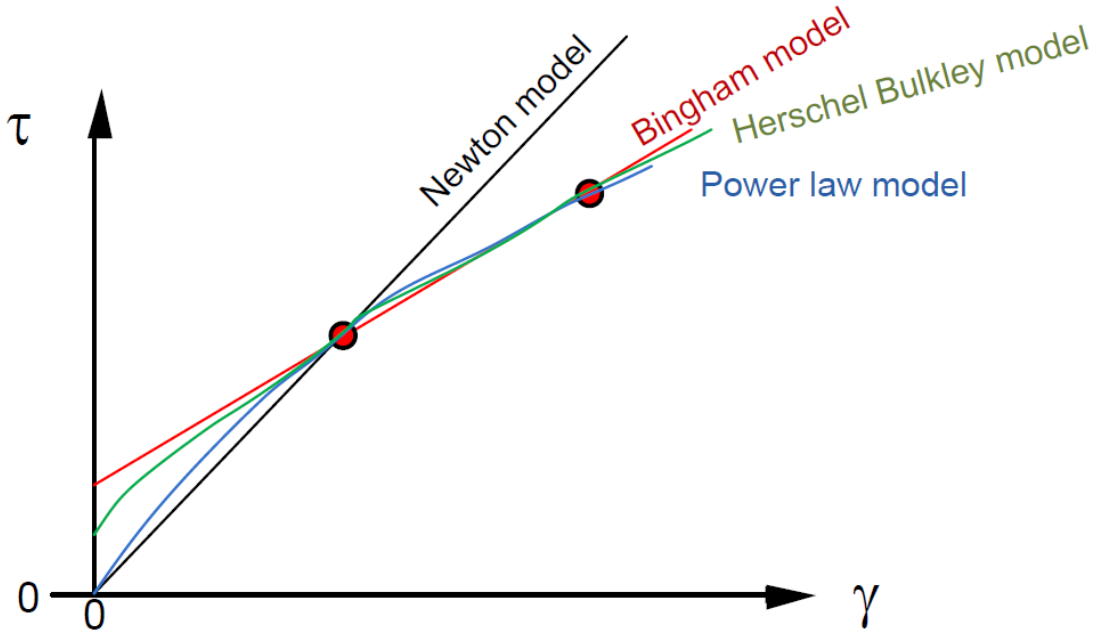

Figure 5.1: Flow curve of the different rheological models. τ is shear stress and γ is shear rate [54]

Drilling fluids are commonly designed with an ability to form a gel-structure during static conditions. This gel-structure causes the internal strength of the drilling fluid to increase at still stand, often expressed as a fluids "gel strength". The purpose of this gel-structure is to keep drilling fluid particles and cuttings in suspension when circulation is ceased. The two parameters shear stress, τ, and shear rate, γ, are used to quantify the flow performance of a fluid. Shear stress is the force required to sustain a constant fluid velocity and shear rate is the rate of change of velocity across the diameter of a fluid-flow. A fluids gel strength is measured at low shear rate after a mud has been at rest for a period of time (commonly either 10 minutes or 10 seconds). In other words, the higher the shear stress is at low shear rates, the higher the gel strength of the fluid is. As illustrated on Figure 5.1, both the Bingham and Herschel Buckley methods are suited for such fluids. For the purpose to estimate annular friction in this case study, the Bingham model has been chosen. For a Bingham fluid, the SI-approach for estimating the effective annular fluid viscosity is as follows [54, 56]:

$$\mu_{eff,ann} = \mu_{pl} + \frac{\tau_0 \cdot (d_o - d_i)}{8 \cdot \bar{v}} \tag{5.13}$$

where μ_{pl} is the plastic viscosity of the fluid and τ_0 is the yield shear stress at zero shear rate, that is, the shear stress during static conditions. Plastic viscosity is defined as $\frac{\Delta\tau}{\Delta\gamma}$, which is equivalent to the slope for the Bingham model line seen in Figure 5.1. The Reynolds

number for the Bingham fluid can now be calculated and the flow rate adjusted to keep the flow in a laminar state. For a Bingham fluid in laminar flow, the annular friction pressure is calculated with the following equation [54, 56]:

$$P_{AF} = \frac{48 \cdot L \cdot \bar{v} \cdot \mu_{eff}}{(d_o - d_i)^2} \tag{5.14}$$

where L is the length of the drill collars/open-hole/casing/liner section being calculated. When the well consists of several sections, independent friction calculations are required for the various sections. This because the annular cross-sectional area is varying, causing the velocity profiles and the effective fluid viscosities to change.

5.1 Planned drilling programs

Tables containing detailed information regarding the planned drilling programs are presented in Appendix C.1. The numbers given in brackets after the effective mud weight represent the effective mud weight at casing shoe depth. The estimated mud weight window for this vertical exploration well is shown in Figure 5.2. As seen on the figure, the estimated fracture pressure gradient begins to deviate from the seawater gradient at roughly 3 150 feet. The water depth at the drill site has therefore been assumed equal to 3 150 feet. Further down, at an estimated depth of 6 920 feet, it is seen that the pore pressure density suddenly drops from an abnormal state to a normal state, meanwhile the fracture pressure is estimated to increase. This gives reason to believe that a thick salt layer is located below this depth. At an estimated depth of 12 540 feet, the pore pressure suddenly increases from a normal state to roughly 13,2 ppg whereas the fracture pressure has decreased slightly. Based on these observations, a thick salt layer has been assumed present between 6 920 and 12 540 feet TVD.

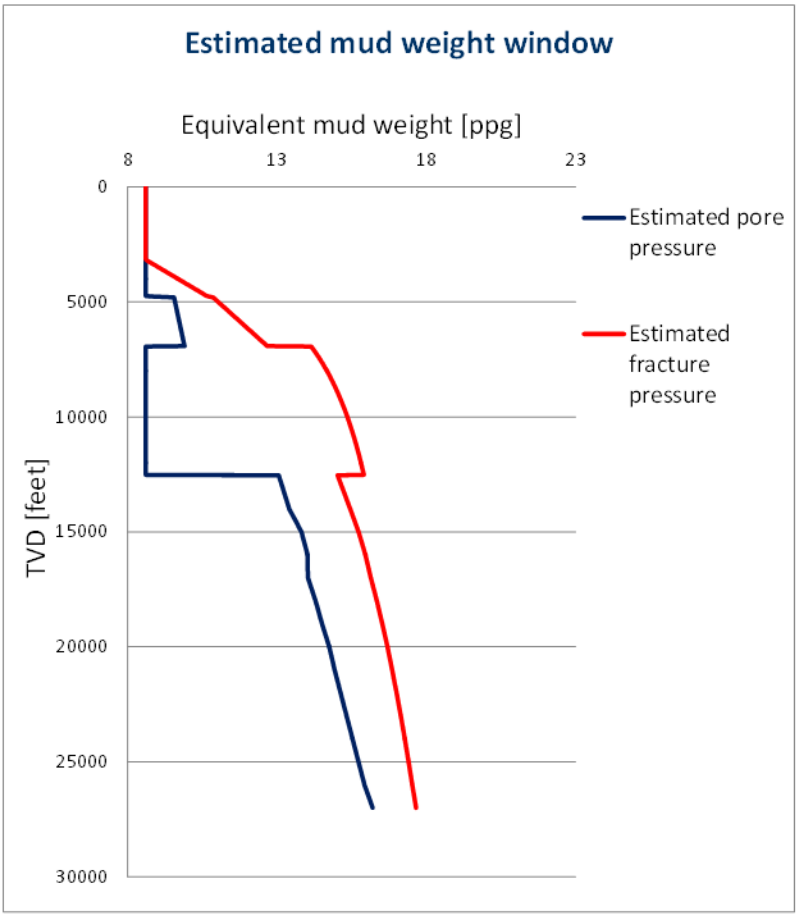

Figure 5.2: Estimated mud weight window.

5.1.1 Conventional drilling

The planned drilling program for conventional drilling is shown in Figure 5.3 and the details are presented in Table C.1 and C.2. The planned bit, casing and liner sizes presented in Appendix C are based on information from the *Drilling data handbook*. Both the 36" and the 26" holes are drilled riserless, this implies that cuttings and drilling fluids are dumped on the seabed, referred to as the *Pump and dump* method. This approach is planned identical for the two upper sections in all the three different variants. The 36" hole is planned drilled with a mud weight equivalent to that of seawater (8,60 ppg), whereas the 26" hole is planned drilled with a mud weight of 9,50 ppg. Sections drilled prior to running the riser and BOP may be composed of two gradients, provided that the density of the drilling fluid is different from the seawater density. This approach has been chosen for the 26" section to better fit the estimated mud weight window. The effective static mud weight for this section has therefore been calculated as follow:

$$EMW_{stat} = \frac{8,60\ ppg \cdot 3\ 150\ feet + 9,50\ ppg \cdot (TVD - 3\ 150\ feet)}{TVD} \tag{5.15}$$

where 8,60 ppg is the seawater gradient, 3 150 feet is the estimated water depth and 9,50 ppg is the drilling fluid density used in this section. The effective dynamic mud weight in this section then becomes:

$$EMW_{dyn} = EMW_{stat} + \frac{P_{AF} + P_C}{g \cdot TVD} \tag{5.16}$$

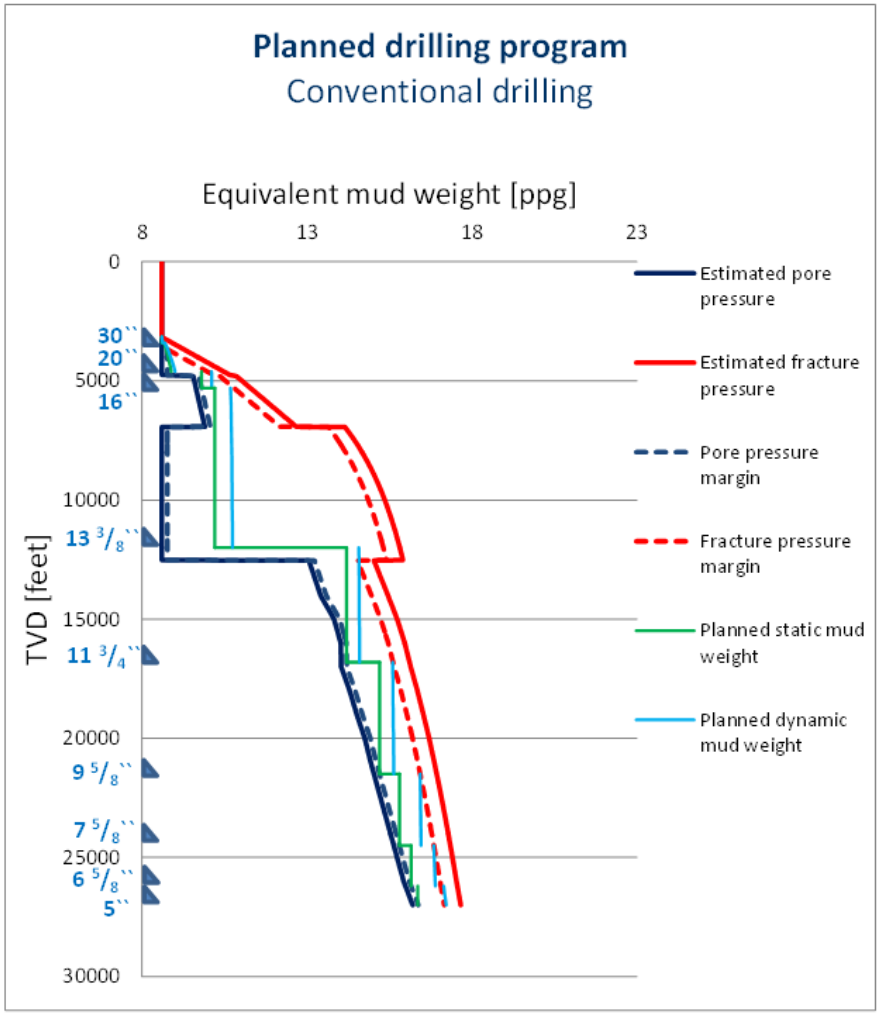

Figure 5.3: Planned drilling program using conventional drilling.

As seen on Figure 5.3, this causes the static and dynamic pressure profiles for this section to be different from the vertical pressure profiles in the other sections. After the 20" surface casing has been run and cemented at 4 600 feet TVD, a BOP is run on a 22" drilling riser. This enables cuttings and drilling fluids to be transported up to the rig, and

conventional drilling is initiated. As seen on the figure, the mud weight window below 12 000 feet becomes relatively narrow, roughly in the range of one to one and a half ppg. This makes it challenging to maintain both the static and dynamic wellbore pressures within the acceptance criteria. Therefore, after the $13\,{}^{3}/_{8}$" casing has been run and cemented, the five inch drill pipe used in the upper sections is replaced with a four inch drill pipe. This will reduce the annular friction loss as the annular cross-sectional area has been increased. According to the drilling plan, a total of nine sections must be drilled and cased if the target depth is to be reached with conventional drilling.

As seen in Table C.1, the planned static and dynamic mud weights does occasionally exceed the acceptance criteria. The narrow mud weight window, in combination with a target depth of 27 000 feet, made it very challenging to plan a conventional drilling program without ever exceeding these limits. In an attempt to reduce the equivalent circulating density, the ROP has been set relatively low to reduce the effect of cuttings, averagely around 50 feet/hour.

5.1.2 Constant Bottom-Hole Pressure MPD

A proposed drilling program using the CBHP MPD variant is illustrated in Figure 5.4 and the details presented in Table C.3. When comparing the planned programs for respectively conventional drilling and CBHP MPD, the most apparent difference is seen below the salt zone. With conventional methods, a total of five sections are required to reach target depth from the lower salt zone. However, if the CBHP variant is chosen, the amount of sections required are reduced from five to three, and the total amount of sections required to reach target depth is reduced from nine to seven. This makes it possible to reach target depth with a larger wellbore diameter and enables a bigger production liner to be set. In this case a $7{}^{5}/_{8}$" production liner is planned at target depth. This is beneficial from both a production and economical point of view. A large production diameter will enhance the production of hydrocarbons due to increased production diameter. Further, a reduction in casing strings leads to less time spent on tripping, casing and cement operations in addition to less steel used in the wellbore, which ultimately reduces the cost of the drilling operation.

During drilling, the dynamic back pressure has been set at a constant pressure of $5 \cdot 10^5$ Pa, with the exception of the $18{}^{1}/_{2}$" section. This enables both the static and dynamic wellbore pressure to be reduced, equivalent to $5 \cdot 10^5$ Pa, in case the wellbore pressure exceeds the fracture pressure and lost circulation occurs. In this particular case, a disadvantage of this approach is seen, especially in the upper wellbore sections. In terms of EMW, the additional pressure applied during dynamic condition decreases with depth, expressed as:

$$EMW = \frac{P_{BHP,\,dyn}}{g \cdot TVD} \tag{5.17}$$

As seen in Table C.3, this causes the effective dynamic mud weight to decrease with increasing depth in the $18^1/_2$", $14^1/_2$" and the $12^1/_4$" sections. However, in the lower two sections, it is seen that the dynamic mud weight begins to increase with depth. This is because the increasing dynamic mud weight induced by annular friction and cuttings are larger than the decreasing trend induced by a constant dynamic back pressure, expressed as:

$$\frac{P_{AF} + P_C}{g \cdot TVD} > \frac{P_{BHP,\,dyn}}{g \cdot TVD} \tag{5.18}$$

Therefore, due to the relatively narrow mud weight window above the salt zone, the dynamic back pressure has been set at a constant pressure of only $1 \cdot 10^5$ Pa in the $18^1/_2$" section. The effect described above may not necessarily be a negative one. In this case, the pore and fracture pressure gradients are expected to increase with respect to depth, with the exception of pore pressure in the salt layer. This effect has therefore been described as a negative one in this context as it counteracts the natural development of the underground pressure regime.

The static effective mud weight has been calculated as described in Table 5.1:

$$EMW_{stat} = \rho_m + \frac{P_{BP,\,stat}}{g \cdot TVD} \tag{5.19}$$

And the dynamic effective mud weight as presented in Table 5.2:

$$EMW_{dyn} = \rho_m + \frac{P_{AF} + P_C + P_{BP,\,dyn}}{g \cdot TVD} \tag{5.20}$$

To compensate for the effect of cuttings, annular friction and dynamic back pressure, the back pressure applied during static conditions is equal to:

$$P_{BP,\,stat} = P_C + P_{AF} + P_{BP,\,dyn} \tag{5.21}$$

where P_C and P_{AF} are calculated using Equations 5.9 and 5.14. The pressures exerted by cuttings and friction increases with increasing depth and reduced annular size (the diameter gets lower for every casing/liner that is run). To compensate for these effects, the static back pressure is continuously increased to keep the bottom hole pressure at a constant level. At the target depth of 27 000 feet, the dynamic back pressure is $5 \cdot 10^5$ Pa, the annular friction pressure is $80,7 \cdot 10^5$ Pa and the effect of cuttings is $2,9 \cdot 10^5$ Pa. This results in an

additional pressure gradient of 0,92 ppg. To compensate for this during static conditions, the back pressure applied during still stand is $88,6 \cdot 10^5$ Pa.

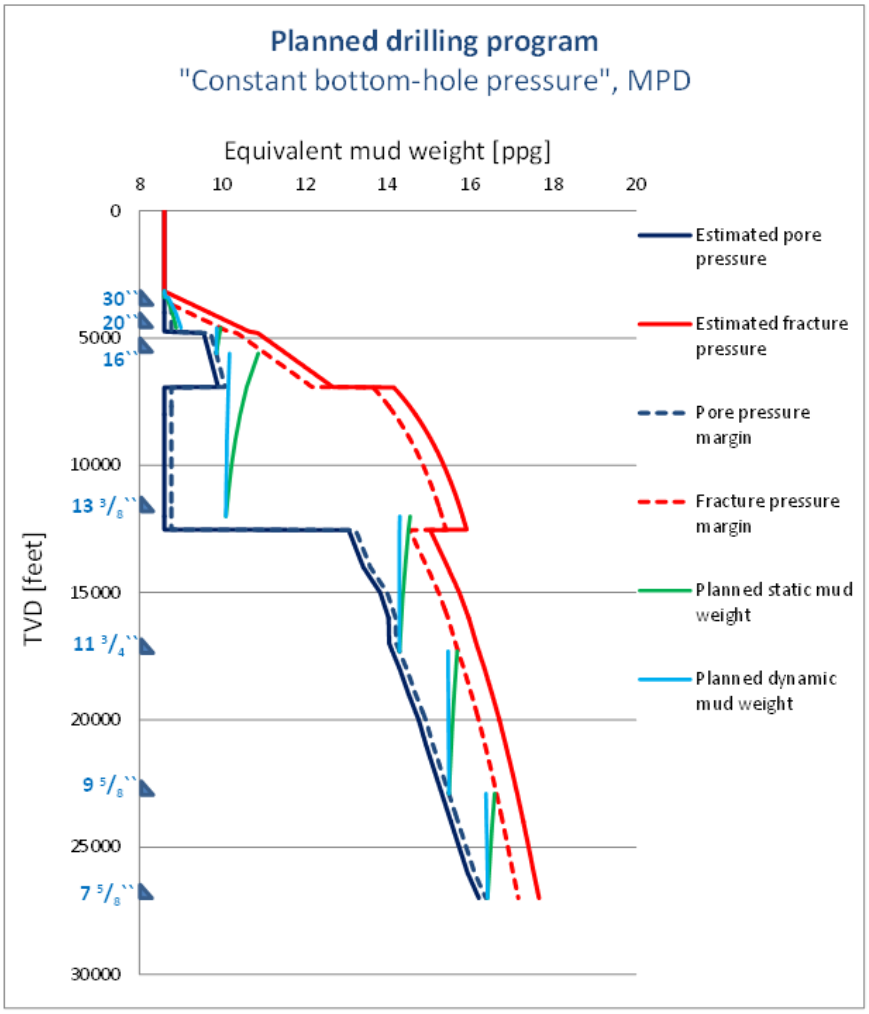

Figure 5.4: Planned drilling program using the MPD variant CBHP.

5.1.3 Controlled Mud Level DGD, MPD

As mentioned in Section 4.3.3, the CML approach can be used in two application modes. In the first mode, the riser is filled during static conditions. When mud circulation and drilling is initiated, the mud level is decreased to compensate for the annular friction and cuttings pressure. The second mode uses a partly evacuated riser during static conditions. When mud circulation and drilling is initiated, the mud level is decreased further to compensate for annular friction and cuttings transport effect. Both of these application modes are presented and discussed below.

AGRs EC-drill is in its current state able to deliver ECD management, and not a "full-

DGD" capability. The application mode, which uses a filled riser, illustrates the current state of this technique. Whereas the application mode with a partly evacuated riser illustrates the possible future, and the advantages it will entail to develop this technique to "full-DGD" capability [60].

Filled riser during static conditions

The advantage of using a filled riser during static conditions presents itself if the subsea pump should fail. If this occurs with a filled riser, the operation can proceed as a conventional drilling operation with conventional well control procedures. In this case, the subsea pump is attached to the riser at a depth of 1 476 feet (450 meters). The planned drilling program for this application mode is presented in Figure 5.5 and the details are given in Table C.4.

As the static mud level is kept at the rig floor, the static effective mud weight is equal to mud weight being used:

$$EMW_{stat} = \rho_m \tag{5.22}$$

When the mud pumps are turned on and the riser level is reduced, two different pressure gradients are formed in the riser. The upper one consists of air at atmospheric pressure, and the lower one is given by the mud weight. Hence, the following equation applies during dynamic conditions:

$$EMW_{dyn} = \frac{\rho_1 \cdot h_1 + \rho_2 \cdot h_2}{TVD} + \frac{P_{AF} + P_C}{g \cdot TVD} \tag{5.23}$$

In order to compensate for the effect of annular friction and cuttings, the dynamic mud level is reduced according to:

$$h_{1,dyn} = \frac{P_{AF} + P_C}{g \cdot TVD} \tag{5.24}$$

As seen in Table C.4, the dynamic mud level is continuously decreased to compensate for the pressures induced by annular friction and transportation of cuttings. At the target depth of 27 000 feet, the annular friction pressure is $77,6 \cdot 10^5$ Pa and the effect of cuttings is $2,9 \cdot 10^5$ Pa. To compensate for this, the mud level is reduced to 415 meters (1 362 feet). As illustrated on Figure 5.5, the dynamic mud weights in this variant bends slightly from left to right. This causes the wellbore pressure during dynamic conditions to better follow the underground pore presure than the CBHP variant does. As seen in Figure 5.4, with the CBHP method the well pressure profile bends from right to left, which is in the opposite

direction of the pore pressure gradient.

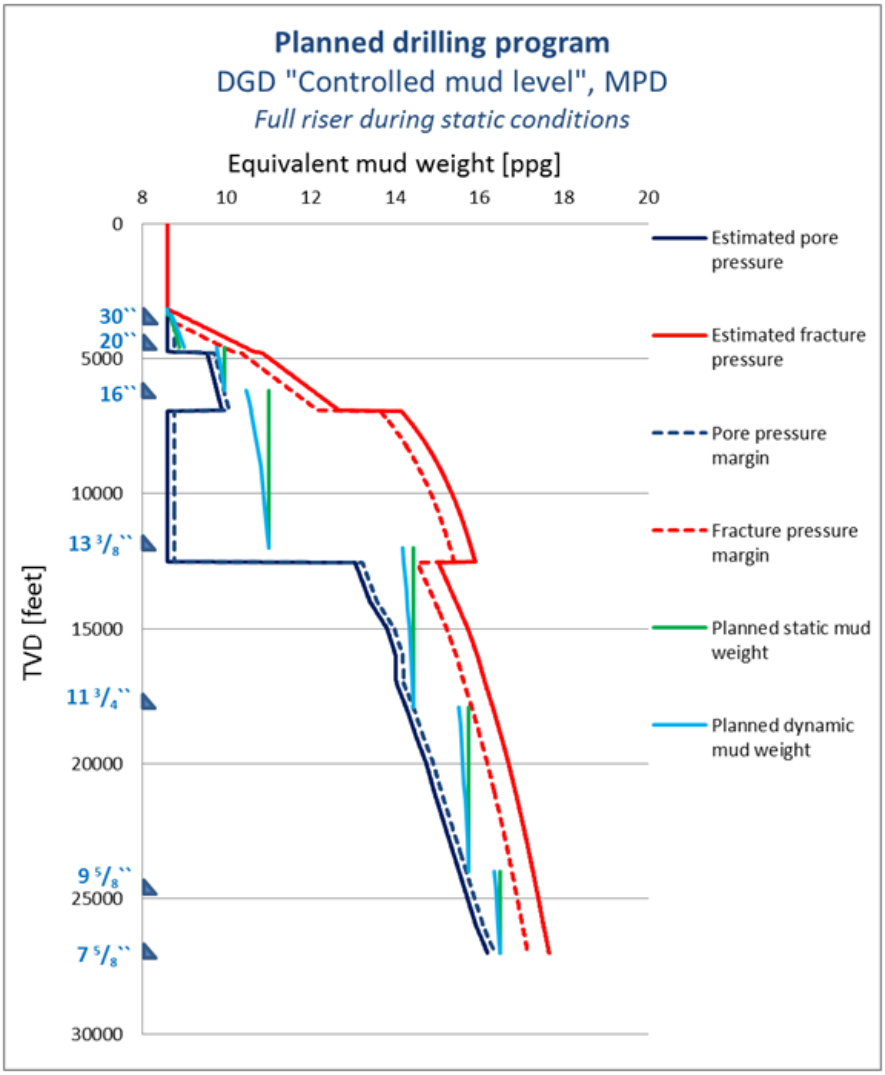

Figure 5.5: Planned drilling program using the CML DGD, MPD approach and a full riser during static conditions.

Partly evacuated riser during static conditions

In this application mode, the subsea pump is attached to the riser slightly deeper than in the previous mode. The subsea pump has been placed at a depth of 600 meters (1 969 feet), enabling a high degree of flexibility regarding regulation and adjustments of the mud level in the riser. The planned drilling program for this application mode is presented in Figure 5.6 and the details are given in Table C.4. When Figure 5.5 and 5.6 are compared, it is seen that a partly evacuated riser during static condition enables the wellbore pressure to better follow the underground pressure environment.

The effective static mud weight for this approach is given by:

$$EMW_{stat} = \frac{\rho_1 \cdot h_1 + \rho_2 \cdot h_2}{TVD} \tag{5.25}$$

The equation used for calculating the dynamic effective mud weight is the same as in the previous application. In order to compensate for the effect of cuttings and friction, the dynamic mud level is reduced with the following amount:

$$h_{1,dyn} = \frac{P_{AF} + P_C}{g \cdot TVD} + h_{1,stat} \tag{5.26}$$

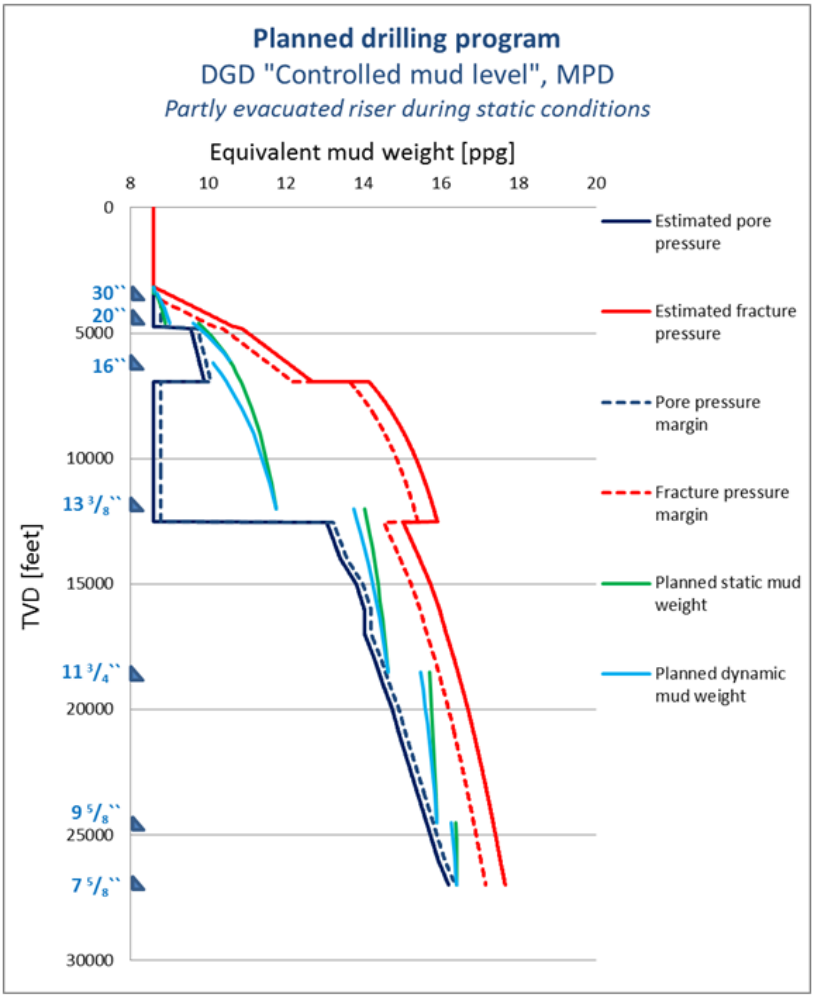

Figure 5.6: Planned drilling program using the CML DGD, MPD approach and a partly evacuated riser during static conditions.

In this case, the riser mud level is continuously regulated to provide a constant BHP at all times. During static conditions, the mud level is kept at a predefined fixed level. However, when drilling is initiated, this level is lowered to compensate for the ever-increasing friction

and cuttings effect. This induces a decreasing trend in the dynamic effective mud weight upwards in the wellbore. Good information about the formation-pore pressure is therefore important to avoid a situation where the dynamic pressure decreases below the formation-pore pressure.

5.2 Actual drilling programs

The well is now drilled in theory using the planned drilling programs in real pressure environments. Tables containing detailed information regarding the updated actual drilling programs are presented in Appendix C.2. Any event that has led to updates during drilling are marked with bold text in these tables. In case the effective mud density drops below or is equal to the pore pressure margin, this is marked with a blue colour. If the effective mud weight either exceeds or is equal to the fracture pressure margin measured at the casing shoe depth, this is marked with a red colour. The numbers presented in brackets after the effective mud weight represents the effective mud weight at the casing shoe depth.

5.2.1 Conventional drilling

The actual drilling program for conventional drilling is illustrated in Figure 5.7 and the details are presented in Table C.6. The first deviation encountered is the estimated seawater depth. This depth was estimated to 3 150 feet. However, when the real pressure environment is investigated, it is seen that the fracture pressure gradient begins to deviate from the normal trend at 3 240 feet rather than at 3 150 feet. The seawater depth at the drill site has therefore been updated to 3 240 feet. Apart from this deviation, the two upper sections are drilled as planned.

After the 20" surface casing has been run and cemented at the planned depth of 4 600 feet, the riser and BOP is run. A LOT is conducted prior to drilling the $18^1/_2$" hole, which measured a fracture pressure of 10,30 ppg. Since this is a lower value than the estimated fracture pressure of 10,47 ppg, the upper well pressure margin is set to 9,80 ppg (10,30 ppg - 0,5 ppg). In order to cope with this reduced margin, the static mud weight has been lowered to 9,50 ppg and the ROP reduced from 25 to 20 feet/hour. When drilling is initiated with this reduced MW and ROP, the dynamic mud weight is estimated to 9,79 ppg, which is 0,01 ppg below the fracture margin. At a depth of 4 800 feet, the MWD tool records a sudden increase in the pore pressure from 9,27 to 9,55 ppg. This will lead to a kick during static conditions, provided that the formation is permeable. The kick is circulated out and the 16" liner is run at this depth, 500 feet earlier than planned.

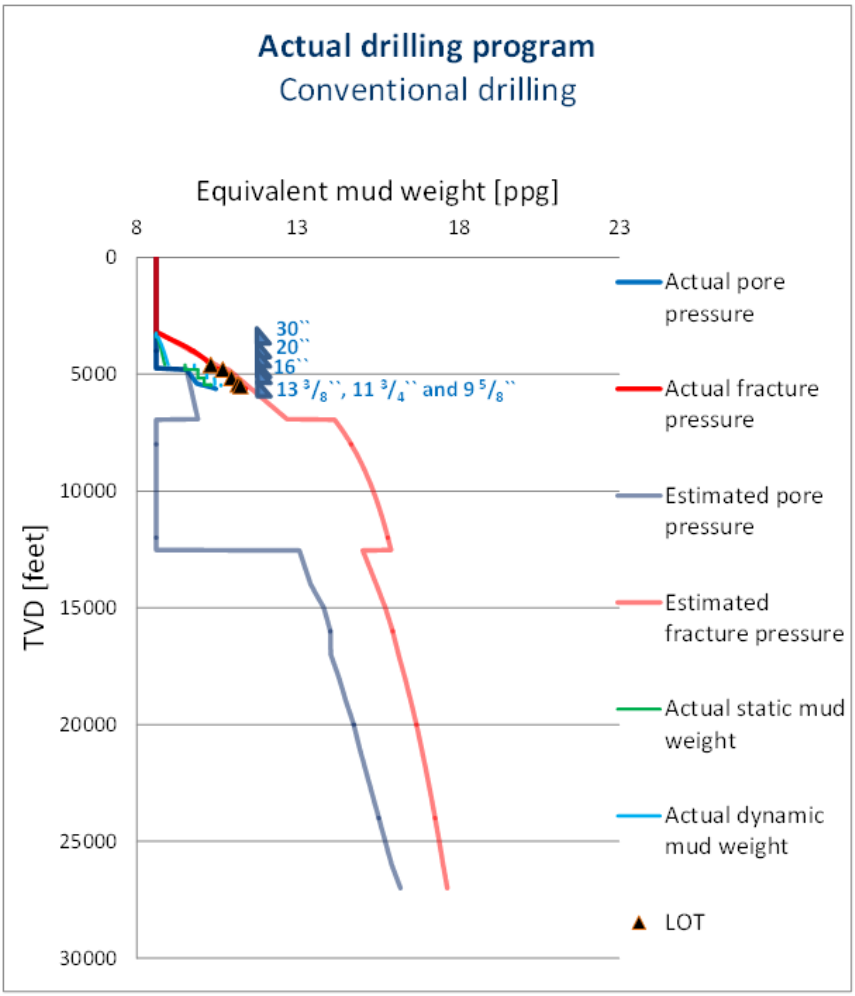

Figure 5.7: Actual drilling program using conventional drilling.

After the aforementioned liner has been set and cemented, a LOT is performed which measures the fracture pressure margin to 10,18 ppg (10,68 - 0,5 ppg), which is only 0,46 ppg above the lower well pressure margin. The static mud weight is set to 9,90 ppg, the ROP to 20 feet/hour and the 14 $^1/_2$" hole is initiated with a dynamic mud weight of 10,17 ppg. At 5 160 feet, the formation-pore pressure is measured to 9,74 ppg which means that the lower acceptable well pressure is 9,91 ppg. This will not result in a kick, but drilling is stopped as the static mud weight is below the pore pressure margin. The 13$^3/_8$" casing is set at 5 160 feet, and the five inch drill pipe is replaced with a four inch drill pipe to reduce the dynamic mud weight. The next sections are drilled with the same strategy as explained above, and casing/liners are run much earlier than planned.

At 5 500 feet, the 9$^5/_8$" liner is run and a LOT is performed. This reveals that the acceptable pressure margin between pore and fracture pressure is only 0,40 ppg. As this margin is not sufficiently large for both static and dynamic pressure conditions, the operation has

been ceased at this depth. The planned versus actual well design is shown in Figure 5.8. It is seen from this figure that there are quite substantial deviations from the planned well design to the actual one. If the target depth is to be reached with this method, the pressure boundaries set for this case would have to be exceeded and the well drilled with potentially extreme losses/influx situations.

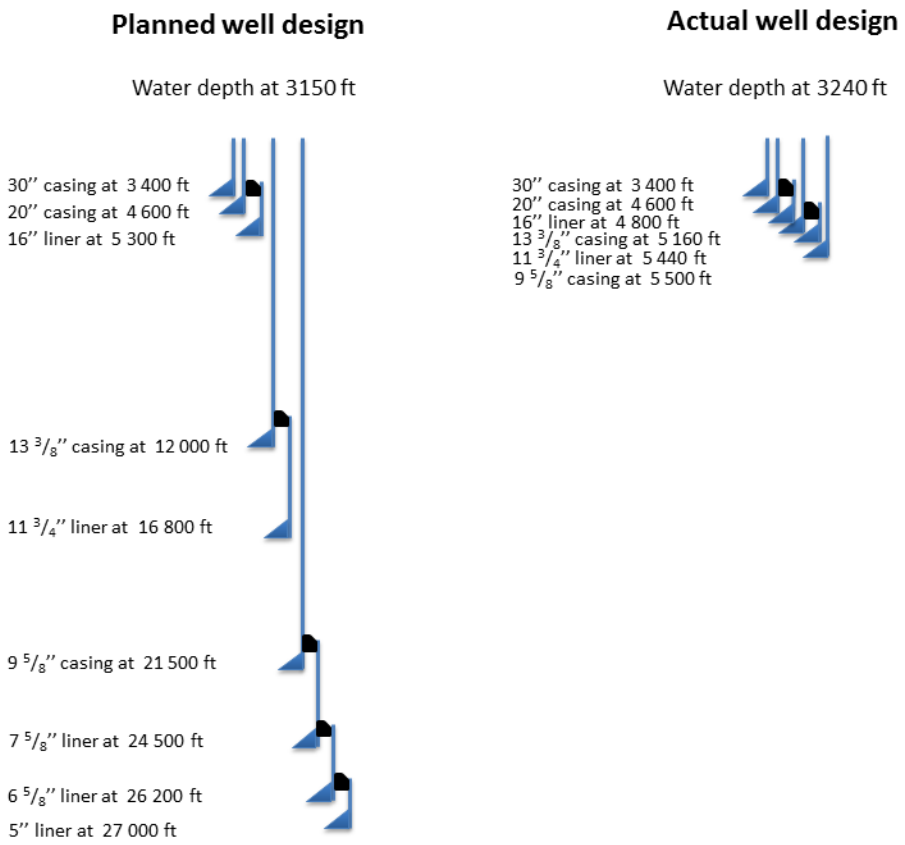

Figure 5.8: Planned versus actual well design for conventional drilling.

5.2.2 Constant Bottom-Hole Pressure, MPD

A remarkable improvement is seen when the well is drilled with CBHP rather than conventional drilling. The two upper sections are drilled according to plan with the exception of the updated water depth. The updated drilling program is shown in Figure 5.9 and the details are presented in Table C.7 and C.8.

The LOT conducted after running the 20" casing indicates a fracture margin of 9,80 ppg, which led to a slight change in the actual drilling program. The mud weight has been reduced from 9,40 ppg to 9,35 ppg and the ROP from 50 to 25 ft/hr, whereas the dynamic

back pressure is kept at the planned $1 \cdot 10^5$ Pa. This results in a static and dynamic mud weight of 9,72 ppg, which is 0,08 ppg below the fracture margin and 0,95 ppg above the pore pressure margin. The $18^1/_2$" hole is then initiated. At 4 820 feet, the formation pore pressure margin is recorded to 9,73 ppg. At this depth, the static back pressure has increased with $0,2 \cdot 10^5$ Pa to compensate for the increased annular friction and cuttings effect. This has caused the static effective mud weight at the 20" casing shoe to increase from the previous value of 9,72 to 9,74 ppg, which is 0,06 ppg below the fracture margin. To cope with the increasing pore pressure at 4 820 feet, the dynamic back pressure is increased from $1 \cdot 10^5$ Pa to $1,8 \cdot 10^5$ Pa. This causes the static back pressure to increase with the same value, resulting in an increase of EMW_{stat} at the 20" casing to 9,79 ppg, only 0,01 ppg below the fracture margin. Drilling is then continued with this increased back pressure until 4 900 feet. At this depth, the measured pore pressure margin is 9,78 ppg whereas EMW_{stat} and EMW_{dyn} equals 9,77 ppg. As the effective static mud weight at the 20" casing shoe is only 0,01 ppg from the fracture margin, it was decided to set the 16" liner at this depth.

It is seen that with the CBHP MPD variant, the 16" liner is run 100 feet deeper than what was possible with conventional drilling. This example illustrates how this variant quickly and effectively is able to adapt to uncertain and narrow pressure margins in the underground. A change of back pressure is conducted in seconds and drilling can proceed uninterrupted. The LOT performed at 4 600 feet indicated a maximum allowed wellbore pressure of 9,80 ppg whereas the pore pressure at 4 900 feet indicated a minimum allowed wellbore pressure of 9,78 ppg. That is a difference of only 0,02 ppg, which illustrates the narrow pressure margin this technique is able to operate within.

After the 16" liner has been run and cemented at 4 900 feet, a LOT is performed. This indicates a fracture margin of 10,26 ppg, triggering the need to reduce the planned mud weight and ROP for this section. In addition, since the measured formation-pore pressure increases with a rapid pace, the initial dynamic back pressure is reduced to $1 \cdot 10^5$ Pa as opposed to the planned $5 \cdot 10^5$ Pa. This will reduce the aforementioned decreasing effect dynamic back pressure has on EMW_{dyn}. Drilling is then initiated from 4 900 feet and the strategy described above regarding regulation of back pressure is followed. Dependent on the situation, the dynamic back pressure is either increased or decreased, aiming to keep the wellbore pressure within the acceptance criteria.

The mud weight window above the salt zone is more narrow in real life than what was initially estimated. The strategy described above for dynamic back pressure has therefore been applied in all sections prior to entering the salt zone. In case a lost circulation incident

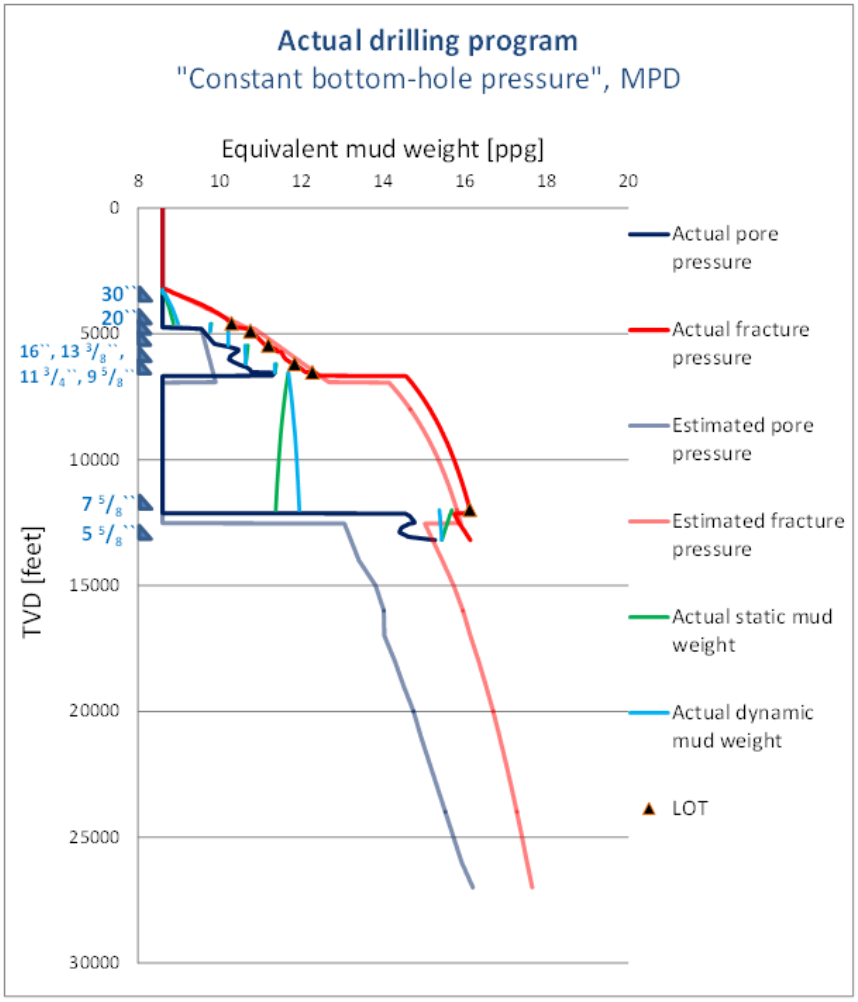

Figure 5.9: Actual drilling program using the MPD variant CBHP.

should be experienced, this enables the wellbore pressure to be decreased equivalent to $1,0 \cdot 10^5$ Pa. In case a lost circulation incident should be experienced, a decrease in BHP equivalent to $1,0 \cdot 10^5$ Pa, may not be enough. However, both the estimated and real pore and fracture pressure gradients are increases continuously above the salt layer. The incidents leading to updated drilling programs are therefore caused by the ever-increasing formation-pore pressure gradient and the continues struggle to stay below the fracture margin measured at the casing shoe depth. This entails that lost circulation will not occur above the salt zone as long as the wellbore pressure is kept below the casing shoe fracture margin.

It is experienced that also this drilling technique is struggling in the narrow mud weight window above the salt zone. The plan was to enter this layer with a $14^1/_2$" hole. However, when the real pressure gradients are used, this layer is entered with a $8^1/_2$" hole which, according to the plan, originally was designated for the target depth. The top of salt is

encountered at a depth of 6 680 feet rather than the expected 6 920 feet. As shown in Table C.8, at a depth of 7 200 feet, EMW_{stat} at the $9^5/_8$" shoe reaches its maximum allowed level. The measured mud weight window above the salt layer is rather narrow, making it difficult to continue drilling. To cope with this situation, it has been decided to switch the point of constant wellbore pressure from the bit to the $9^5/_8$" casing shoe. The estimated mud weight window in this layer is very wide, enabling safe pressure fluctuations at the bit depth. EMW_{stat} is set equal to EMW_{dyn} (11,68 ppg) at 6 540 feet, and drilling continues uninterrupted until 12 000 feet is reached. The $7^5/_8$" liner is set at this depth, according to the plan, as the pressure environment below the salt layer is highly uncertain.

At 12 000 feet, it has been decided to drill a contingency section. A LOT is performed and a $6^7/_8$" hole is drilled with CBHP set at the bit depth. As the estimated fracture margin below the salt layer is 14,53 ppg, it has been decided to stay below this value when exiting the salt. At 12 140 feet, the formation-pore pressure margin suddenly increases from 8,77 to 14,72 ppg, indicating that the salt is exited. The wellbore pressure gradient at this point is only 14,15 ppg, which is 0,57 ppg below the margin. To cope with this situation, the dynamic back pressure is increased from $5,0 \cdot 10^5$ to $35,0 \cdot 10^5$ Pa, which brings the effective mud weights up to 14,84 ppg. It is experienced that the real pore pressure below the salt layer is 1,50 ppg higher than initially estimated. It has therefore been assumed that also the fracture pressure is higher than originally estimated. The fracture pressure measured at the LOT is therefore used as the upper limit for the continued drilling operation. Drilling proceeds to a depth of 13 200 feet, continuously increasing the dynamic back pressure to compensate for the increasing formation-pore pressure. At this depth, it becomes challenging to continue safe drilling and the $6^5/_8$" liner is run. It would be possible to drill yet another contingency section ($5^3/_4$"), but is seems highly unlikely that this would be sufficient to reach the target depth of 27 000 feet. The drilling operation has therefore been ceased at this depth. The planned versus actual well design for the CBHP MPD variant is presented in Figure 5.10. It is seen that this variant is able to drill longer section than conventional drilling was, but the target depth of 27 000 feet was not reached.

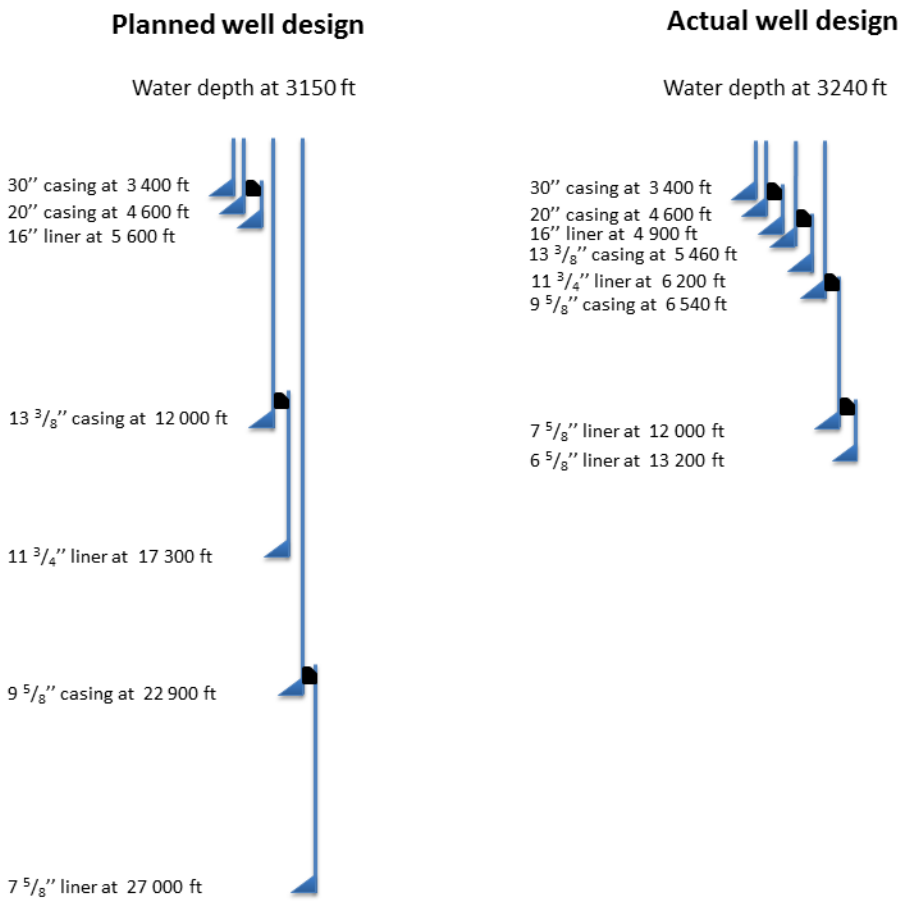

Figure 5.10: Planned versus actual well design for CBHP MPD.

5.2.3 Controlled Mud Level DGD, MPD

Filled riser during static conditions

The actual drilling program for the CML variant with a filled riser during static conditions is illustrated in Figure 5.11 and the details are presented in Table C.9 and C.10. The well pressure profile for this variant looks quite similar to the CBHP MPD variant. Also this variant requires four sections to be drilled in the upper, narrow mud weight window.

After the surface casing has been set at 4 600 feet, the riser and BOP has been run and the LOT conducted, drilling is initiated with the CML approach. The LOT measures a lower fracture prssure margin than estimated (9,80 ppg) and the mud weight is therefore set to 9,80 ppg to avoid fracturing the formation during drilling. The operation is commenced and drilling proceeds until 4 960 feet. At this depth, the pore pressure margin increases to 9,81 ppg which triggers the need to stop drilling and run the 13 $^{3}/_{8}$" casing.

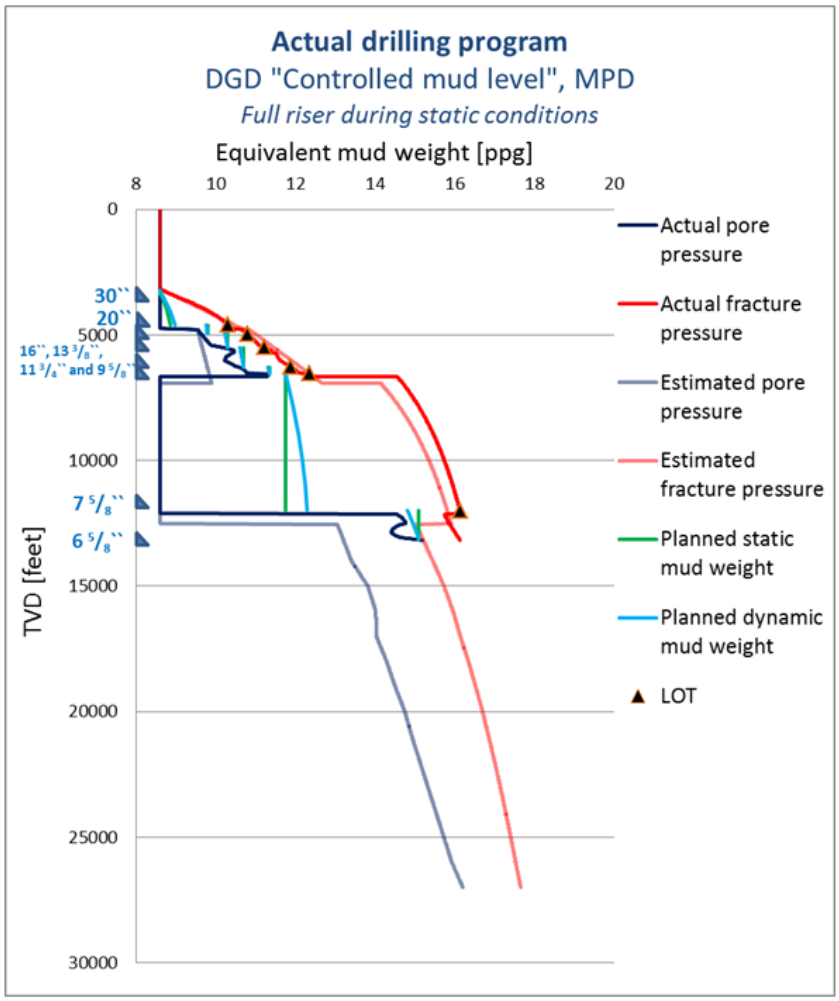

Figure 5.11: Actual drilling program using the CML DGD, MPD approach and a full riser during static conditions.

It is experienced that also this technique is struggling prior to entering the salt layer. A total of four sections are required from 4 600 feet to 6 540 feet, which is equivalent to the CBHP variant. At 6 680 feet, the top of salt is entered with a $8^1/_2$" hole and drilling proceeds until 7 850 feet. At this depth, the dynamic mud weight is equal to the pore pressure margin at 6 560 feet (11,51 ppg). To cope with this situation, the same strategy as was performed with the CBHP variant has been chosen. The dynamic mud level is set to a fixed level of 87 meters, which causes the dynamic and static effective mud weights to be equal at the casing shoe. This enables drilling to continue until 12 000 feet and a 7 $^5/_8$" liner is set at this depth.

The LOT performed at 12 000 feet indicates a higher fracture pressure margin than estimated, 15,63 ppg as opposed to the estimated 15,31 ppg. In order to stay below the estimated fracture margin when exiting the salt, the mud weight is set to 14,50 ppg and

$6^{7}/_{8}$" contingency hole is drilled. When the base of salt is breached at 12 140 feet, the measured pore pressure margin is 14,72 ppg which results in a kick. A mud weight with a density of 14,80 ppg is circulated into the wellbore to bring the well in overbalance and drilling is continued. At 12 240 feet, the pore pressure margin is measured to 14,82 ppg, which triggers the need to increase the mud weight further. It has been chosen to increase the mud weight to 15,10, which enables drilling to continue until 13 140 feet. At this depth, the pore pressure margin is measured to 15,15 ppg. It has been decided to cease the operation at this depth as the actual fracture pressure in this interval is highly uncertain. The disadvantage experienced with this technique is the inability to increase or decrease the wellbore pressure without changing the mud weight. However, if riser is kept partly evacuated during static conditions, this would have been possible as is demonstrated in the next case.

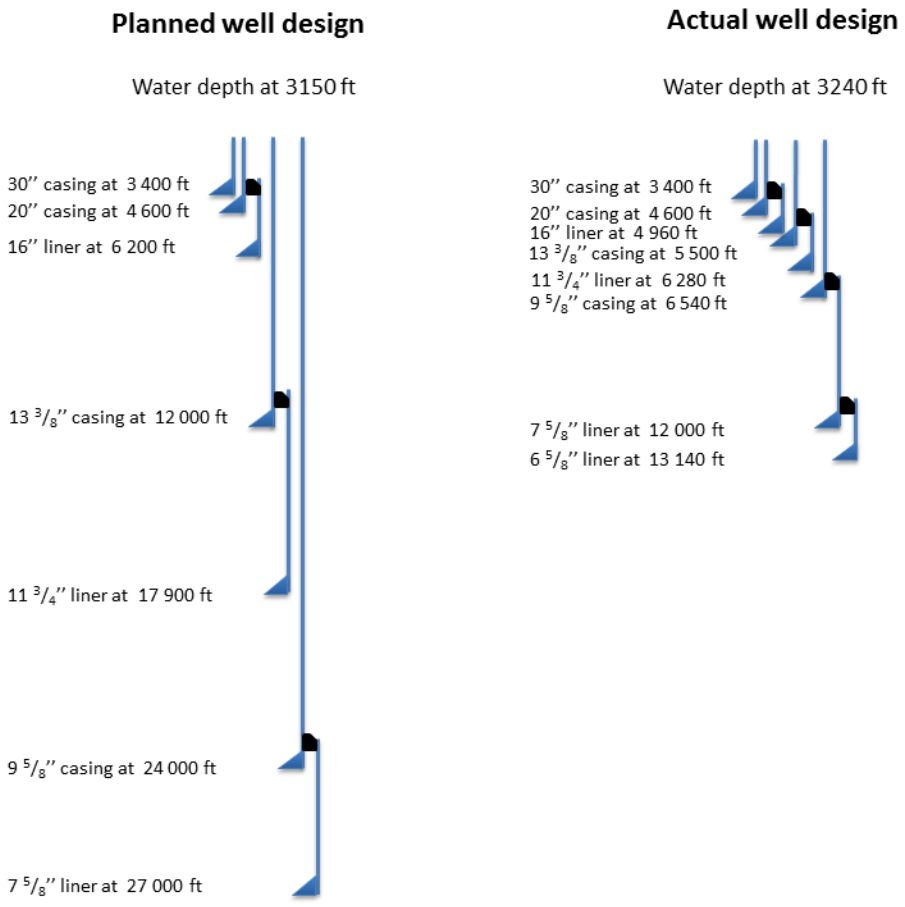

Figure 5.12: Planned versus actual well design for the CML DGD, MPD with a full riser during static conditions.

Partly evacuated riser during static conditions

The actual drilling program for the CML variant, with a partly evacuated riser during static conditions, is illustrated in Figure 5.13. The details are presented in Table C.11 and C.12. The advantages offered by this technique are in particular seen in the upper wellbore sections. As seen in the figure, the downhole wellbore pressure is manipulated to better match the measured pore and fracture gradients. Ultimately, this makes it possible to drill each section longer prior to setting casing, compared to any of the aforementioned techniques.

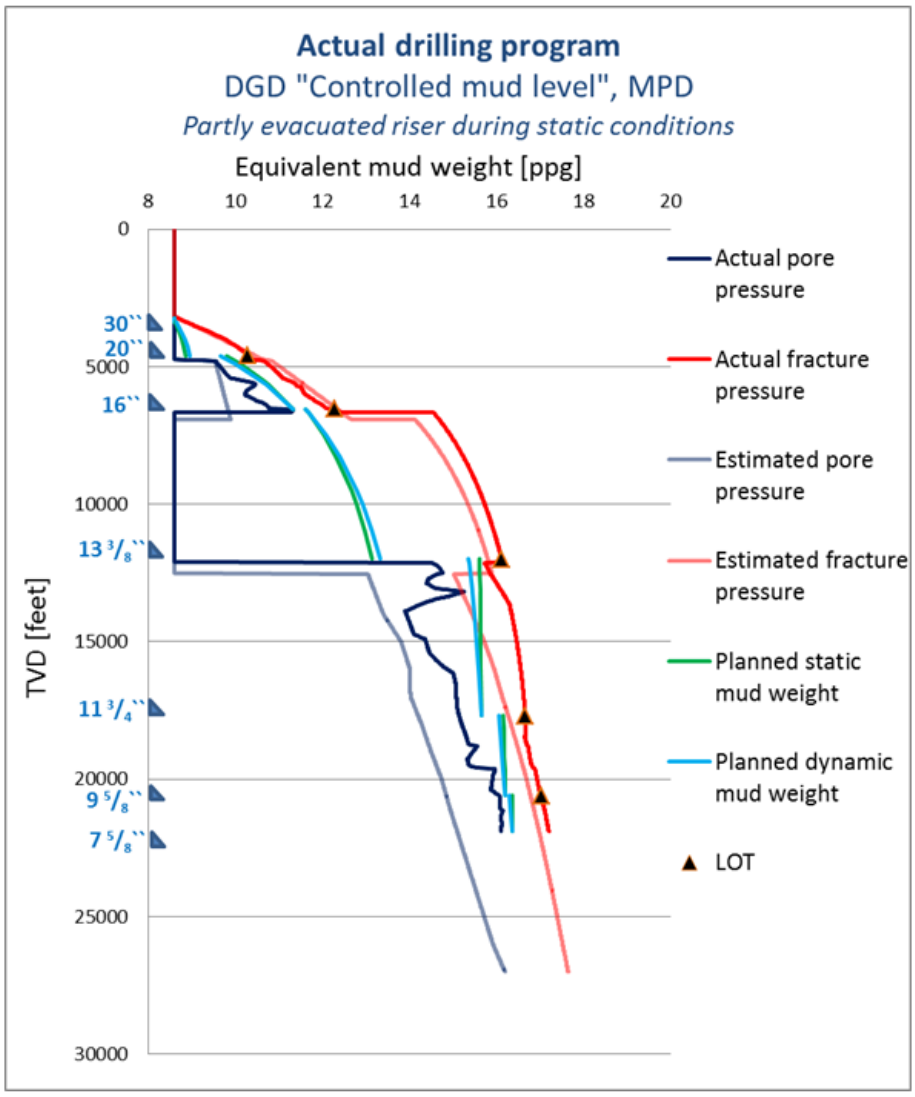

Figure 5.13: Actual drilling program using the CML DGD, MPD approach and a partly evacuated riser during static conditions

After the surface casing has been set at 4 600 feet, the riser and BOP has been run and the LOT conducted, drilling is initiated with the partly evacuated CML approach. As seen on the actual drilling program, no changes are performed at this point and drilling is initiated according to the plan until 5 500 feet is reached. At this depth, the measured formation-pore pressure is 10,33 ppg whereas the effective mud weights are 10,28 ppg. A possible solution to this scenario would be to increase the static mud level in the riser. However, as the effective static mud level at the casing shoe is only 0,04 ppg below the maximum level, another approach has been selected. A more dense drilling fluid is circulated into the wellbore (15,00 ppg), while gradually lowering the static mud level to 490 meter. As seen in Table C.11, this causes the effective mud weights at 5 500 feet to increase, whereas the effective static mud weight at the casing shoe depth is kept constant. Drilling is resumed until 6 540 feet. According to the plan, this section was intended to cease at 6 200 feet, but it was decided to continue drilling with the updated drilling plan until 6 540 feet. Between 6 520 and 6 540 feet, the pore pressure margin suddenly increases from 10,95 to 11,39 ppg. This triggered the need to set the 16" liner at this depth, making this section 340 feet longer than planned. When the well is drilled with this dual gradient variant, only one section is required after the surface casing prior to entering the salt layer.

After the 16" liner has been set, a LOT is carried out at 6 540 feet, indicating a fracture margin of 11,78 ppg. This section is drilled with the updated mud weight of 15,00 ppg and a static mud level of 450 meter. At 6 680 feet, the pore pressure suddenly drops to a normal pressure gradient, indicating that the salt layer has been entered. Drilling is continued uninterrupted until 8 300 feet. The ever-decreasing dynamic mud level has caused the effective dynamic mud weight at 6 560 feet to decrease below the measured formation-pressure margin. To cope with this situation, the same approach has been selected here as was performed with the aforementioned CML application mode. The point of constant wellbore pressure is changed from the bit depth to the 16" liner shoe depth. This enables drilling to continue until the planned depth of 12 000 feet in the salt layer.

The $12^1/_4$" section is initiated according to the plan and the well pressure is kept below the estimated fracture margin at the base of the salt. When the salt layer is exited at 12 140 feet, 400 feet earlier than estimated, the measured pore pressure margin is 14,72 ppg. This triggered the need to increase the static mud level from 400 to 200 meter as the pore pressure is much higher than expected. As drilling advances, it is experienced that the pore pressure continues to increase. To compensate for this, the static mud level is gradually increased. When the bit reaches 17 700 feet, the effective dynamic mud weight at 13 200 feet is equal to the measured pore pressure margin, and the effective static mud weight is only 0,01 ppg below the fracture margin. This triggered the need to cease drilling and run

the $11^3/_4$" liner.

As seen in Table C.12, the $9^5/_8$" casing is set at 20 580 feet, whereas the $7^5/_8$" liner is set at 21 900 feet. The real pore and fracture pressure information ends at this depth, and the operation has therefore been ceased. Of the discussed drilling techniques, it is seen that this variant best matches the planned well design.

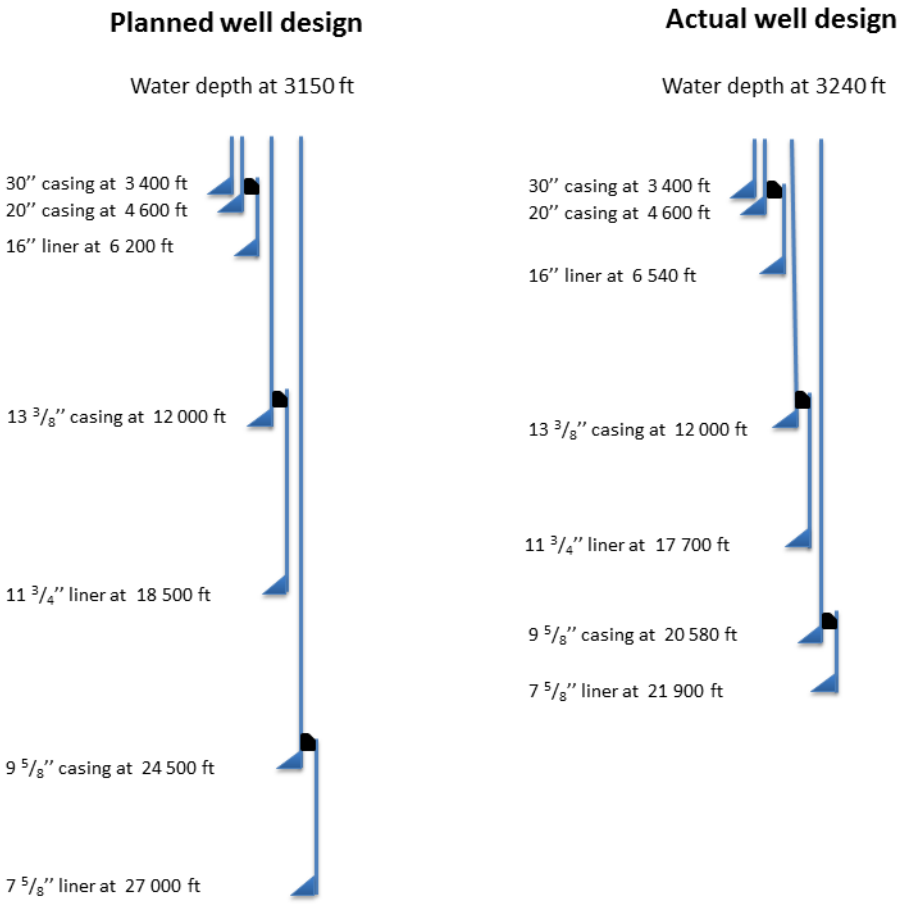

Figure 5.14: Planned versus actual well design for the CML DGD, MPD with a partly evacuated riser during static conditions.

Chapter 6

Discussion and evaluation

The case study showed clear advantages of using MPD over conventional drilling in narrow and uncertain pressure regimes. CBHP and both applications of CML were able to drill through, and past the (presented) salt layer. Where the latter of the CML mode shows the advantage of using a partly evacuated riser in a narrow and rapidly increasing pressure environment.

As illustrated in Figure 6.1, production of oil and gas from deep waters has steadily increased since the race for deepwater reservoirs began in the early 1990s. By 2015, it is expected that the oil production from deep water reservoirs will reach 10 million barrels/day, which will cover approximately 10 % of the global demand for oil. Drilling in these conditions are often associated with narrow and unpredictable mud windows, high amounts of costly NPT and increased risk. The oil and gas industry works determined to minimize the costs and risks related to the development of deep water fields. With unique challenges, such as unstable boreholes and vast amounts of salt, there is a need for innovative techniques to develop these areas in a safe and effective manner [8].

The Deepwater Horizon accident serves as a strong reminder of the catastrophic outcome an uncontrollable event in deep waters may entail. Eleven people lost their lives, seventeen were injured and nearly five million barrels (0,8 m^3) of oil were released to the environment. As a consequence of this, there has been an increased focus on enhancing the safety in deepwater drilling. The International Oil and Gas Technology concluded in their annual report, as of 2011, that [59]: "*The industry is still recovering from the repercussions of the Macondo incident in the Gulf of Mexico. Many operators now consider that the use of MPD techniques on the Macondo well might have facilitated the early identification of an imminent "kick", which would have allowed the implementation of effective mitigation action* [59]."

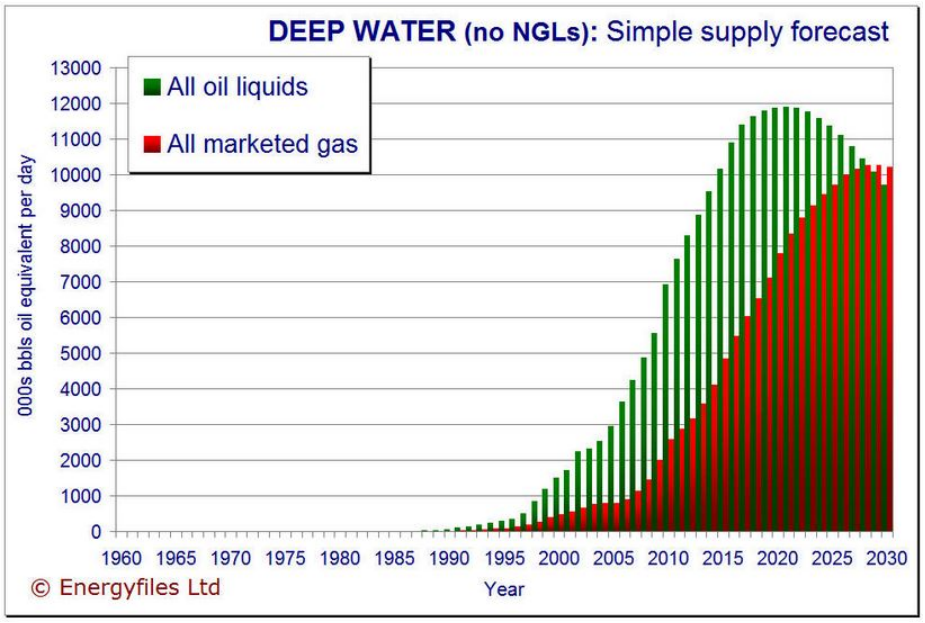

Figure 6.1: Illustration of global hydrocarbon production from deep waters [57].

6.1 Interpretation of results

Implementing MPD in a deepwater well in the Gulf of Mexico (ref. Chapter 5) showed clear advantages in terms of target depth. A tighter mud window than expected brought conventional drilling to a standstill after 5 500 feet whereas CBHP and both applications of CML were able to drill through, and past the (presented) salt layer to a total depth of roughly 13 000 feet. Drilling with CML and a partly evacuated riser would allow drilling to continue all the way to 21 900 feet.

As can be seen on Figure 6.2, the real mud weight window is narrower than the predicted, which makes conventional drilling both risky and uneconomical. The most noticeable difference took place in the narrow and rapidly increasing pressure regimes around 4 600 to 6 600 feet. With conventional drilling it becomes impossible to drill this section without defying the defined pressure boundaries, and face potentially huge amounts of fluid loss/influx.

The same challenges as CBHP MPD were experienced when the CML method was used with a static filled riser. Conventional drilling proved inadequate in this interval and both the CBHP and CML had to use four sections to complete the interval. A significant difference was experienced when the static riser level was reduced. This allowed the narrow pressure regime from 4600 to 6600 feet to be drilled with only one section. This was achieved by lowering the riser lever and using a dense drilling fluid, which enabled the well pressure profile to better "follow" the underground pressure environment. With the current technology you need AGRs RMR method to allow for this approach to be taken.

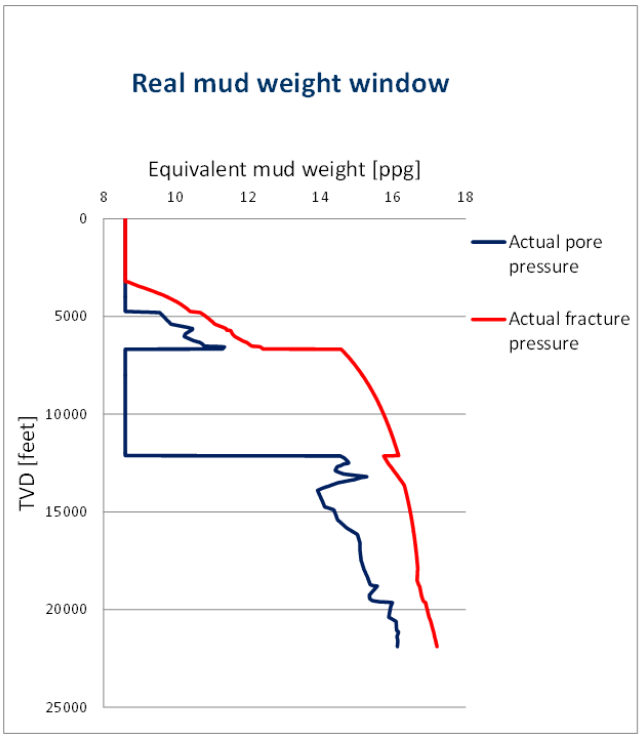

Figure 6.2: The real mud weight window presented in the case study

Figure 6.3 below shows a typical Dual Gradient mud profile when the RMR method is implemented. The 30x32" hole would be in this case be limited to 8,9 ppg if the well was drilled with a riser, and can with RMR be increased to 10,5 ppg. RMR allows for the 26" hole to be drilled with 13,5 ppg, where it previously was limited to 11,0 ppg. The effect of this, is increased drilling margins, allowing extended hole depths. The optimal solution for the well presented would be to implement AGRs RMR method in the upper section, and then proceed with the CBHP variant. This would enable the top hole sections to be drilled with a pressure profile that better "follows" the pore and fracture pressure gradients. Whereas the lower sections would be drilled with the operation flexibility offered by CBHP [60].

The next step will be to develop the AGRs CML variant, EC-drill, into a "full DGD" post-BOP capability. This will be a logical next step after the successful field trial of AGRs CML variant, EC-drill, conducted on the Troll field in the spring of 2014 [60]. On May 13, 2014, the enhanced drilling department of AGR published a press release regarding the Troll pilot, stating that: "*EC-Drill made it possible for Statoil to minimise losses, while the amount of drilling mud used was reduced by approximately 70 per cent in relation to comparable wells. Following the Troll Pilot, Statoil is due to introduce EC-Drill to the Gulf of Mexico later in the year, on the Maersk Developer, for a multi-well project* [61]."

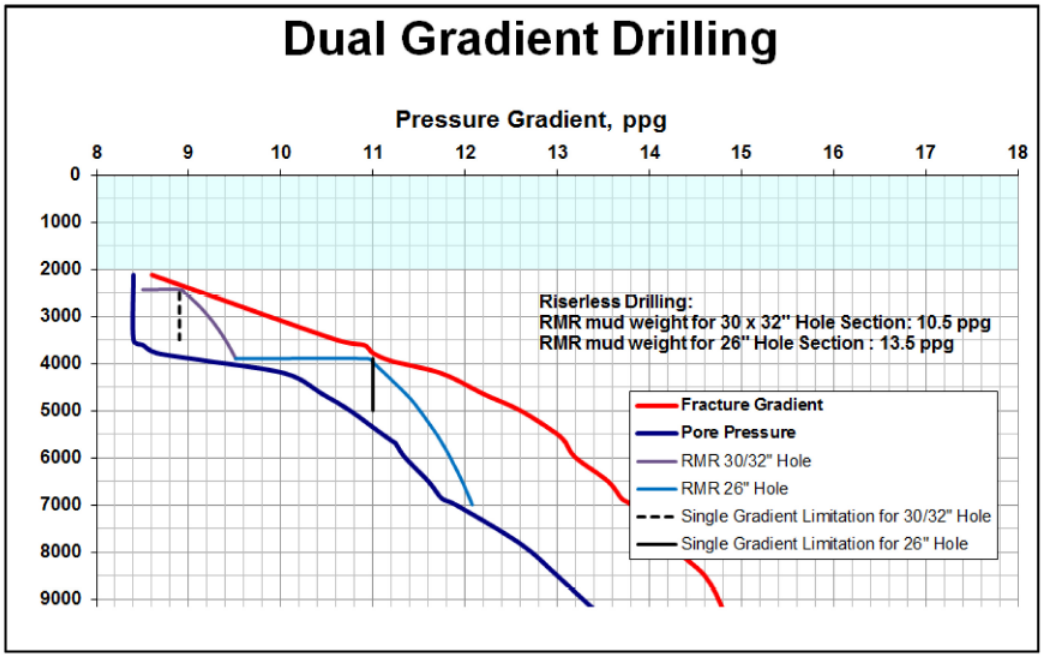

Figure 6.3: Typical mud profile for the RMR method, notice how this method is able to manipulate the mud profile to better match the mud weight window [60]

The development of the EC-drill technique into a "full DGD" technique will require modified well control procedures to enable a kick to be circulated out of the wellbore without fracturing the formation. *Ziegler et.al 2013* states that it will be possible to develop the EC-drill technology into a "full DGD" Controlled Annular Mud Level with modified well control equipment. As discussed in this thesis, this will enable increased operational flexibility in narrow and rapidly increasing pressure environments [62].

Chapter 7

Conclusion

The concluding remarks of this thesis are summarized below:

- To meet the worlds increasing demand for oil and gas, the petroleum industry has extended its portfolio to also include deepwater reservoirs. However, drilling under these conditions are risky, and a huge responsibility lies upon the production companies in doing so in a safe manner.
- MPD increases the drillability and safety while reducing the amount of costly NPT in narrow and unpredictable mud weight windows. This makes MPD a sustainable candidate for safe and cost-effective drilling in deep water depths.
- Development of AGRs EC-drill into a "full DGD" technique will enable the well pressure profile to better "follow" and adapt to the underground pore and fracture pressure gradients. The overall advantage of this will be a reduction in the amount of casing strings required to reach target depth.

Nomenclature

Symbol	
β	Failure angle caused by shear failure
Δh	Difference in height
Δt	Acoustic wave velocity
Δt_{normal}	Normal acoustic wave velocity
μ_{eff}	Effective fluid viscosity
$\mu_{eff,ann}$	Effective annular fluid viscosity
μ_{pl}	Plastic viscosity
ρ	Density
$\bar{\rho}_a$	Average annular density
ρ_c	Cuttings density
ρ_{lam}	Light annular mud density
ρ_m	Drilling fluid density
ρ_1	Upper fluid/gas density
ρ_2	Lower fluid density
σ	Total stress
σ_h	Minimum horizontal stress
σ_H	Maximum horizontal stress
σ_i	Principal stress
σ_n	Normal stress
σ_v	Vertical stress
σ'_i	Effective principal stress
σ'_h	Effective minimum horizontal stress
σ'_v	Effective vertical stress
σ'_1	Maximum effective stress
σ'_3	Minimum effective stress
τ	Shear stress
τ_0	Yield shear stress

Continued on next page

– Continued from previous page

Symbol	
φ	Angle of internal friction
A	Area
C_0	Uniaxial compressive strength
$\bar{C}_c$	Average concentration of cuttings
$C_{c,i}$	Initial concentration of cuttings
d	d'exponent
d_c	dc-exponent
$d_{c,normal}$	dc-exponent in a normally pressured formation
d_{bit}	Bit diameter
d_i	Inner annulus diameter
d_o	Outer annulus diameter
D	Vertical depth
$D_{formation}$	Depth below seabed
D_w	Water depth
F	Force
g	Gravity constant
$h_{top,frac}$	Vertical depth down to first fractured zone
h_1	Vertical height of upper fluid/gas
h_2	Vertical height of lower fluid
$h_{1,dyn}$	Vertical height of upper fluid/gas during dynamic conditions
$h_{1,stat}$	Vertical height of upper fluid/gas during static conditions
$h_{2,dyn}$	Vertical height of lower fluid during dynamic conditions
$h_{2,stat}$	Vertical height of lower fluid during static conditions
L	Length
P_{AF}	Annular friction pressure
$P_{BP,dyn}$	Surface back pressure applied during dynamic conditions
$P_{BP,stat}$	Surface back pressure applied during static conditions
P_C	Pressure exerted by cuttings
$P_{Collapse}$	Collapse pressure
P_f	Formation-pore pressure
$P_{f,est}$	Estimated formation-pore pressure
P_{frac}	Fracture pressure
$P_{frac,est}$	Estimated fracture pressure
$P_{hydrostatic}$	Hydrostatic head of drilling fluid

Continued on next page

– *Continued from previous page*

Symbol	
P_i	Rock failure pressure
P_{normal}	Normal pore pressure
P_{ovb}	Overburden pressure
P_w	Well pressure
P_{water}	Hydrostatic head of water
$P_{well,actual}$	Actual well pressure
$P_{well,planned}$	Planned well pressure
Q_c	Amount of cuttings generated during drilling
Q_m	Drilling fluid flow rate
$Q_{tot,a}$	Total annular flow rate
R	Resistivity
R_{normal}	Resistivity in a normally pressured formation
Re	Reynolds number
R_t	Cuttings transport ratio
S_0	Inherent shear strength
T_o	Tensile strength
$\bar{v}$	Average fluid velocity
v_{slip}	Slipping velocity of cuttings
v_t	Cuttings transport velocity

Abbreviations	
BHA	Bottom-hole assembly
BHP	Bottom-hole pressure
BHP_{dyn}	Dynamic bottom-hole pressure
BHP_{stat}	Static bottom-hole pressure
BOP	Blow out preventer
BSEE	Bureau of Safety and Environmental Enforcement
CBHP	Constant Bottom-Hole Pressure
CCS	Continuous circulation system
CML	Controlled Mud Level
DAPC	Dynamic Annular Pressure Control
DGD	Dual Gradient Drilling
DSV	Drillstring valve
ECD	Equivalent circulating density
EDS	Enhanced Drilling Solutions
EMW	Equivalent mud weight
E&P	Exploration and production
FCP	Fracture Closure Pressure
FIT	Formation integrity test
FPP	Fracture propagation pressure
GOM	Gulf of Mexico
HSE	Health, safety and environment
IADC	International Association of Drilling Contractors
LAM	Light annular mud
LCM	Lost circulation material
LOP	Leak-Off Pressure
LOT	Leak-Off Test
LRRS	Low Riser Return System
MAASP	Maximum allowable annular surface pressure
MPA	Megapascal
MPD	Managed Pressure Drilling
MWD	Measurements while drilling
NOV	National Oilwell Varco
NPT	Non-Productive Time
NTNU	Norwegian University of Science and Technology
ORS	Ocean Risers System

Continued on next page

– *Continued from previous page*

Abbreviations	
PMCD	Pressurized Mud-Cap Drilling
PWD	Pressure-while-drilling
RCD	Rotating Control Device
RFC	Returns-Flow-Control
RMR	Riserless Mud Return
ROP	Rate of penetration
RPM	Revolutions per minute
SICP	Shut-in casing pressure
TVD	Total vertical depth
UBD	Underbalanced drilling
WOB	Weight on bit
WD	Water depth
XLOT	Extended Leak-Off Test

Bibliography

[1] "Why High Gas Prices Are Here to Stay", [Online], Downloaded from: http://tinyurl.com/lcgv4ge, (accessed 02.06.2014)

[2] "National Commission on the BP Deepwater Horizon Oil Spill and Offshore Drilling", [Online], Downloaded from: http://www.cs.ucdavis.edu/~rogaway/classes/188/materials/bp.pdf, (accessed 02.06.2014)

[3] "The Deep Offshore: Billions of Barrels" [Online], Downloaded from: http://tinyurl.com/n8chhod, (accessed 31.03.2014)

[4] Perez, M.A., Clyde ,R., and D'Ambrosio, P. et.al. "Meeting the Subsalt Challenge", Oilfield Review 20. October 01, 2008. https://www.slb.com/~/media/Files/resources/oilfield_review/ors08/aut08/meeting_the_subsalt_challenge.pdf

[5] "Deepwater Operations" [Online], Downloaded from: http://tinyurl.com/lxy4d92, (accessed 07.03.2014)

[6] "Reduce Non-Productive Time (NPT)" [Online], Downloaded from: http://tinyurl.com/kppvnac (accessed 13.02.2014)

[7] Pritchard, D., "Real-time data offers critical tool to redefine well control, safety", [online], Downloaded from: http://tinyurl.com/og6648z, (accessed 13.02.2014)

[8] Kjoesnes, I., Gaassand, S. and Stave, R. et.al "ECD Management Toolbox for Floating Drilling Units", OTC-25292, this paper was prepared for presentation at the Offshore Technology Conference, Houston, Texas, U.S.A., 05-08 May 2014. http://dx.doi.org/10.4043/25292-MS

[9] International Association of Drilling Contractors "Managed Pressure Drilling" [online], Downloaded from: http://www.iadc.org/ubo-mpd-committee/subcommittees/ (accessed 31.01.2014).

[10] Rehm, B. et.al "Managed Pressure Drilling", Gulf Publishing Company, Houston, Texas, USA., 2008.

[11] Fjær, E., Holt, R.M., Horsrud, P. et.al 2008, "Petroleum Related Rock Mechanics", second edition, Development in Petroleum Science, Elsevier

[12] Olsen, E. J., "Managed Pressure Drilling (MPD), Subsea, History in Brief, Drilling Technology", Lecture presented in the unit "TPG4215, Høyavviksboring" at NTNU, 12 October 2012.

[13] Langley, W. D. and Dunsavage, P. M., "Pollution Control in the Oil Industry - From Spindletop to Santa Barbara", SPE-3096-MS, this paper was prepared for the 45th Annual Fall Meeting of the Society of Petroleum Engineers of AIME, Houston, Texas, U.S.A., 4-7 October 1970. http://dx.doi.org/10.2118/3096-MS

[14] Helgeland, L., Andersen, A. A. and Kvalheim, F. O. et.al "Gas kick due to hydrates in the drilling for offshore natural gas and oil", Project in the Unit, TPG4140 NATURGASS at NTNU, autumn 2012.

[15] Wenaas, A., "Investigating the Consequences Reservoir Depletion Induced Stress Entails", Specialization Project in the Unit TPG4520-Drilling Engineering at NTNU, autumn 2013.

[16] Skalle, P., 2012 "Pressure Control During Oil Well Drilling", Ventus Publishing ApS, Downloaded from: www.bookboon.com

[17] Fredrik, C. G., 2003 "A critical review of currently available pore pressure methods and their input parameters: glaciations and compaction of north sea sediments", Durham theses, Durham University. Available at Durham E-Theses Online: http://etheses.dur.ac.uk/4090/

[18] Osypov, K., Yang, Y., Bachrach, R. et.al "Assessing the risk of drilling hazards using seismic uncertainty analysis", [Online], Downloaded from: http://tinyurl.com/pel9nmx, (accessed 25.05.2014)

[19] Breckels, I.M. and van Eekelen H.A.M., "Relationship Between Horizontal Stress and Depth in Sedimentary Basins", this paper forms part Journal of Petroleum Technology, Volume 34, Number 9, pages 2191-2199., September 1982. http://dx.doi.org/10.2118/10336-PA

[20] Bartlit, F. H., Sankar, S. N. and Grimsley, S. C., 2011 "Chief Counsel's Report, National Commission on the BP Deepwater Horizon Oil Spill and Offshore Drilling, Chapter 2 - Drilling for Oil in Deepwater", [Online] Downloaded from: http://www.eoearth.org/files/164401_164500/164423/full.pdf, (accessed 05.06.2014)

[21] Rocha, L. A. S., Junqueira, P. and Roque, J. L., "Overcoming Deep and Ultra Deepwater Drilling Challenges", OTC 15233, this paper was prepared for presentation at the 2003 Offshore Technology Conference, Houston, Texas, U.S.A., 5–8 May 2003. http://dx.doi.org/10.4043/15233-MS

[22] "Design evolution of a subsea BOP, Blowout preventer requirements get tougher as drilling goes ever deeper" [Online], Downloaded from: http://www.drillingcontractor.org/dcpi/dc-mayjune07/DC_May07_BOP.pdf, (accessed 04.06.2014)

[23] "Deepwater Horizon Accident Investigation Report", internal investigation performed by BP., September 8, 2010. [Online], Downloaded from: http://tinyurl.com/36lcn49, (accessed 01.04.2014)

[24] Fitzgerald, B., Breen, P. M., and Patrick, J. H. "Making the Safety Case Work - Post Macondo and Montara", SPE-158199-MS, this paper was prepared for presentation at the International Conference on Health, Safety and Environment in Oil and Gas Exploration and Production, Perth, Australia., 11-13 September 2012. http://dx.doi.org/10.2118/158199-MS

[25] The Telegraph, "BP accuses drilling partner of lack of disclosure over Deepwater accident", [Online], Downloaded from: http://tinyurl.com/l7udnwk, (accessed 05.06.2014)

[26] "Gulf drilling ban lifted if you 'play by the (new) rules" [Online], Downloaded from: http://www.nbcnews.com/id/39633824/ns/us_news-environment/t/gulf-drilling-ban-lifted-if-you-play-new-rules/#.U49-Y_lESoM, (accessed 04.06.2014)

[27] Olin, J. M., "Should BP be Liable for Economic Losses due to the Moratorium on Oil Drilling Imposed After the Deepwater Horizon Accident¿' [Online], Downloaded from: http://www.law.harvard.edu/programs/olin_center/papers/pdf/Shavell_708.pdf, (accessed 04.06.2014)

[28] Hammond, A., Forbes "Four Years On, The Legacy Of Deepwater Horizon Remains Intensely Controversial For The Oil Industry", [Online] Downloaded from http://tinyurl.com/lq5r5vv, (accessed 04.06.2014)

[29] Olsen, E. J., "Managed Pressure Drilling, What It Is and What It Is Not", Lecture presented in the unit "TPG4215, Høyavviksboring" at NTNU, 12 October 2012.

[30] Kinn, A. A., "Comparison of Methods Enabling MPD from Floaters", Specialization Project in the Unit TPG4520-Drilling Engineering at NTNU, autumn 2013.

[31] "IADC, Drilling Lexicon", [Online], Downloaded from: http://www.iadclexicon.org/equivalent-circulating-density-ecd/ (accessed 11.05.2014)

[32] Golan, M., "IADC RIGPASS, Underbalanced Drilling Orientation", Professor at NTNU.

[33] Olsen, E. J., "Underbalanced Operations, IADC Riggpass", Lecture presented in the unit "TPG4215, Høyavviksboring" at NTNU, 06 October 2012.

[34] "A new technology for reducing the density of drilling fluid", [Online], Downloaded from: http://www.egyptoil-gas.com/admin/industry/Technology%20&%20Solutions%20Issue%207%20July%202007.pdf, (acessed 13.05.2014)

[35] Olsen, E. J., "UBO Theory" Lecture presented in the unit "TPG4215, Høyavviksboring" at NTNU, 06 October 2012.

[36] Malloy, K. P., Stone, R., Medley, G. H. et.al. "Managed-Pressure Drilling: What It Is and What It Is Not", SPE-122281-MS, this paper was prepared for presentation at the IADC/SPE Managed Pressure Drilling and Underbalanced Operations Conference and Exhibition, San Antonio, Texas., 12-13 February 2009. http://dx.doi.org/10.2118/122281-MS

[37] Smith, K., "Fundamentals of Managed Pressure Drilling", Lecture presented in the unit "TPG4215, Høyavviksboring" at NTNU, 12 October 2012.

[38] Haghshenas, A., Paknejad, A. S., Rehm, B. et.al 2008, "'The Why and Basic Principles of Managed Well-Bore Pressure", Chapter one, Gulf Publishing Company.

[39] [Online], Downloaded from: http://www.drilling-mud.org/, (accessed 17.03.2014)

[40] Qutob, H., "Managed Pressure Drilling: Drill the Un-Drillable", [Online], Downloaded from: http://www.spe.org/dl/docs/2012/qutob.pdf, (accessed 19.03.2014)

[41] Nauduri, S., Medley, G. H., and Schubert, J.J. "MPD: Beyond Narrow Pressure Windows", SPE-122276-MS, this paper was prepared for the IADC/SPE Managed Pressure Drilling and Underbalanced Operations Conference & Exhibition, San Antonio, Texas, USA., 12-13 February 2009. http://dx.doi.org/10.2118/122276-MS

[42] Darmawan, G. R., Susilo, S. D., and Toralde, J. S. "Successful Installation and Operation of Downhole Isolation Valve Combined with Pressurized Mud Cap Drilling to Safely Develop Sour Gas, Fractured-limestone Reservoir in Gundih Field, Indonesia", SPE-140269-MS, this paper was prepared for presentation at the SPE European Health, Safety and Environmental Conference in Oil and Gas Exploration and Production, Vienna, Austria., 22-24 February 2011. http://dx.doi.org/10.2118/140269-MS

[43] Toralde, J. S. S., "Pressurised Mud Cap Drilling", [Online], Downloaded from: http://www.spe.org/training/courses/PMCD.php, (accessed 18.03.2014)

[44] Rojas, F., Mathews, T. P., Jayah, M. N. et.al. "Implementation of PMCD to Explore Carbonate Reservoirs from Semi-Submersible Rigs in Malaysia results in Safe and Economical Drilling Operations", SPE-163479-MS, this paper was prepared for presentation at the SPE/IADC Drilling Conference, Amsterdam, The Netherlands., 5-7 March 2013. http://dx.doi.org/10.2118/163479-MS

[45] "Weatherford, Pressurized Mud-Cap Drilling" [Online], Downloaded from: https://www.youtube.com/watch?v=-qpNxyI0OXk, (accessed 18.03.2014)

[46] Smith, K. L., Gault, A. D., and Witt, D. E. et.al. "SubSea MudLift Drilling Joint Industry Project: Delivering Dual Gradient Drilling Technology to Industry", SPE-71357-MS, this paper was prepared for presentation at the SPE Annual Technical Conference and Exhibition, New Orleans, Louisiana., 30 September – 3 October 2001. http://dx.doi.org/10.2118/71357-MS

[47] "A Deepwater Breakthrough: The Launch Window for Dual Gradient Drilling Technology", [Online], Downloaded from: http://www.pacificdrilling.com/files/doc_news/dualgradientdrilling.pdf, (accessed 14.05.2014)

[48] "RMR - Riserless Mud Recovery", [Online], Downloaded from: http://www.enhanced-drilling.com/solutions/rmr-riserless-mud-recovery, (accessed 15.05.2014)

[49] "Riserless mud recovery moves into deepwater", [Online], Downloaded from: http://tinyurl.com/qdekr86, (accessed 27.05.2014)

[50] "LRRS treads fine line within drilling window", [Online], Downloaded from: http://tinyurl.com/pnn5s37, (accessed 15.05.2014)

[51] "Enhanced Drilling, Managed Pressure Drilling", [Online], Downloaded from: http://tinyurl.com/ne6hp2r, (accessed 27.05.2014)

[52] "AGR, Enhanced Drilling, What we do, What's new? What's the value?", [Online], Downloaded from: http://m-innovate.statoil.com/StatoilTechnologyInvest/Documents/AGR%20Enhanced%20Drilling.pdf, (accessed 15.05.2014)

[53] Weatherford "Application Answers: Returns-Flow-Control Drilling" [Online], Downloaded from: http://www.weatherford.com/ECMWEB/groups/web/documents/weatherfordcorp/WFT021446.pdf, (accessed 24.03.2014)

[54] Skalle, P., 2012 "Drilling Fluid Engineering", Ventus Publishing ApS, Downloaded from: www.bookboon.com

[55] Skalle, P., 2012 "Exercises within Drilling Fluid Engineering", Ventus Publishing ApS, Downloaded from: www.bookboon.com

[56] "Schlumberger, The Oilfield Glossary", [Online], Downloaded from: http://www.glossary.oilfield.slb.com/, (accessed 11.05.2014)

[57] Energy Files "Deep Water" [Online], Downloaded from: http://www.energyfiles.com/global/deepwater.html, (accessed 31.03.2014)

[58] Faucon, B., "Oil Companies Go Deep" [Online], Downloaded from (requires access): http://tinyurl.com/lxxp8pl, (accessed 01.04.2014)

[59] "International Oil and Gas Technology, Annual Report for the year ended 31 December 2011", [Online], Downloaded from: http://www.international-ogt.com/archive/ar2011.pdf

[60] Stave, R., "Implementation of Dual Gradient Drilling", OTC-25222-MS, this paper was prepared for presentation at the Offshore Technology Conference, Houston, Texas, U.S.A., 5-8 May 2014. http://dx.doi.org/10.4043/25222-MS

[61] "Success for Enhanced Drilling's EC-Drill® technology on Troll pilot with Statoil" [Online], downloaded from http://www.enhanced-drilling.com/bilder/Troll_Pilot_success_for_Enhanced_Drillings_EC-Drill_-_13.05.14.pdf, (accessed 07.06.2014)

[62] Ziegler, R., Sabri, M. S. A. and Idris, M. R. "First Successful Commercial Application of Dual Gradient Drilling in Ultra-Deepwater GOM", SPE-166272-MS, this paper was prepared for presentation at the SPE Annual Technical Conference and Exhibition, New Orleans, Louisiana, USA, 30 September-2 October, 2013. http://dx.doi.org/10.2118/166272-MS

[63] Godhavn, J. M., "Managed Pressure Drilling (MPD)", Lecture presented in the Unit "TPG4215 Høyavviksboring" at NTNU, 26 October 2012.

[64] 'Managed pressure drilling erases the lines", [Online], Downloaded from: http://www.slb.com/~/media/Files/resources/oilfield_review/ors11/spr11/managed_pressure.pdf, (accessed 06.05.2014)

[65] Sangesland, S., "Well Barriers", Lecture presented in the Unit "TPG4215 Høyavviksboring" at NTNU, 29 October 2012.

[66] "Norsok Standard D-010, Well integrity in drilling and well operations", Revised the 3rd of August 2004, [Online], Downloaded from: http://www.govmin.gl/images/stories/petroleum/norsok/D-010r3_Well_integrity_in_drilling_and_well_operation.pdf, (accessed 03.05.2014)

[67] Mæland, M., "Managed Pressure Drilling, The Solaris Prospect - HPHT Exploration well", Master Thesis at NTNU in Petroleum Geoscience and Engineering, spring 2013.

[68] Kaasa, G.-O., Stamnes, Ø. N. and Aamo, O. M. et.al "Simplified Hydraulics Model Used for Intelligent Estimation of Downhole Pressure for a Managed-Pressure-Drilling Control System", SPE-143097-PA, this paper was accepted for presentation at the SPE/IADC Managed Pressure Drilling and Underbalanced Operation & Exhibition, Denver, USA., 5-6 April 2011. http://dx.doi.org/10.2118/143097-PA

[69] "MPD opens door to new well control options in deepwater", [Online], Downloaded from: http://tinyurl.com/pokmgep, (accessed 04.05.2014)

[70] "Continuous Circulation Drilling System", [Online], Downloaded from: http://maris-eu.com/ccd.html, (accessed 05.05.2014)

[71] "Managed pressure drilling? What is it anyway¿', [Online], Downloaded from: http://tinyurl.com/pmhnjrd, (accessed 05.05.2014)

Appendix A

MPD equipment/software

Table A.1: Required/optional equipment and software used in an automated CBHP MPD operation [63].

Equipment/software	Use	Optional/required
Annular seal	Provide back pressure	Required
Chokes	Adjust back pressure	Required
Hydraulic model	Compute back pressure	Required
Control System	Adjust choke	Required
Back pressure pump	Adjust back pressure without circulation	Optional
Flow meter	Detect kicks/losses	Optional
Continuous circulation system	Provide circulation and hole cleaning during connections	Optional

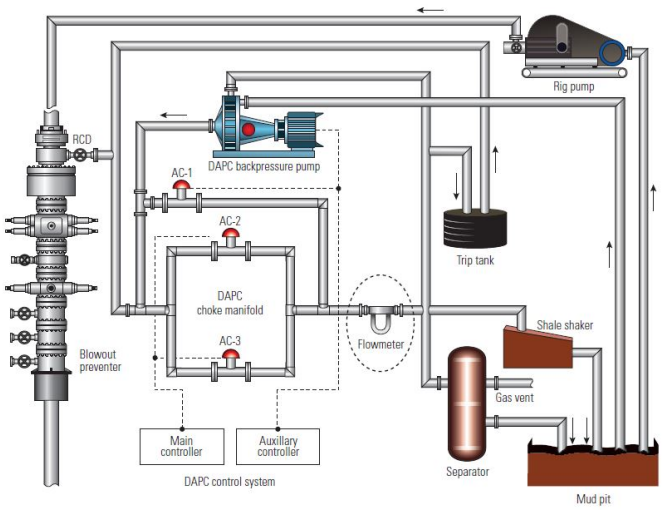

Figure A.1: Illustration of the Dynamic Annular Pressure Control (DAPC) closed circulation system. The DAPC system is designed to manage the BHP during both static and dynamic conditions [10, 64].

A.1 Annular seal

During all types of well operations (drilling, production, intervention and plug and abandonment operations) two independent pressure barriers are normally required [65]. According to the well integrity standard, NORSOK D-010, a well barrier is defined as:

"*An envelope of one or several barrier elements preventing fluids or gasses from flowing unintentionally from the formation, into another formation or to surface* [66]."

During a drilling operation, the primary pressure barrier consists of the hydrostatic drilling fluid pressure exerted on the formation. In case the primary pressure barrier should fail, a drilling blow out preventer functions as the secondary pressure barrier. In addition, elements such as a high pressure riser, wellhead, the last casing installed and the casing cement forms part of the secondary well barrier envelope [65, 66].

An essential part of MPD is to generate a surface back pressure in the annulus. This requires a seal to be formed between the flowing pressurized fluid in the annulus and surface during the drilling operation. A drilling BOP can offer such a sealing capability, but only as a temporary solution. If used as a more permanent solution, the stationary sealing elements in the BOP will be worn down due to drill string rotation. To cope with this problem, the industry has developed rotating annular seals. A rotating annular seal does not function as a replacement for the BOP, but as a supplement. Thus, the primary barrier during a MPD operation consists of hydrostatic drilling fluid pressure and the rotating annular seal, whereas the drilling BOP (placed below the rotating annular seal) functions as the secondary barrier. [65, 67].

The following two variations of rotating annular seals are in use [10]:

- Rotating control device (passive system)
- Rotating annular preventer (active system)

The main difference between the passive and active system, is that the passive system utilizes well pressure to apply sealing, whereas the active system uses external hydraulic pressure. Of which the passive system is by far the most commonly used. High-pressure RCDs make up more than 90 % of the rotating annular seals used in MPD operations, the RCD is further described below [30, 67].

A.1.1 Rotating control device (RCD)

The RCD is a rotating packer that seals around the drill pipe using an annular sealing element. This causes the returning, pressurized drilling fluid to be diverted to the choke manifold, see Figure A.2. The sealing element used in the RCD is deliberately undersized with $^{1}/_{2}$" - $^{7}/_{8}$" to the drill pipe diameter, and it must therefore be forced onto the pipe. This forms a tight seal around the pipe in the annulus, even at zero-pressure conditions. Increasing differential pressure across the element causes the sealing capability to be enhanced. This is described as a passive activation system. The annular seal element rotates with the pipe, thus limiting rotational wear, and is sealed into a bearing assembly, which is cooled and lubricated by a circulating hydraulic system [10].

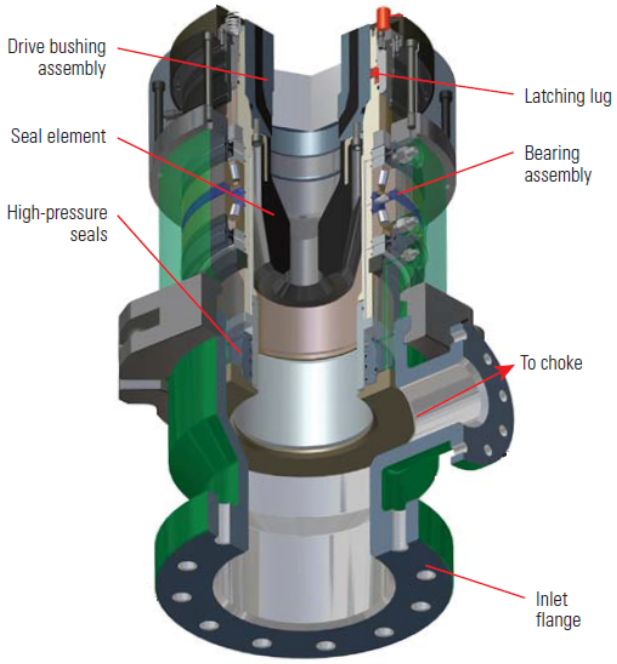

Figure A.2: Rotating control device [64].

The most common failure mode for passive RCDs are low-pressure leakage in the sealing element around the drill pipe or drill collar. Packers get worn down over time, and at a certain point it is no longer able to provide sealing at low pressures. Such a leak is often detected on the drill floor during a tripping or connection operation [10, 67].

A.2 Chokes

The choke is another vital equipment used in MPD. Its function is to regulate the surface back pressure exerted in the annulus. One or two choke valves, placed downstream of the rotating seal (see Figure A.1), carries out this task through choking the returning fluid

flow from the wellbore. The annuli back pressure is then adjusted through regulating the opening of the choke valve, see Figure A.3 [10, 30].

The choke valve can either be controlled manually or automatically. Of which, the automatic option enables a more accurate and fast response to unexpected pressure changes, than the manual. As a redundancy, two chokes are often installed in parallel downstream of the rotating annular preventer. This allows for one of them to regulate the flow rate whereas the other is closed. If the one regulating the flow rate fails, the other can take over. The failed choke is taken out and either replaced or repaired [10, 30].

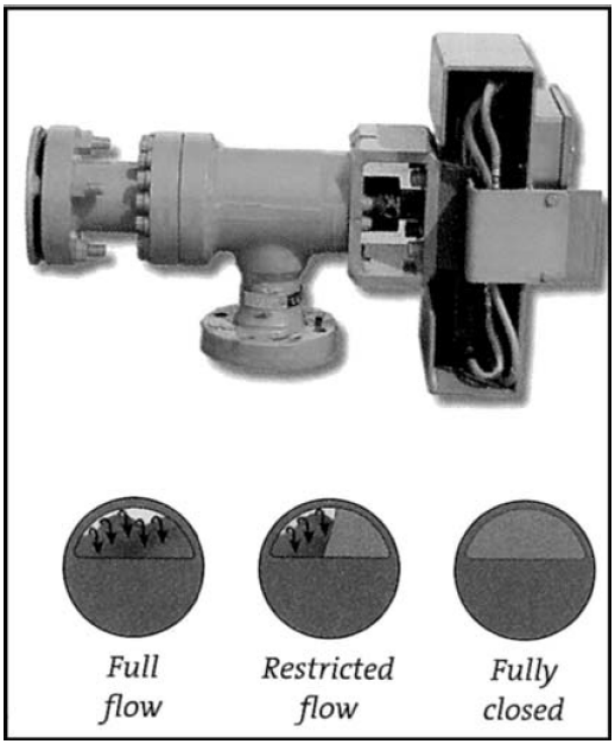

Figure A.3: M-I SWACO 10K Super Choke and choke plates [10].

A.3 Hydraulic model

An essential part of an automated MPD system is the hydraulic model, which provides continuous real-time estimates of the BHP. The hydraulic model compares the estimated BHP against the desired BHP, and provides an estimate of the choke pressure required to match the BHP set point. This estimate is then transmitted to the control unit which regulates the choke position, see Figure A.4 [68].

The hydraulic model is in many cases the limiting factor when it comes to pressure accuracy in a MPD operation. Much effort has therefore been invested into developing advanced

models that takes into account all the aspects of the drilling hydraulics. Despite the effort put into these models, some parameters are difficult to predict as they are highly uncertain and slowly changing. Such as the friction coefficients along the wellbore, the amount of gas dissolved in the drilling fluid, or external boundary conditions like uncertain reservoir temperature. Continuous calibration is hence a vital part of a real-time hydraulic model, used to accurately predict the BHP. Valuable calibration information is gathered from topside and downhole presure measurements [68].

A.4 Control system

In an automated MPD system, a control system provides automatic and continuous regulation of the choke valves position. Based on information from the hydraulic model, combined with a feedback algorithm, the control system adjusts the choke valves position. Continuously attempting to provide the requested back pressure. As illustrated in Figure A.4, the control system automatically controls the back pressure pump, further described in Section A.5 [68].

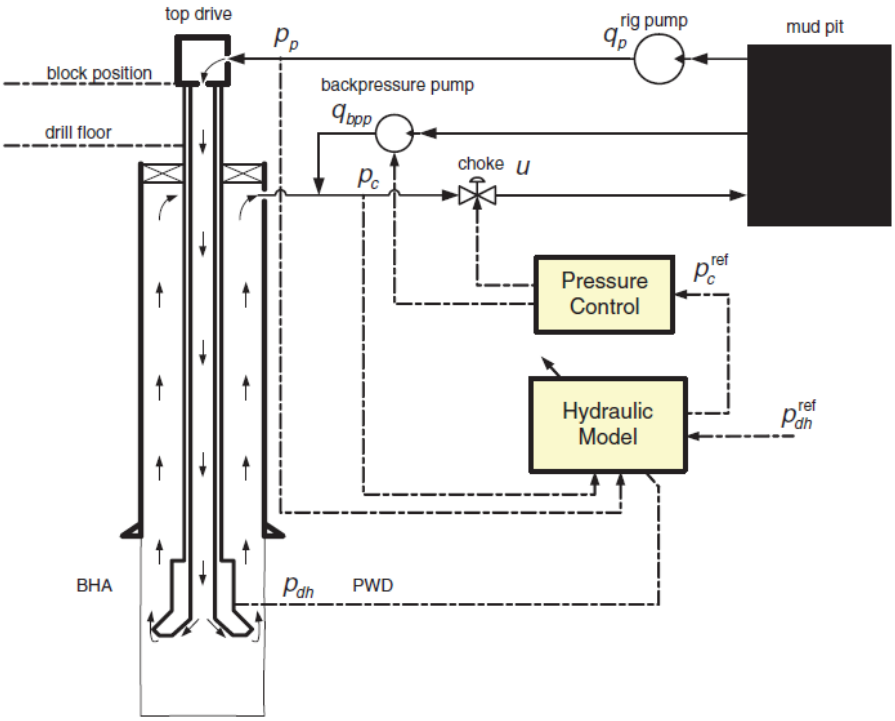

Figure A.4: Workflow schematic of an automated MPD operation, illustrating how the hydraulic model and the control system communicates and provides back pressure [68].

A.5 Back pressure pump

As long as a sufficient volume of mud flows through the aforementioned choke valve(s), there will be back pressure. When the flow rate slows down, the choke begins to close, attempting to keep a stable back pressure. However, if the flow rate should suddenly stop, the choke will close completely to trap the remaining back pressure. The amount of back pressure trapped depends on how quickly the choke reacted and responded to the non-existent flow rate scenario. However, in the event of a sudden and unexpected loss of wellbore pressure, it is unlikely that the choke will respond and close fast enough to trap the entire back pressure. Lost back pressure stays lost until flow from the well is either resumed or provided from another source. A lost back pressure scenario implies loss of pressure control in the wellbore, and possibly also total loss of well control if the mud weight window is narrow [10].

One solution to this problem is to provide fluid flow from an external source. Some MPD systems are therefore equipped with its own on-demand back pressure pump (See Figure A.1). The back pressure pumps used in the DAPC-system is a low volume, triplex pump connected to the choke manifold, and automatically controlled by the control system. If the control system senses that the choke is unable to provide the requested back pressure, the back pressure pump is automatically turned on. The pressure and fluid flow through the choke then increases and the requested back pressure from the hydraulic model is delivered. A scenario involving lost back pressure, is in such a manner effectively avoided [10].

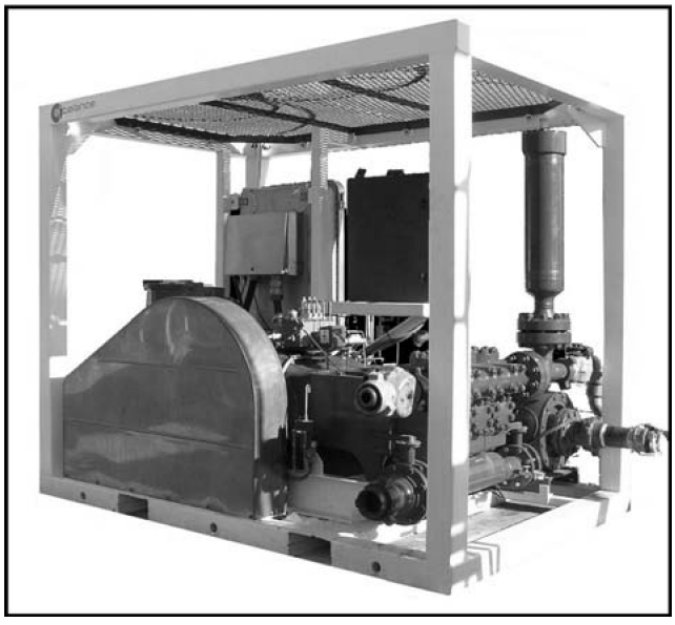

Figure A.5: A DAPC back pressure pump [10]

A.6 Flow meter

A flow meter is an optional, but nevertheless a very useful equipment used in MPD. Its purpose is to measure the flow rate downstream of the choke, illustrated in Figure A.1. A flow meter, in combination with an automated control system, enables quick detection and immediate reaction if mud losses or fluid influx occur. This is performed by comparing the actual flow rate, measured by the flow meter, against the predicted flow rate. Actions are taken if the two values differ with a certain amount. Mud losses or influx are typically detected before the lost or gained volume reaches 0,5 barrels, which is approximately 80 litres. The automatic control system then signals the choke valves to either open (mud lost) or throttle (fluid influx) dependent on the situation. In the case of a kick, the choke valves are signalled to throttle until sufficient amount of back pressure is applied and the influx stops. The situation is typically brought under control before the total lost or gained volume has reached 2 barrels, which is approximately 320 litres [30, 63].

The Coriolis flowmeter is, as opposed to other flow meter types, able to provide very accurate flow rate measurements of fluids containing solids. This makes it ideal for use on returning drilling fluid as they contain cuttings. A Coriolis flowmeter used in a MPD operation is illustrated in Figure A.6 [10].

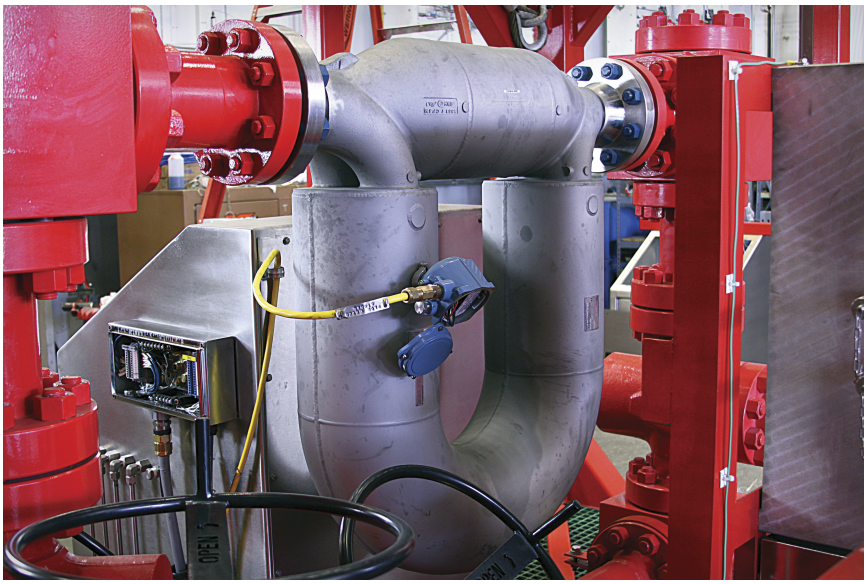

Figure A.6: Coriolis flow meter used in a MPD operation [69].

A.7 Continuous circulation system

A continuous circulation system (CCS) enables the BHP to remain more or less constant during drill pipe connections. The system minimizes the positive and negative pressure fluctuations encountered during drill pipe connections. This results in shorter total connection time, improved wellbore stability and improved hole cleaning. In addition, problems related to gas migration during connections are reduced [10].

A CCS set-up is shown in Figure A.7, the system is developed by National Oilwell Varco (NOV). When a connection is to be made, the lower and upper pipe rams, illustrated on the figure, closes around the drill pipe and creates a sealed chamber. Mud is then pumped into the sealed chamber, through the black hoses on the figure, until the pressure outside the drill string is equal to the pressure inside it. The drill pipe connection is then broke and the loose drill string raised. When the raised drill string is clear of the blind ram, it closes and circulation from the top drive is stopped. Mud is then circulated from the lower black hose into the open-end drill pipe, and hence, circulation is maintained. Pressure is bled off in the upper pressure-section and the upper pipe ram opened. The drill pipe is then lifted out of the CCS-unit, and a new stand of drill pipe is guided into the unit. The sequence described above now repeats itself in reverse order, which allows a new stand to be connected to the open-end drill pipe. Drilling then continuous with uninterrupted wellbore circulation, and a stable ECD. [70].

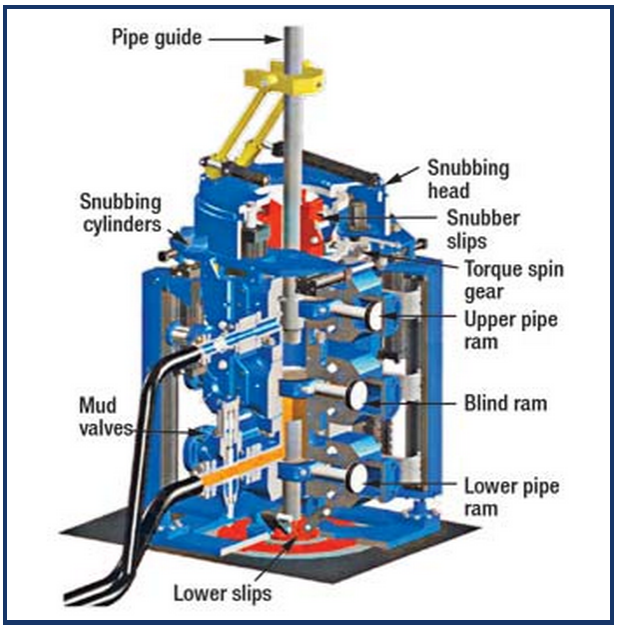

Figure A.7: Continuous circulation system set-up, developed by NOV [71].

The CCS has proven to be a safe and reliable system, enabling successful drilling in high-

pressure/high-temperature fields and wells drilled in narrow mud weight windows. The system has also proved valuable when drilling into reservoirs. Problems experienced with formation damage and impaired production in the reservoir can be reduced with a continuous circulation system [10].

Appendix B

DGD approaches and systems

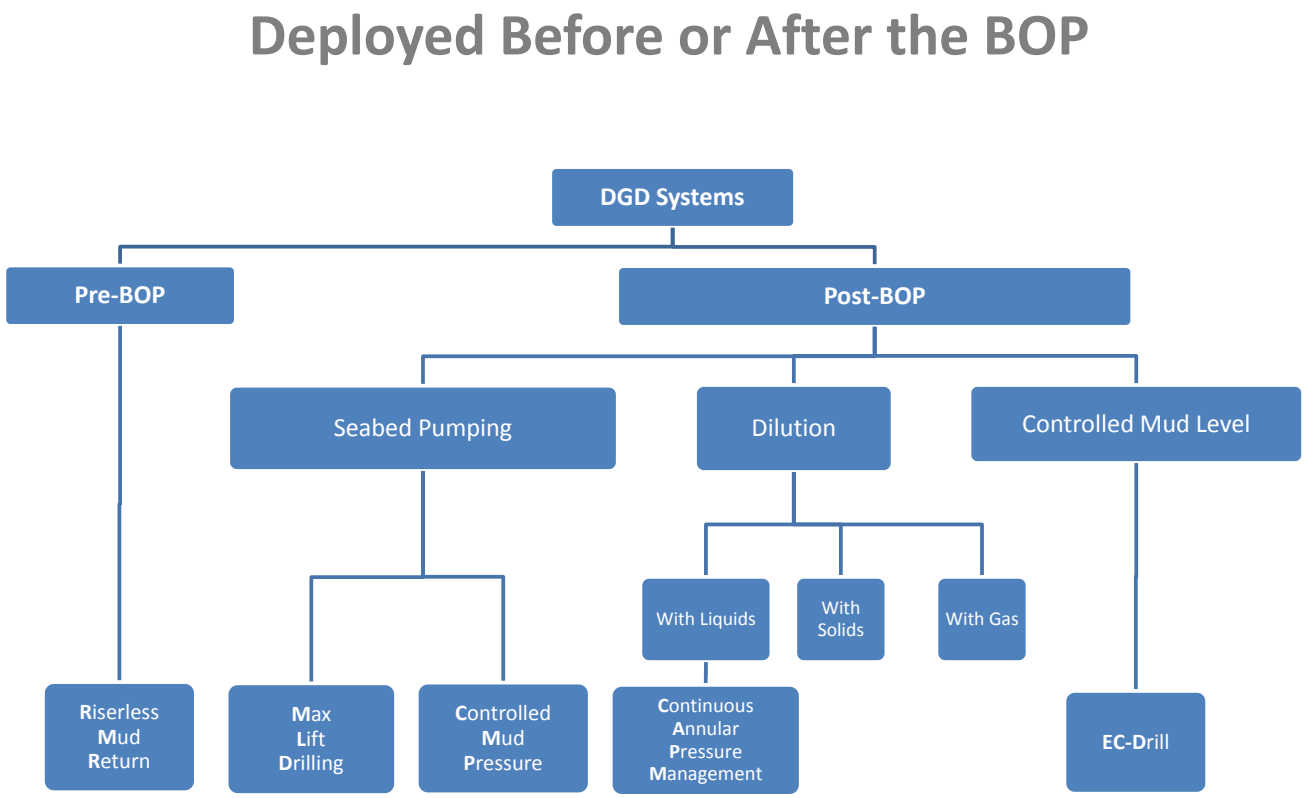

Figure B.1: Dual gradient drilling approaches and systems [9].

Appendix C

Case study

C.1 Planned drilling programs

The following parameters are used in the planned drilling programs:

- *Hole size*: The hole diameter of the section in inches (1 inch = 0,0254 meters).
- *Casing/liner size*: The diameter of the casing/liner in inches.
- *TVD*: The total vertical depth in feet (1 feet = 0,3048 meters).
- EMW_{stat}: Effective static mud weight in ppg (1 ppg is 119,8 kg/m^3).
- *ROP*: Rate of penetration in feet/hour (1 feet/hour = $8,47 \cdot 10^{-5}$).
- Q_m: The flow rate delivered by the mud pump in litres per minute.
- $\bar{C}_C$: The average concentration of cuttings in the borehole during drilling in %.
- P_{AF}: The annular friction pressure caused by circulation, noted in Pascal.
- P_C: The pressure exerted by the weight of cuttings in the borehole, noted in Pascal.
- EMW_{dyn}: Effective dynamic mud weight in ppg.
- $\rho_{f,\,est}$: The estimated pore pressure margin (pore pressure + 0,17 ppg).
- $\rho_{frac,\,est}$: The estimated fracture pressure margin (fracture pressure - 0,5 ppg).
- $P_{BP,stat}$: The static back pressure applied in the CBHP MPD variant, noted in Pascal.
- $P_{BP,dyn}$: The dynamic back pressure applied in the CBHP MPD variant, noted in Pascal.
- $h_{1,\,stat}$: The static mud level in the riser with the CML DGD variant, noted in meters.
- $h_{1,\,dyn}$: The dynamic mud level in the riser with the CML DGD variant, noted in meters.

Hole size [*inch*]	Casing/liner size [*inch*]	TVD [*feet*]	EMW$_{stat}$ [*ppg*]	ROP [*ft/h*]	Q$_m$ [*lpm*]	$\bar{C}_C$ %	P$_{AF}$ [*bar*]	P$_C$ [*bar*]	EMW$_{dyn}$ [*ppg*]	$\rho_{f,\,est}$ [*ppg*]	$\rho_{frac,\,est}$ [*ppg*]
36”	30” conductor pipe	3 150	8,60 (**8,60**)	20	3 500	2,5	0	0	8,60 (**8,60**)	8,77	8,11
	30” shoe	3 400	8,60 (**8,60**)	20	3 500	2,5	0,1	0,2	8,63 (**8,60**)	8,77	8,41
26”	20” surface casing	3 400	8,67[1] (8,67)	30	3 000	2,3	0,1	0,2	8,69 (**8,69**)	8,77	8,41
	20” shoe	4 600	8,88 (8,67)	30	3 000	2,3	0,6	1,2	9,0 (**8,69**)	8,77	9,97
Run	*BOP on 22” riser*										
18 $^1/_2$”	16” liner	4 600	9,80 (*9,80*)	25	3 000	1,0	3,6	1,5	10,11 (*10,11*)	8,77	9,97
	16” shoe	5 300	9,80 (*9,80*)	25	3 000	1,0	4,2	1,7	10,11 (*10,11*)	9,80	10,79
14 $^1/_2$”	13 $^3/_8$” casing	5 300	10,20 (*10,20*)	100	2 500	2,8	4,3	4,8	10,68 (*10,68*)	9,80	10,79
	13 $^3/_8$” shoe	12 000	10,20 (*10,20*)	100	2 500	2,8	12,3	10,9	10,74 (*10,68*)	8,77	15,31
Change	*to 4” drill pipe*										
12 $^1/_4$”	11 $^3/_4$” liner	12 000	14,20 (*14,20*)	50	2 500	1,0	13,7	2,2	14,57 (*14,57*)	8,77	15,31
	11 $^3/_4$” shoe	16 800	14,20 (*14,20*)	50	2 500	1,0	20,5	3,1	14,59 (*14,57*)	14,20	15,60
10 $^5/_8$”	9 $^5/_8$” casing	16 800	15,20 (*15,20*)	50	2 000	1,0	21,2	2,3	15,59 (*15,59*)	14,20	15,60
	9 $^5/_8$” shoe	21 500	15,20 (*15,20*)	50	2 000	1,0	29,7	3,0	15,62 (*15,59*)	15,20	16,43
8 $^1/_2$”	7 $^5/_8$” liner	21 500	15,80 (*15,80*)	50	1 500	0,8	46,1	2,2	16,43 (*16,43*)	15,20	16,43
	7 $^5/_8$” shoe	24 500	15,80 (*15,80*)	50	1 500	0,8	54,8	2,5	16,45 (*16,43*)	15,80	16,84

Table C.1: Planned drilling program using conventional drilling.

[1]The mud weight used in the 26” hole is 9,50 ppg and the section is drilled with the *Pump and Dump* approach.

Hole size [*inch*]	Casing/liner size [*inch*]	TVD [*feet*]	EMW$_{stat}$ [*ppg*]	ROP [*ft/h*]	Q$_m$ [*lpm*]	$\bar{C}_C$ %	P$_{AF}$ [*bar*]	P$_C$ [*bar*]	EMW$_{dyn}$ [*ppg*]	$\rho_{f,\,est}$ [*ppg*]	$\rho_{frac,\,est}$ [*ppg*]
6 $^7/_8$”	6 $^5/_8$” liner	24 500	16,15 (*16,15*)	50	1 000	0,8	57,9	2,2	16,83 (*16,83*)	15,80	16,84
	6 $^5/_8$” shoe	26 200	16,15 (*16,15*)	50	1 000	0,8	66,8	2,3	16,89 (*16,83*)	16,15	17,05
5 $^3/_4$”	5” liner	26 200	16,35 (*16,35*)	40	750	0,6	72,5	1,6	17,14 (*17,14*)	16,15	17,05
	5” shoe	27 000	16,35 (*16,35*)	40	750	0,6	81,7	1,7	17,21 (*17,14*)	16,37	17,16

Table C.2: Planned drilling program using conventional drilling, continued.

Hole size [inch]	Casing/liner size [inch]	TVD [feet]	MW [ppg]	ROP [ft/h]	Q [lpm]	$\bar{C}_C$ %	P_{AF} [10^5Pa]	P_C [10^5Pa]	$P_{BP,dyn}$ [10^5Pa]	EMW_{dyn} [ppg]	$P_{BP,stat}$ [10^5Pa]	EMW_{stat} [ppg]	$\rho_{f,\,est}$ [ppg]	$\rho_{frac,\,est}$ [ppg]
36”	30” conductor pipe	3 150	8,60	20	3 500	2,5	0	0	0	8,60 (*8,60*)	0	8,60 (*8,60*)	8,77	8,11
	30” shoe	3 400	8,60	20	3 500	2,5	0,1	0,2	0	8,63 (*8,60*)	0	8,60 (*8,60*)	8,77	8,41
26”	20” surface casing	3 400	9,50	30	3 000	2,3	0,1	0,2	0	8,69 (*8,69*)	0	8,67 (*8,67*)	8,77	8,41
26”	20” shoe	4 600	9,50	30	3 000	2,3	0,6	1,2	0	9,00 (*8,69*)	0	8,88 (*8,67*)	8,77	9,97
Run	*BOP on 22” riser*													
18 $^1/_2$”	16” liner	4 600	9,40	50	3 000	1,9	3,6	3,1	1,0	9,87 (*9,87*)	7,7	9,87 (*9,87*)	8,77	9,97
	16” shoe	5 600	9,40	50	3 000	1,9	4,4	3,8	1,0	9,86 (*9,87*)	9,2	9,86 (*9,96*)	9,85	11,04
14 $^1/_2$”	13 $^3/_8$” casing	5 600	9,40	100	2 500	2,8	5,0	5,6	5,0	10,18 (*10,18*)	15,6	10,18 (*10,18*)	9,85	11,04
	Top of salt	6 920	9,40	100	2 500	2,8	6,6	6,8	5,0	10,14 (*10,18*)	18,5	10,14 (*10,32*)	10,07	12,17
	13 $^3/_8$” shoe	12 000	9,40	100	2 500	2,8	12,6	11,9	5,0	10,01	29,5	10,01 (*10,87*)	8,77	15,31
12 $^1/_4$”	11 $^3/_4$” liner	12 000	13,70	100	2 500	2,0	15,4	4,8	5,0	14,29 (*14,29*)	25,2	14,29 (*14,29*)	8,77	15,31
	Bottom of salt	12 540	13,70	100	2 500	2,0	16,3	5,0	5,0	14,29 (*14,29*)	26,3	14,29 (*14,31*)	13,22	14,53
	11 $^3/_4$” shoe	17 300	13,70	100	2 500	2,0	24,1	6,9	5,0	14,28 (*14,29*)	36,0	14,28 (*14,54*)	14,28	15,70
10 $^5/_8$”	9 $^5/_8$” casing	17 300	14,85	100	2 000	1,9	27,4	5,1	5,0	15,46 (*15,46*)	37,5	15,46 (*15,46*)	14,28	15,70
	9 $^5/_8$” shoe	22 900	14,85	100	2 000	1,9	39,6	6,8	5,0	15,48 (*15,46*)	51,4	15,48 (*15,68*)	15,48	16,63
8 $^1/_2$”	7 $^5/_8$” liner	22 900	15,50	50	1 500	0,8	64,0	2,5	5,0	16,37 (*16,37*)	71,5	16,37 (*16,37*)	15,48	16,63
	7 $^5/_8$” shoe	27 000	15,50	50	1 500	0,8	80,7	2,9	5,0	16,42 (*16,37*)	88,6	16,42 (*16,58*)	16,37	17,16

Table C.3: Planned drilling program using the MPD variant CBHP

Hole size [inch]	Casing/liner size [inch]	TVD [feet]	MW [ppg]	ROP [ft/h]	Q [lpm]	$\bar{C}_C$ [%]	P_{AF} [10^5Pa]	P_C [10^5Pa]	$h_{1,\,stat}$ [meter]	EMW_{stat} [ppg]	$h_{1,\,dyn}$ [meter]	EMW_{dyn} [ppg]	$\rho_{f,\,est}$ [ppg]	$\rho_{frac,\,est}$ [ppg]
36”	30” conductor pipe	3 150	8,60	20	3 500	2,5	0	0	0	8,60 *(8,60)*	0	8,60 *(8,60)*	8,77	8,11
	30” shoe	3 400	8,60	20	3 500	2,5	0,1	0,2	0	8,60 *(8,60)*	0	8,63 *(8,60)*	8,77	8,41
26”	20” surface casing	3 400	9,50	30	3 000	2,3	0,1	0,2	0	8,67 *(8,67)*	0	8,69 *(8,69)*	8,77	8,44
26”	20” shoe	4 600	9,50	30	3 000	2,3	0,6	1,2	0	8,88 *(8,67)*	0	9,00 *(8,69)*	8,77	9,97
Run	*BOP on 22” riser*													
18 $^1/_2$”	16” liner	4 600	9,95	75	3 000	2,9	1,5	1,9	0	9,95 *(9,95)*	29	9,95 *(9,95)*	8,77	9,97
	16” shoe	6 200	9,95	75	3 000	2,9	2,8	3,4	0	9,95 *(9,95)*	53	9,95 *(9,78)*	9,95	11,57
14 $^1/_2$”	13 $^3/_8$” casing	6 200	11,00	100	2 500	2,8	3,2	3,0	0	11,00 *(11,00)*	48	11,00 *(11,00)*	9,95	11,57
	Top of salt	6 920	11,00	100	2 500	2,8	4,1	3,6	0	11,00 *(11,00)*	59	11,00 *(10,93)*	10,07	12,17
	13 $^3/_8$” shoe	12 000	11,00	100	2 500	2,8	10,1	7,8	0	11,00 *(11,00)*	139	11,00 *(10,47)*	8,77	15,31
12 $^1/_4$”	11 $^3/_4$” liner	12 000	14,45	100	2 500	2,0	13,4	3,2	0	14,45 *(14,45)*	98	14,45 *(14,45)*	8,77	15,31
	Bottom of salt	12 540	14,45	100	2 500	2,0	14,3	3,4	0	14,45 *(14,45)*	104	14,45 *(14,43)*	13,23	14,53
	11 $^3/_4$” shoe	17 900	14,45	100	2 500	2,0	23,0	5,3	0	14,45 *(14,45)*	167	14,45 *(14,18)*	14,43	15,82
10 $^5/_8$”	9 $^5/_8$” casing	17 900	15,75	100	2 000	1,9	23,3	3,6	0	15,75 *(15,75)*	145	15,75 *(15,75)*	14,43	15,82
	9 $^5/_8$” shoe	24 000	15,75	100	2 000	1,9	36,7	5,0	0	15,75 *(15,75)*	225	15,75 *(15,52)*	15,70	16,78
8 $^1/_2$”	7 $^5/_8$” liner	24 000	16,50	75	1 500	1,2	65,4	2,5	0	16,50 *(16,50)*	351	16,50 *(16,50)*	15,70	16,78
	7 $^5/_8$” shoe	27 000	16,50	75	1 500	1,2	77,6	2,9	0	16,50 *(16,50)*	415	16,50 *(16,35)*	16,37	17,16

Table C.4: Planned drilling program using the CML MPD, DGD approach and a full riser during static conditions.

Hole size [inch]	Casing/liner size [inch]	TVD [feet]	MW [ppg]	ROP [ft/h]	Q [lpm]	$\bar{C}_C$ [%]	P_{AF} [10^5Pa]	P_C [10^5Pa]	$h_{1,\,stat}$ [meter]	EMW_{stat} [ppg]	$h_{1,\,dyn}$ [meter]	EMW_{dyn} [ppg]	$\rho_{f,\,est}$ [ppg]	$\rho_{frac,\,est}$ [ppg]
36”	30” conductor pipe	3 150	8,60	20	3 500	2,5	0	0	0	8,60	0	8,60 *(8,60)*	8,77	8,11
	30” shoe	3 400	8,60	20	3 500	2,5	0,1	0,2	0	8,6	0	8,63 *(8,63)*	8,77	8,41
26”	20” surface casing	3 400	9,50	30	3 000	2,3	0,1	0,2	0	8,67	0	8,69 *(8,69)*	8,77	8,44
26”	20” shoe	4 600	9,50	30	3 000	2,3	0,6	1,2	0	8,88	0	9,00 *(8,69)*	8,77	9,97
Run	*BOP on 22” riser*													
18 $^1/_2$”	16” liner	4 600	13,00	75	3 000	2,9	1,5	1,3	350	9,76 *(9,76)*	368	9,76 *(9,76)*	8,77	9,97
	16” shoe	6 200	13,00	75	3 000	2,9	2,8	2,3	350	10,59 *(9,76)*	383	10,59 *(9,61)*	9,95	11,57
14 $^1/_2$”	13 $^3/_8$” casing	6 200	13,00	100	2 500	2,8	3,2	2,2	350	10,59 *(10,59)*	386	10,59 *(10,59)*	9,95	11,57
	Top of salt	6 920	13,00	100	2 500	2,8	4,1	2,7	350	10,84 *(10,59)*	394	10,84 *(10,53)*	10,07	12,17
	13 $^3/_8$” shoe	12 000	13,00	100	2 500	2,8	10,1	5,9	350	11,76 *(10,59)*	455	11,76 *(10,12)*	8,77	15,31
12 $^1/_4$”	11 $^3/_4$” liner	12 000	15,75	100	2 500	2,0	13,4	2,4	400	14,03 *(14,03)*	485	14,03 *(14,03)*	8,77	15,31
	Bottom of salt	12 540	15,75	100	2 500	2,0	14,3	2,5	400	14,10 *(14,03)*	490	14,10 *(14,00)*	13,23	14,53
	11 $^3/_4$” shoe	18 500	15,75	100	2 500	2,0	24,0	4,0	400	14,63 *(14,03)*	551	14,63 *(13,74)*	14,57	15,93
10 $^5/_8$”	9 $^5/_8$” casing	18 500	16,50	100	2 000	1,9	24,3	2,9	275	15,70 *(15,70)*	416	15,70 *(15,70)*	14,57	15,93
	9 $^5/_8$” shoe	24 500	16,50	100	2 000	1,9	37,5	4,0	275	15,89 *(15,70)*	489	15,89 *(15,48)*	15,80	16,84
8 $^1/_2$”	7 $^5/_8$” liner	24 500	16,50	75	1 500	1,2	67,0	2,6	50	16,39 *(16,39)*	409	16,39 *(16,39)*	15,80	16,84
	7 $^5/_8$” shoe	27 000	16,50	75	1 500	1,2	77,2	2,9	50	16,40 *(16,39)*	463	16,40 *(16,27)*	16,37	17,16

Table C.5: Planned drilling program using the CML MPD, DGD approach and a partly evacuated riser during static conditions

C.2 Actual drilling programs

These additional parameters are introduced in the actual drilling programs:

- LOT: The Leak-Off Test conducted prior to drilling a new section, given in terms of fracture pressure margin (LOT - 0,5 ppg).
- $\rho_{f\,real}$: The measured pore pressure during drilling, given in terms of pore pressure margin (pore pressure + 0,17 ppg)

Hole size [*inch*]	Casing/liner size [*inch*]	TVD [*feet*]	EMW$_{stat}$ [*ppg*]	ROP [*ft/h*]	Q$_m$ [*lpm*]	$\bar{C}_C$ %	P$_{AF}$ [*bar*]	P$_C$ [*bar*]	EMW$_{dyn}$ [*ppg*]	*LOT* [*ppg*]	$\rho_{f\ real}$ [*ppg*]
36”	30” conductor pipe	**3 240**	8,60	20	3 500	2,5	0	0	8,60		
	30” shoe	3 400	8,60	20	3 500	2,5	0,1	0,2	8,62		
26”	20” surface casing	3 400	9,50 (8,64)	30	3 000	2,3	0,1	0,1	8,67		
	20” shoe	4 600	9,50 (8,87)	30	3 000	2,3	0,7	1,1	9,0		
Run	*BOP on 22” riser*										
18 $^1/_2$”	16” liner	4 600	**9,50**	**20**	3 000	0,8	3,6	1,2	9,79	9,80	8,77
		4 780	9,50	20	3 000	0,8	3,7	1,3	9,79		9,44
	16” shoe	**4 800**	9,50	20	3 000	0,8	3,7	1,3	9,79		9,72
14 $^1/_2$”	13 $^3/_8$” casing	**4 800**	**9,90**	**20**	2 500	0,6	3,8	0,9	10,17	10,18	9,72
		5 140	9,90	20	2 500	0,6	4,2	1,0	10,18		9,90
	13 $^3/_8$” shoe	**5 160**	9,90	20	2 500	0,6	4,2	1,0	10,18		9,91
Change	*to 4” drill pipe*										
12 $^1/_4$”	11 $^3/_4$” liner	**5 160**	**10,10**	**25**	**2 000**	0,6	4,8	1,1	10,42	10,44	9,91
		5 420	10,10	25	2 000	0,6	5,2	1,1	10,43		10,10
	11 $^3/_4$” shoe	**5 440**	10,10	25	2 000	0,6	5,2	1,1	10,43		10,16
10 $^5/_8$”	9 $^5/_8$” casing	**5 440**	**10,30**	**25**	2 000	0,5	5,3	0,8	10,61	10,64	10,16
		5 480	10,30	25	2 000	0,5	5,3	0,8	10,61		10,27
	9 $^5/_8$” shoe	**5 500**	10,30	25	2 000	0,5	5,4	0,9	10,62		10,33
8 $^1/_2$”	7 $^5/_8$” liner	**5 500**	10,32	**20**	1 500	0,3	7,8	0,6	10,74	10,73	10,33
Stops drilling,	*mud weight window*	*is closed*									

Table C.6: Actual drilling program using conventional drilling.

Hole size [inch]	Casing/liner size [inch]	TVD [feet]	MW [ppg]	ROP [ft/h]	Q [lpm]	$\bar{C}_C$ %	P_{AF} [10^5Pa]	P_C [10^5Pa]	$P_{BP,dyn}$ [10^5Pa]	EMW_{dyn} [ppg]	$P_{BP,stat}$ [10^5Pa]	EMW_{stat} [ppg]	LOT [ppg]	$\rho_{f\ real}$ [ppg]
36”	30” conductor pipe	**3 240**	8,60	20	3 500	2,5	0	0	0	8,60 (*8,60*)	0	8,60 (*8,60*)		
	30” shoe	3 400	8,60	20	3 500	2,5	0,1	0,2	0	8,63 (*8,60*)	0	8,60 (*8,60*)		
26”	20” surface casing	3 400	9,50	30	3 000	2,3	0,1	0,2	0	8,66 (*8,66*)	0	8,64(*8,64*)		
26”	20” shoe	4 600	9,50	30	3 000	2,3	0,6	1,2	0	8,98 (*8,66*)	0	8,87(*8,64*)		
Run	*BOP on 22” riser*													
18 $^1/_2$”	16” liner	4 600	**9,35**	**25**	3 000	1,0	3,6	1,6	1,0	9,72 (*9,72*)	6,2	9,72 (*9,72*)	9,80	8,77
		4 820	9,35	25	3 000	1,0	3,8	1,7	1,0	9,72 (*9,72*)	6,4	9,72 (*9,74*)		9,73
		4 820	9,35	25	3 000	1,0	3,8	1,7	**1,8**	9,77 (*9,77*)	7,2	9,77 (*9,79*)		9,73
	16” shoe	4 900	9,35	25	3 000	1,0	3,8	1,7	1,8	9,77 (*9,77*)	7,3	9,77 (*9,79*)		9,78
14 $^1/_2$”	13 $^3/_8$” casing	**4 900**	**9,80**	**25**	2 500	0,7	4,0	1,2	**1,0**	10,15 (*10,15*)	6,2	10,15 (*10,15*)	10,26	9,78
		5 460	9,80	25	2 500	0,7	4,7	1,3	1,0	10,16 (*10,16*)	7,0	10,16 (*10,20*)		10,21
	13 $^3/_8$” shoe	5 460	9,80	25	2 500	0,7	4,7	1,3	**2,0**	10,21 (*10,21*)	8,0	10,21 (*10,26*)		10,21
12 $^1/_4$”	11 $^3/_4$” liner	**5 460**	**10,25**	**25**	2 500	0,5	5,8	0,9	**1,0**	10,64 (*10,64*)	7,7	10,64 (*10,64*)	10,69	10,21
		6 000	10,25	25	2 500	0,5	6,7	1,0	1,0	10,65 (*10,64*)	8,7	10,65 (*10,69*)		10,41
		6 000	10,25	25	2 500	0,5	6,7	1,0	**0,6**[1]	10,63 (*10,63*)	8,3	10,63 (*10,67*)		10,41
		6 200	10,25	25	2 500	0,5	7,0	1,0	0,6	10,64 (*10,63*)	8,6	10,64 (*10,69*)		10,61
10 $^5/_8$”	9 $^5/_8$” casing	**6 200**	**10,75**	**50**	2 000	1,0	7,4	1,8	**1,0**	11,21 (*11,21*)	10,2	11,21 (*11,21*)	11,30	10,61
		6 540	10,75	50	2 000	1,0	8,2	1,9	1,0	11,22 (*11,21*)	11,1	11,22 (*10,23*)		11,39
		6 540	10,75	50	2 000	1,0	8,2	1,9	**4,0**	11,35 (*11,35*)	14,1	11,35 (*11,38*)		11,39

Table C.7: Actual drilling program using the MPD variant CBHP

[1]The measured pore pressure gradient at 5 660 feet is 10,63 ppg. In order to stay above the pore pressure at this depth, the dynamic back pressure can be reduced to a maximum of 0,6 bar.

Hole size [inch]	Casing/liner size [inch]	TVD [feet]	MW [ppg]	ROP [ft/h]	Q_m [lpm]	$\bar{C}_C$ %	P_{AF} [10^5Pa]	P_C [10^5Pa]	$P_{BP,dyn}$ [10^5Pa]	EMW_{dyn} [ppg]	$P_{BP,stat}$ [10^5Pa]	EMW_{stat} [ppg]	LOT [ppg]	$\rho_{f\ real}$ [ppg]
8 $^1/_2$"	7 $^5/_8$" liner	**6 540**	**11,00**	50	1 500	0,8	12,8	1,6	**1,0**	11,66 (*11,66*)	15,4	11,66 (*11,66*)	11,78	11,39
	Top of salt	6 680	11,00	50	1 500	0,8	13,4	1,6	1,0	11,67 (*11,66*)	16,0	11,66 (*11,68*)		8,77
		7 200 [2]	11,00	50	1 500	0,8	15,5	1,7	1,0	11,71 (*11,66*)	18,2	11,71 (*11,78*)		8,77
		7 200	11,00	**100**	1 500	1,6	15,5	3,45	**0**	11,74 (***11,68***)	16,0	11,62 (***11,68***)		8,77
	7 $^5/_8$" shoe	12 000	11,00	**100**	1 500	1,6	35,0	5,8	0	11,95 (*11,68*)	16,0	11,37 (*11,68*)		8,77
Drill	*contingency section*													
6 $^7/_8$"	**6 $^5/_8$" liner**	12 000	13,00	75	1 000	1,2	40,1	3,2	5	14,12[3] (*14,12*)	48,3	14,12 (*14,12*)	15,63	8,77
	Bottom of salt	**12 140**	13,00	75	1 000	1,2	41,6	3,3	5	14,15 (*14,16*)	49,9	14,15 (*14,12*)		14,72
		12 140	13,00	75	1 000	1,2	41,6	3,3	**35**	14,84 (*14,86*)	79,9	14,84 (*14,82*)		14,72
		12 300	13,00	75	1 000	1,2	43,3	3,3	35	14,85 (*14,90*)	81,6	14,85 (*14,82*)		14,86
		12 300	13,00	75	1 000	1,2	43,3	3,3	**45**	15,08 (*15,13*)	91,6	15,08 (*15,06*)		14,86
		13 140	13,00	75	1 000	1,2	52,2	3,5	45	15,14 (*15,34*)	100,7	15,14 (*15,06*)		15,15
		13 140	13,00	75	1 000	1,2	52,2	3,5	**55**	15,35 (*15,58*)	110,7	15,35 (*15,29*)		15,15
		13 200	13,00	75	1 000	1,2	52,8	3,5	55	15,36 (*15,59*)	111,3	15,36 (*15,29*)		15,45
		13 200	13,00	75	1 000	1,2	52,8	3,5	**59**	15,44 (*15,68*)	115,3	15,44 (*15,38*)		15,45

Table C.8: Actual drilling program using the MPD variant CBHP, continued.

[2]Switch point of constant pressure to the 9 $^5/_8$" casing shoe as the expected margins in the salt zone are large
[3]The estimated fracture margin below the salt zone (12 540 feet) is 14,53 ppg, stays below this.

Hole size [inch]	Casing/liner size [inch]	TVD [feet]	MW [ppg]	ROP [ft/h]	Q [lpm]	$\bar{C}_C$ [%]	P_{AF} [10^5Pa]	P_C [10^5Pa]	$h_{1,\,stat}$ [meter]	EMW_{stat} [ppg]	$h_{1,\,dyn}$ [meter]	EMW_{dyn} [ppg]	LOT [ppg]	$\rho_{f\ real}$ [ppg]
36”	30” conductor pipe	**3 240**	8,60	20	3 500	2,5	0	0	0	8,60 (*8,60*)	0	8,60 (*8,60*)		
	30” shoe	3 400	8,60	20	3 500	2,5	0,1	0,2	0	8,60 (*8,60*)	0	8,63 (*8,60*)		
26”	20” surface casing	3 400	9,50	30	3 000	2,3	0,1	0,1	0	8,64 (*8,64*)	0	8,66 (*8,66*)		
26”	20” shoe	4 600	9,50	30	3 000	2,3	0,7	1,1	0	8,67 (*8,64*)	0	8,97 (*8,66*)		
Run	*BOP on 22” riser*													
18 $^1/_2$”	16” liner	4 600	**9,80**	75	3 000	2,9	1,5	1,9	0	9,80 (*9,80*)	30	9,80 (*9,80*)	9,80	8,77
		4 960	9,80	75	3 000	2,9	1,8	2,3	0	9,80 (*9,80*)	35	9,80 (*9,76*)		9,81
14 $^1/_2$”	13 $^3/_8$” casing	**4 960**	10,30	100	2 500	2,8	1,9	2,1	0	10,30 (*10,30*)	33	10,30 (*10,30*)	10,30	9,81
	13 $^3/_8$” shoe	5 500	10,30	75	2 500	2,8	2,5	2,6	0	10,30 (*10,30*)	42	10,30 (*10,24*)		10,33
12 $^1/_4$”	11 $^3/_4$” liner	5 500	10,70	100	2 500	2,0	3,8	1,8	0	10,70 (*10,70*)	44	10,70 (*10,70*)	10,73	10,33
	11 $^3/_4$” shoe	6 280	10,70	100	2 000	2,0	5,1	2,3	0	10,70 (*10,70*)	58	10,70 (*10,61*)		10,74
10 $^5/_8$”	9 $^5/_8$” casing	**6 280**	11,35	100	2 000	1,9	5,1	2,0	0	11,35 (*11,35*)	53	11,35 (*11,35*)	11,39	10,74
	9 $^5/_8$” shoe	6 540	11,35	100	2 000	1,9	5,7	2,1	0	11,35 (*11,35*)	58	11,35 (*11,31*)		11,39
8 $^1/_2$”	7 $^5/_8$” liner	**6 540**	11,75	75	1 500	1,2	10,8	1,3	0	11,75 (*11,75*)	87	11,75 (*11,75*)	11,78	11,39
	Top of salt	6 680	11,75	75	1 500	1,2	11,3	1,3	0	11,75 (*11,75*)	92	11,75 (*11,72*)		8,77
		7 850	11,75	75	1 500	1,2	16,1	1,7	0	11,75 (*11,75*)	129	11,75 (*11,50*)		8,77
		7 850	11,75	75	1 500	1,2	16,1	1,7	0	11,75 (*11,75*)	**87**[1]	11,95 (*11,75*)		8,77
	7 $^5/_8$” shoe	12 000	11,75	75	1 500	1,2	33,0	3,1	0	11,75 (*11,75*)	87	12,31 (*11,75*)		8,77

Table C.9: Actual drilling program using the CML MPD, DGD approach and a full riser during static conditions.

[1]The pore pressure measured at 6 560 feet is 11,51 ppg. When the bit is at 7 850 feet, the effective dynamic mud weight at this depth is 11,51 ppg. It has been decided to switch the point of constant wellbore pressure to the 9 $^5/_8$” casing shoe.

Hole size [inch]	Casing/liner size [inch]	TVD [feet]	MW [ppg]	ROP [ft/h]	Q [lpm]	$\bar{C}_C$ [%]	P_{AF} [10^5Pa]	P_C [10^5Pa]	$h_{1,\,stat}$ [meter]	EMW_{stat} [ppg]	$h_{1,\,dyn}$ [meter]	EMW_{dyn} [ppg]	LOT [ppg]	$\rho_{f\ real}$ [ppg]
6 $^7/_8$”	**6 $^5/_8$” liner**	12 000	14,50	75	1 000	1,2	55,6	1,7	0	14,50[2] (*14,50*)	337	14,50 (*14,50*)	15,63	8,77
	Bottom of salt	**12 140**	14,50	75	1 000	1,2	57,1	1,8	0	14,50 (*14,50*)	346	14,50 (*14,47*)		14,72
		12 140	**14,80**	75	1 000	1,2	57,1	1,8	0	14,80 (*14,80*)	339	14,80 (*14,76*)		14,72
		12 240	14,80	75	1 000	1,2	58,1	1,8	0	14,80 (*14,80*)	345	14,80 (*14,74*)		14,82
		12 240	**15,10**	75	1 000	1,2	58,1	1,7	0	15,10 (*15,10*)	337	15,10 (*15,04*)		14,82
	6 $^5/_8$” shoe	13 140	15,10	75	1 000	1,2	67,6	1,9	0	15,10 (*15,10*)	392	15,10 (*14,81*)		15,15

Table C.10: Actual drilling program using the CML DGD, MPD approach and a full riser during static conditions, continued.

[2]The estimated fracture margin below the salt zone (12 540 feet) is 14,53 ppg, stays below this.

Hole size [inch]	Casing/liner size [inch]	TVD [feet]	MW [ppg]	ROP [ft/h]	Q [lpm]	$\bar{C}_C$ [%]	P_{AF} [10^5Pa]	P_C [10^5Pa]	$h_{1,\,stat}$ [meter]	EMW_{stat} [ppg]	$h_{1,\,dyn}$ [meter]	EMW_{dyn} [ppg]	LOT [ppg]	$\rho_{f\ real}$ [ppg]
36”	30” conductor pipe	**3 240**	8,60	20	3 500	2,5	0	0	0	8,60 (*8,60*)	0	8,60 (*8,60*)		
	30” shoe	3 400	8,60	20	3 500	2,5	0,1	0,2	0	8,60 (*8,60*)	0	8,63 (*8,60*)		
26”	20” surface casing	3 400	9,50	30	3 000	2,3	0,1	0,1	0	8,64 (*8,64*)	0	8,66 (*8,66*)		
26”	20” shoe	4 600	9,50	30	3 000	2,3	0,7	1,1	0	8,67 (*8,64*)	0	8,97 (*8,66*)		
Run	*BOP on 22” riser*													
18 $^1/_2$”	16” liner	4 600	13,00	75	3 000	2,9	1,5	1,3	350	9,76 (*9,76*)	368	9,76 (*9,76*)	9,80	8,77
		5 500	13,00	75	3 000	2,9	2,3	1,2	350	10,28 (*9,76*)	377	10,28 (*9,68*)		10,33
		5 500	**15,00**	75	3 000	2,9	2,3	1,2	**490**	10,62 (*9,76*)	510	10,62 (*9,69*)		10,33
		6 540	15,00	75	3 000	2,9	3,1	1,7	490	11,31 (*9,76*)	517	11,31 (*9,61*)		11,39
		6 540	15,00	75	3 000	2,9	3,1	1,7	**485**	11,35 (*9,81*)	512	11,35 (*9,66*)		11,39
14 $^1/_2$”	13 $^3/_8$” casing	**6 540**	15,00	**75**	2 500	2,1	3,6	1,3	**450**	11,61 (*11,61*)	477	11,61 (*11,61*)	11,78	11,39
	Top of salt	**6 680**	15,00	75	2 500	2,1	3,7	1,3	450	11,69 (*11,61*)	479	11,69 (*11,61*)		8,77
		8 300[1]	15,00	75	2 500	2,1	5,7	1,8	450	12,33 (*11,61*)	493	12,33 (*11,50*)		8,77
		8 300	15,00	75	2 500	2,1	5,7	1,8	450	12,33 (*11,61*)	**477**	12,42 (*11,61*)		8,77
	13 $^3/_8$” shoe	12 000	15,00	75	2 500	2,1	10,1	3,0	450	13,16 (*11,61*)	477	13,35 (*11,61*)		8,77

Table C.11: Actual drilling program using the CML DGD, MPD approach and a partly evacuated riser during static conditions.

[1]The pore pressure measured at 6 560 feet is 11,51 ppg. When the bit is at 8 300 feet, the effective dynamic mud weight at this depth is 11,51 ppg. It has been decided to switch the point of constant wellbore pressure to the 16” liner shoe.

Hole size [inch]	Casing/liner size [inch]	TVD [feet]	MW [ppg]	ROP [ft/h]	Q [lpm]	$\bar{C}_C$ [%]	P_{AF} [10^5Pa]	P_C [10^5Pa]	$h_{1,\ stat}$ [meter]	EMW_{stat} [ppg]	$h_{1,\ dyn}$ [meter]	EMW_{dyn} [ppg]	LOT [ppg]	$\rho_{f\ real}$ [ppg]
12 $^1/_4$"	11 $^3/_4$" liner	12 000	15,75	100	2 500	2,0	13,3	2,4	400	14,03[2] (*14,03*)	485	14,03 (*14,03*)	15,63	8,77
	Bottom of salt	**12 140**	15,75	100	2 000	2,0	13,5	2,4	400	14,05 (*14,03*)	486	14,05 (*14,02*)		14,72
		12 140	15,75	100	2 000	2,0	13,5	2,4	**200**	14,90 (*14,89*)	286	14,90 (*14,88*)		14,72
		12 460	15,75	100	2 000	2,0	14,1	2,5	200	14,92 (*14,89*)	289	14,92 (*14,87*)		14,93
		12 460	15,75	100	2 000	2,0	14,1	2,5	**175**	15,03 (*15,00*)	264	15,03 (*14,98*)		14,93
		13 140	15,75	100	2 000	2,0	15,2	2,6	175	15,06 (*15,00*)	271	15,06 (*14,95*)		15,15
		13 140	15,75	100	2 000	2,0	15,2	2,6	**100**	15,36 (*15,32*)	196	15,36 (*15,27*)		15,15
		13 200	15,75	100	2 000	2,0	15,3	2,7	100	15,36 (*15,32*)	197	15,36 (*15,27*)		15,45
		13 200	15,75	100	2 000	2,0	15,3	2,7	**30**	15,63 (*15,62*)	127	15,63 (*15,57*)		15,45
	11 $^3/_4$" shoe	17 700[3]	15,75	100	2 000	2,0	22,6	3,8	30	15,66 (*15,62*)	173	15,66 (*15,37*)		15,32
10 $^5/_8$"	9 $^5/_8$" casing	**17 700**	16,50	100	2 000	1,9	22,9	2,8	**200**	16,89 (*15,89*)	333	15,89 (*15,89*)	16,17	15,32
		19 620	16,50	100	2 000	1,9	27,1	3,1	200	15,95 (*15,89*)	356	15,95 (*15,82*)		16,02
		19 620	16,50	100	2 000	1,9	27,1	3,1	**110**	16,20 (*16,16*)	266	16,20 (*16,09*)		16,02
	9 $^5/_8$" shoe	20 580	16,50	100	2 000	1,9	29,2	3,3	110	16,21 (*16,16*)	278	16,21 (*16,06*)		16,23
8 $^1/_2$"	7 $^5/_8$" liner	**20 580**	16,50	75	1 500	1,2	54,6	2,1	50	16,37 (*16,37*)	342	16,37 (*16,37*)	16,53	16,23
	7 $^5/_8$" shoe	21 900[4]	16,50	75	1 500	1,2	60,0	2,3	50	16,38 (*16,37*)	371	16,38 (*16,29*)		16,29

Table C.12: Actual drilling program using the CML DGD, MPD approach and a partly evacuated riser during static conditions, continued.

[2]The estimated fracture margin below the salt zone (12 540 feet) is 14,53 ppg, stays below this.
[3]When the bit is 17 700 feet, the effective dynamic mud density at 13 200 feet is at the measured formation-pore pressure margin of 15,45 ppg.
[4]The real pore and fracture data ends at 21 900 feet. Drilling has therefore been ceased at this depth.